STRUCTURE AND FUNCTION RELATIONSHIPS IN TROPONIN C PROBED BY SITE-DIRECTED MUTAGENESIS

by

Genny Trigo-Gonzalez

B.A., Universidad de Valparaiso, Chile, 1982

Thesis submitted in partial fulfillment of

the requirements for the degree of

Master of Science.

in the Department

of

Chemistry

SIMON FRASER UNIVERSITY

March 1992

APPROVAL

Name: Genny Trigo-Gonzalez

Degree: Master of Science

Title of thesis: Structure and Function Relationships in Troponin-C Probed by Site-Directed Mutagenesis

Examining Committee:

Chair: Dr. D. Sutton

Dr. T. Borgford, Assistant Professor
Senior Supervisor

Dr. B. M. Pinto, Associate Proffesor
Supervisory Committee

Dr. R. B. Cornell, Assistant Professor
Supervisory Committee

Dr. S. Holdcroft, Assistant Professor
Internal Examiner
Department of Chemistry
Simon Fraser University

PARTIAL COPYRIGHT LICENSE

I hereby grant to Simon Fraser University the right to lend my thesis, project or extended essay (the title of which is shown below) to users of the Simon Fraser University Library, and to make partial or single copies only for such users or in response to a request from the library of any other university, or other educational institution, on its own behalf or for one of its users. I further agree that permission for multiple copying of this work for scholarly purposes may be granted by me or the Dean of Graduate Studies. It is understood that copying or publication of this work for financial gain shall not be allowed without my written permission.

Title of Thesis/Project/Extended Essay:

STRUCTURE AND FUNCTION RELATIONSHIPS IN TROPONIN-C PROBED BY SITE-DIRECTED MUTAGENESIS.

Author:

(signature)

GENNY TRIGO-GONZALEZ

(name)

April 10th 1992

(date)

ABSTRACT

Troponin C (TnC) is a protein located on the thin filament of skeletal and cardiac muscle fibres. Calcium induces a conformational change in TnC which is communicated to the other protein components of the thin filament, triggering muscle contraction. By site-directed mutagenesis, tryptophan residues were introduced into the high-affinity domain of TnC at position 105 (mutant FW105), and into the low-affinity domain at position 29 (mutant FW29). Since wild type TnC does not contain either tyrosine or tryptophan, Trp-29 and Trp-105 were used as site-specific reporters of metal ion binding and conformational change. The spectral properties of FW29, and FW105 and of a double mutant (FW29/FW105) were examined by absorbance and fluorescence methods.

Calcium induced significant changes in the near-UV absorbance spectra, fluorescence emission spectra and far-UV circular dichroism of all three proteins. Magnesium induced changes in the spectral properties of FW105 and FW29/FW105 only. Calcium induced a 1.22 fold decrease in the fluorescence quantum yield of FW105, whereas magnesium induced a 1.6 fold increase. This suggests that calcium and magnesium ions differ in their influence on the conformation of the high-affinity sites. Tryptophan substitutions allowed low- and high-affinity sites to be titrated independently of one another. Hill coefficients derived from titration curves indicate cooperative calcium binding in both low- and high-affinity sites.

The binding of calcium by TnC produces a significant increase in the helical content of the protein. Site-directed mutagenesis was used to study the relationship between calcium ion binding and α-helix stability. Amino acid substitutions were made at position 130, the N-cap position of helix G, in FW105. The binding properties of the mutants were monitored using Trp-105 as reporter group in fluorescence experiments. The high-affinity binding constants increased in the series Ile < Gly < Asp < Asn < Thr <

Ser. The substitutions did not affect the degree of cooperativity between the high-affinity sites. The results suggest a close thermodynamic relationship between the stability of helix G and high-affinity calcium ion binding in TnC. This relationship may be a way by which calcium binding proteins with helix-loop-helix motifs fine-tune ion affinity.

DEDICATION

To my parents, for their love

ACKNOWLEDGMENTS

I am very grateful to my supervisor Dr. Thor Borgford for his professional guidance, for being so encouraging, for creating such a nice working atmosphere and for being there in my dark days.

Thanks to B.C Health Care Research Foundation for supporting this work.

Special thanks to Kevin Neden, Greg Awang, Gabe Kalmar, Debbie Carson and Kathy Racher for helping me with their expertise and advice at different stages in my work.

Thanks to everyone in Thor's lab for their warmth and joy of living.

Thanks to all my friends in Canada, my family in this beautiful country.

TABLE OF CONTENTS

Page

LIST OF TABLES

Page

LIST OF FIGURES

Page

LIST OF ABBREVIATIONS

ATPase	Adenosine triphosphatase
BSA	Bovine serum albumin
CIP	Calf intestine alkaline phosphatase
dATP	2'- deoxyadenosine 5'- triphosphate
dCTP	2'- deoxycytidine 5'- triphosphate
dGTP	2'- deoxyguanosine 5'- triphosphate
dTTP	2'- deoxythymidine 5'- triphosphate
DEAE-	Diethylaminoethyl-
DTT	DL-dithiothreitol
EGTA	Ethyleneglycolbis-(aminoethylether) tetra-acetic acid
EDTA	Ethylenediamine tetra-acetic acid
FPLC	Fast protein liquid chromatography
HPLC	High performance liquid chromatography
MOPS	3 - [N-Morpholino] propanesulfonic acid
PAP	Linear polyacrylamide
PMSF	Phenylmethyl sulfonyl fluoride
RNase A	Ribonuclease A
RNase T1	Ribonuclease T1
rATP	Adenosine 5'- triphosphate
SDS	Sodium dodecyl sulfate
PAGE	Polyacrylamide gel electrophoresis
TFA	Trifluoracetic acid
TRIS	Tris (hydroxymethyl) methylamine

1. INTRODUCTION

1.1. Troponin C and Muscle Contraction

The contraction of skeletal muscle is a process that involves the coordinated activity of proteins of the thin and thick filament in muscle fibers(1, 2) (Figure 1.1-A). The thick filament is composed of myosin, a protein that has an enzyme ATPase activity. The thin filament is composed of the proteins tropomyosin, actin and the troponin complex. When actin forms a complex with myosin, called actomyosin, there is an increase in the ATPase activity of myosin. The hydrolysis of ATP by myosin provides the energy necessary for muscle contraction. In the early 1960s it was known that micromolar concentrations of calcium were required for ATP hydrolysis in myofibrils. Ebashi in 1963 (3) and Ebashi *et. al* in 1964 (4) found calcium sensitivity in a tropomyosin-like protein. In the presence of this protein, actomyosin preparations and myofibrils became calcium sensitive. Ebashi in 1968 (5) isolated from native tropomyosin, a new protein from the thin filament that he called troponin. Troponin was identified as the protein that bound calcium. The actomyosin preparation was calcium sensitive only in the presence of both troponin and tropomyosin. In the early 1970s, Greaser and Gergely (6, 7), using sodium dodecyl sulfate (SDS) polyacrylamide gels and ion exchange chromatography in 6 M urea, established that troponin consists of three polypeptide subunits. Troponin T (TnT) is the tropomyosin binding subunit, troponin I (TnI) inhibits the actomyosin ATPase activity and troponin C (TnC) is the calcium-binding subunit.

Muscle contraction is initiated by the increase of intracellular calcium concentration that follows the release of Ca^{2+} from the sarcoplasmic reticulum. The contraction / relaxation process is regulated by the binding of Ca^{2+} to the troponin

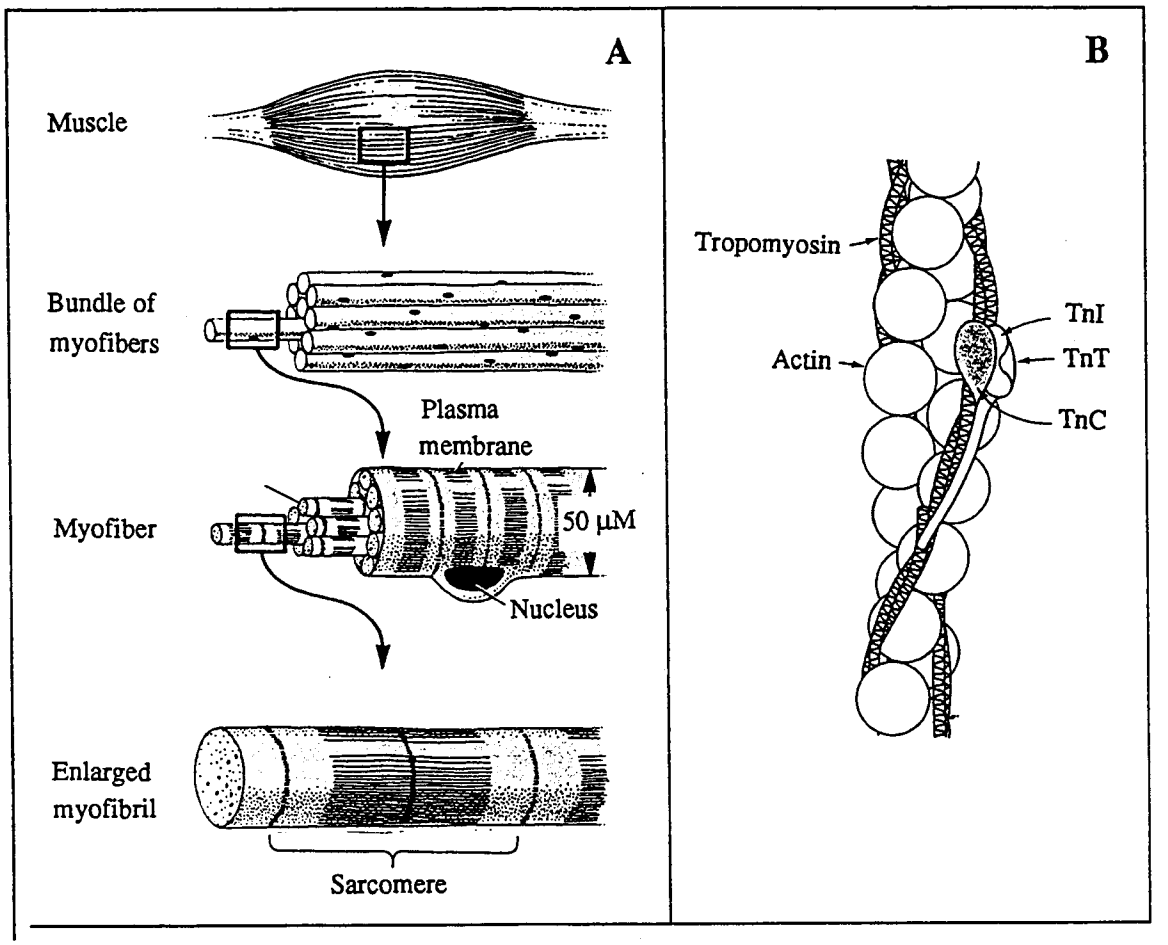

FIGURE 1.1. Organization of Skeletal Muscle

(A) Levels of organization in skeletal muscle. Muscle cells, or myofibers, are formed of many filaments, or myofibrils. Myofibrils are divided in sarcomeres, the functional unit of muscle contraction (adapted from (8)). (B) Representation of the thin filament (adapted from (9)). One tropomyosin molecule spans seven actin monomers. One troponin molecule occurs one third of the distance from the carboxyl-terminal end of each tropomyosin molecule.

complex, more specifically, to its TnC subunit. Calcium binds to TnC and the protein undergoes a conformational change that is transmitted to the other proteins of the thin filament. TnI dissociates from actin, allowing tropomyosin to move. This results in the formation of the actomyosin complex, increase in actomyosin ATPase activity and muscle contraction.

The binding of calcium to troponin C is an important event in the process of muscle contraction, and it is one of the objectives of this thesis project, to characterize this interaction. The study of the interaction between calcium and troponin C and of the relationships between the function and the structure of TnC is important in understanding the molecular details of the regulation of muscle contraction by the troponin complex.

Studies of the relationship between function and structure of TnC are possible since the gene encoding TnC and the three-dimensional crystal structure of the protein are now available. The first TnC sequence determined was that of rabbit skeletal muscle, by Collins *et.al.* (10). The sequence of chicken skeletal muscle TnC was first determined by Wilkinson (11), and it has been recently revised and corrected by DNA sequencing methods (12). The protein has 162 amino acids and a molecular weight of 18,400. It contains no tyrosine, no tryptophan residues and only one of each cysteine, histidine and proline residues. The protein is acidic, due to the high content of glutamic and aspartic acid. The three dimensional X-ray crystal structure has been reported for both turkey TnC (13) and chicken TnC (14). The molecule assumes a dumbbell shape in which the globular amino and carboxy domains are linked by a long central α-helix (Figure 1.2). Two relatively low-affinity, calcium-specific binding sites are present in the N-terminal domain (sites I and II). Two relatively high-affinity sites able to bind either calcium or magnesium are present in the C-terminal domain (sites III and IV). The structural unit of the metal binding sites is characterized by a helix-loop-helix (H-L-H) configuration (Figure 1.3). At the N-terminal domain, helix A-site I-helix B and helix C-site II-helix D form a pair of H-L-H motifs joined by a linking peptide. At the C-domain, helix E-site

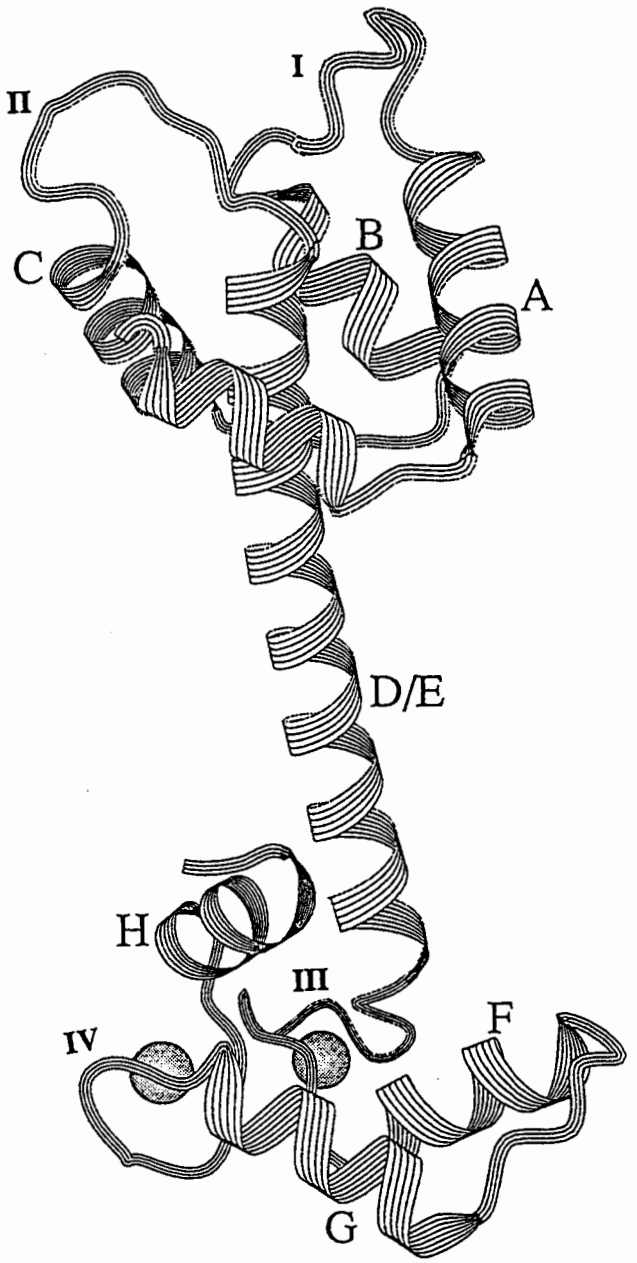

FIGURE 1.2. Ribbon Structure of Troponin C

Representation of the crystal structure of skeletal troponin C (1). The calcium binding sites are labeled I to IV. The helices are labeled A to H.

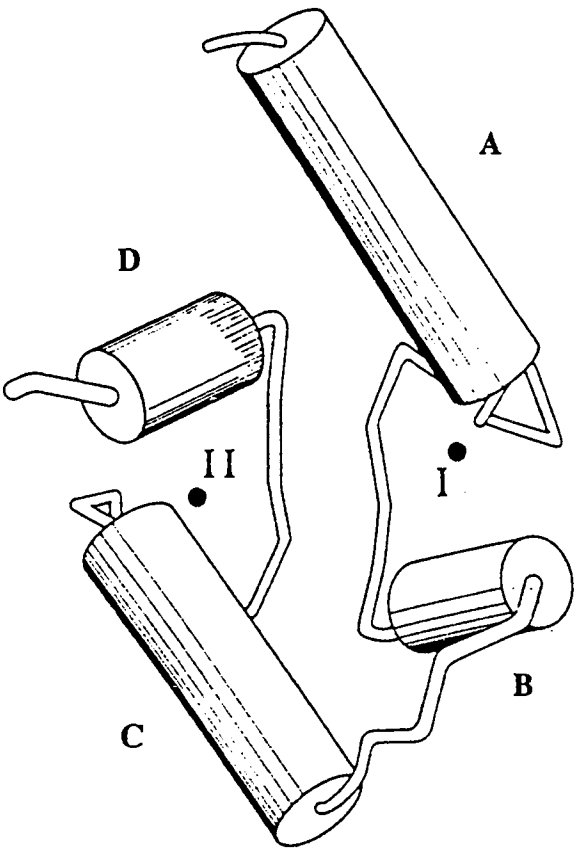

FIGURE 1.3. Helix-Loop-Helix Structural Motif

Schematic representation of the Helix-Loop-Helix motif (adapted from (15)). Helices are labeled A to D. Calcium binding site are labeled I and II.

III-helix F and helix G-site IV-helix H are also joined by a linking peptide. The functional unit exists as a pair of H-L-H motifs rather than an individual binding site (15). This is a structural feature common to a family of highly homologous calcium binding proteins such as Calmodulin, Parvalbumin, and Calbindin (15). Understanding more about the relationships between structure and function in TnC can indirectly contribute to the knowledge of other calcium binding proteins that are structurally related to TnC, as well as contribute to our general understanding of protein structure and function.

A variety of methods have been used to estimate binding constants for the Ca^{2+}-specific sites (low-affinity) and for the Ca^{2+}/Mg^{2+} (high-affinity) sites in TnC. Binding constants for the Ca^{2+}/Mg^{2+} sites have been estimated by equilibrium dialysis (16, 17), titration of covalently bound fluorescent probes (extrinsic probes) (18,19,20), by using Ca^{2+} sensitive electrodes (21) and by titration of the far-UV ellipticity of the protein (22,23). Binding constants for low-affinity Ca^{2+}-specific sites have been more difficult to estimate because suitable intrinsic reporters are unavailable and since calcium binding at low-affinity sites is only responsible for about 30% to 40% of the change in the far U.V. ellipticity associated with Ca^{2+} binding. Unfortunately, the results derived from these experiments are contradictory with respect to whether there is cooperativity in the binding of calcium to the protein which is isolated from the other proteins of the fiber.

Genes encoding chicken (24) and rabbit (25) TnC have been cloned, sequenced and expressed in *Escherichia coli*. This has made it possible for relationships between the structure and activity of TnC to be examined by site-directed mutagenesis of the cloned genes (12, 20, 26). Since chicken TnC lacks tryptophan and tyrosine residues, it is an attractive protein for the site-specific introduction of one of these amino acids as a reporter group in a convenient location of the sequence. The presence of a single chromophore allows one to unambiguously assign changes in the spectral features of the protein, to changes in the environment of that residue. In this study of chicken TnC, site-

directed mutagenesis was used to substitute Phe-29 or Phe-105 by a Trp residue creating the mutant proteins FW29 and FW105, respectively, and also the double mutant FW29/ FW105. In the wild type chicken muscle TnC, Phe-29 is located at the carboxy-terminal end of helix A, adjacent to Ca^{2+} binding site I (residues 30-41) (Figure 1.4). The substitution of Phe-29 by Trp allowed the assignment of spectral features to position 29 in the low-affinity sites. Phe-105 is located at the carboxy-terminal end of helix E, adjacent to Ca^{2+} binding site III (residues 106-117) (Figure 1.4.) and occupies, in the high affinity sites, an equivalent position to that of Phe-29. The substitution of Phe-105 by Trp (mutant FW105) allows Trp-105 to be used as a probe for metal binding events occurring at the C-terminal domain of TnC.

In the first part of the project, the spectral properties of Trp residues introduced by site-directed mutagenesis at position 29 and 105 were used to monitor metal binding in the N and C-terminal domains of chicken TnC. In the second part of the project, calcium binding to the high-affinity sites of TnC was monitored by using Trp at position 105 as an intrinsic reporter. The proteins were analysed by absorption and fluorescence methods.

1.2. Cooperativity in Calcium Binding

Many studies have addressed the question about cooperativity in the binding of calcium by TnC, however, the issue of cooperativity has not been resolved. Cooperativity was found to occur in the binding of Ca^{2+} to the structurally related proteins Calbindin, Parvalbumin and Calmodulin (27, 28, 29). Based on the high homology between these Ca^{2+} binding proteins, cooperativity is also likely to be found in TnC. Studies using circular dichroism (22, 23), ^{1}H-NMR (22, 30), and fluorescence (31), show that, in solution, TnC undergoes Ca^{2+}-induced conformational changes. The X-ray crystal structure (14) shows that two calcium-binding sites are covalently joined by a peptide

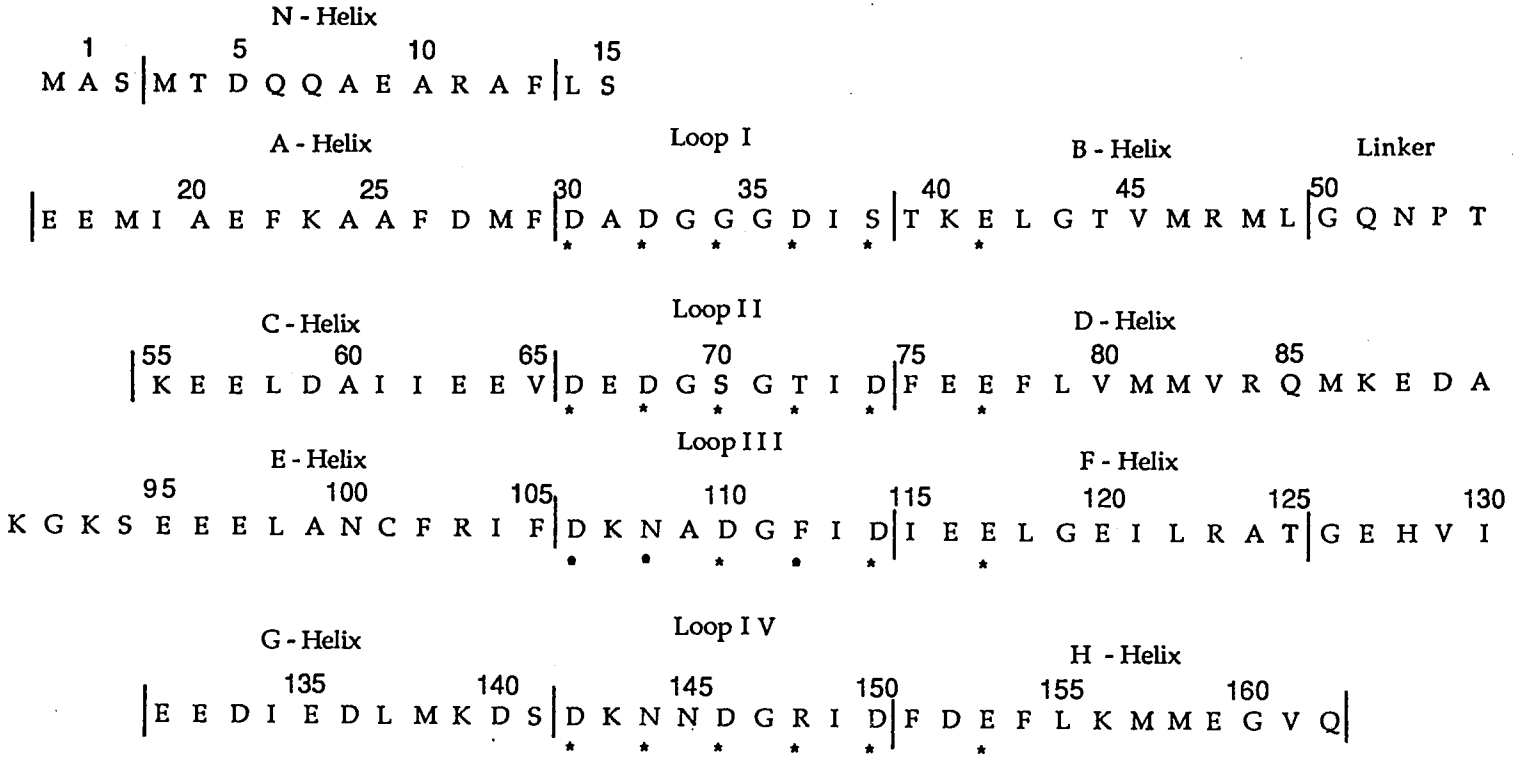

FIGURE 1.4. Amino acid Sequence and Organization of Recombinant TroponinC

The sequence of recombinant chicken troponin-C (24) is presented in one letter code and organized according to the homology between binding sites (adapted from (15)). The recombinant protein, purified from the vector pLcIIFX-TnC, has an additional methionine residue at its amino terminus. The sequence is numbered from the second residue so as to be consistent with the non-recombinant protein. Residues directly or indirectly involved in coordinating metal ions are indicated by asterisk.

segment. It also shows that there is a close packing between adjacent binding sites due to favorable non-covalent interactions between neighboring H-L-H motifs. There are strong hydrophobic interactions, especially between helices A/D and B/D in the N-terminal domain and between helices E/H in the C-terminal domain. There are also hydrophobic interactions between sites I and II and hydrogen bond interactions between sites I and II and between sites III and IV. Therefore, the conformational changes that one site undergoes upon Ca^{2+} binding will have an effect in the adjoining site. It is then reasonable to believe that there is cooperativity in the binding of calcium to TnC.

In whole muscle fibre, measurements of the calcium dependence of tension development (32) and of actomyosin ATPase activity (33), suggested cooperative metal ion binding. Studies which measure calcium-binding by equilibrium dialysis in TnC isolated from the other fiber components(16) and by using a metallochromic indicator (34) suggest that the sites are non-interacting. Cooperativity was not found between sites in Ca^{2+} fluorescence titrations of extrinsic probes attached to TnC (33, 35). However, there are some reports of cooperativity between sites III and IV (19, 36, 37, 38). With respect to sites I and II ,no cooperativity has been demonstrated (18, 20, 38), except for the recent evidence found using a combination of site-directed mutagenesis and equilibrium dialysis methods (17). Cooperativity has not been clearly demonstrated in TnC, possibly because the techniques used so far, measure binding to all four sites simultaneously. In equilibrium dialysis experiments there is the possibility of oxidation of methionine and / or cysteine residues, which may alter the functional and Ca^{2+} binding properties of TnC (26). When extrinsic probes are used, their non-polar nature may favour interactions with hydrophobic regions of the protein and this may be disruptive to TnC. This could be responsible for the apparent loss of interactions between sites.

Tryptophan substitutions by site-directed mutagenesis are an alternative to chemical methods for the introduction of reporter groups in chicken TnC. Tryptophan mutants are a promising model system for the study of the interaction between calcium

and TnC. In the first part of the project described in this thesis, the properties of the mutants FW29, FW105 and of the double mutant FW29/FW105 were studied. The use of the fluorescence of Trp-29 or Trp-105 in the single mutants have the clear advantage over other techniques used in the study of TnC, of measuring binding of Ca^{2+} to the high- and low-affinity sites, independently.

1.3. Stability of Helices and Calcium Binding

Alpha helices are a common element in the secondary structure of proteins. The amino acid residues that form an α-helix have backbone dihedral angles, phi and psi, that are near -60° and -40°, respectively (39). The characteristic hydrogen bonding pattern is one in which the >N-H group of one amino acid is the donor, and the >C=O of the amino acid four residues toward the C-terminal end of the protein is the acceptor. However, the >N-H donors in the first four residues of the helix, and the >C=O acceptors in the last four residues lack intrahelical partners. This leads to the hypothesis that helix formation requires the presence of amino acid residues towards the helix termini, whose side chains can hydrogen bond to the unpaired chain >N-H or >C=O groups (40). That is, at the N-terminal end of the helix there should be an amino acid whose side chain is able to serve as a hydrogen-bond acceptor. At the C-terminal end there should be an amino acid whose side chain can serve as a hydrogen-bond donor. However, when the crystal structure of proteins is examined, this side chain to main chain hydrogen bond at the termini of helices is not always observed. This might indicate that the stabilizing effect of hydrogen bonds at the helix termini could be of great importance in the nascent helix, but that it is not always required for the stability of the mature protein (40, 41).

There is evidence that electrostatic interactions are important in the stabilization of α-helices (42). It is recognized that the helix backbone has a considerable dipole moment. The α-helix macro dipole has its origins in the dipole of the individual peptide

units, whose dipole moment in an α-helix are aligned almost parallel to the helix axis. Thus, the C-terminal constitutes the negative end, and the N-terminal constitutes the positive end, each having a half unit charge (43). One of the effects of the electric field in α-helices may be that negatively charged groups close to the N-terminal or positively charged groups close to the C-terminal end of the helix could interact favorably with the electrostatic field of the helix. The stability of α-helices has been, in many cases, attributed to this type of interaction of charged residues with the helix dipole (44, 45, 46).

A recent survey of protein structures (47) from the Brookhaven protein database revealed preferences for amino acids at specific positions in α-helices. It was shown that there is a preference for negatively charged residues to be located close to the N-terminal end of helices and of positively charged residues at the C-terminal. This can be explained if the dipolar nature of the α-helix is considered. In this structural survey, the N-cap and C-cap were defined as the residues in a helix "whose α carbon lies approximately in the cylinder formed by the helix backbone and along the helical spiral path". The first and last residues in helices can contribute to helix stability in different ways. A preference at the N-cap position for residues whose side chain can hydrogen bond to the main chain was observed, such as threonine, serine, asparagine, aspartic acid. These results support the hydrogen bond hypothesis,that is, that these amino acids are preferred because they can stabilize the helix due to their H-bonding capacities. In the case of aspartic acid, however, its stabilizing effect at the N-cap position can also be explained in terms of the helix dipole. The negatively charged side chain of aspartic acid could interact favourably with the helix dipole at the N-terminal (positive) end of helices.

Synthetic peptides have been used to study the effect of amino acids in the stability of α-helices (45, 46, 48, 49). Experiments show that there is a pH dependence of the helical content, which demonstrates the importance of ionizable groups in the stability of the helices. The results indicate that charged residues stabilize α-helices by

favorable interactions with the helix dipole. Using site-directed mutagenesis, charged amino acid substitutions at helix termini have been shown to stabilize the structure of the enzymes T4 lysozyme (50, 51) and *Bacillus amyloliquefaciens* ribonuclease (a.k.a. Barnase) (52) by their interaction with the helix dipole. In an attempt to verify that there is a preference for certain amino acids at the N-cap position, multiple substitutions were made at the N-cap in two helices in the enzyme Barnase (53). The only substitution that was found to be stabilizing was that of threonine by aspartic acid, with an increase in the stabilizing energy of only 0.1 kcal/mol. The substitution of threonine by asparagine resulted in destabilization, in contrast with what was expected from the structural survey (47). Thus, it appeared that substitutions at N-cap residues must be considered in the context of the surrounding protein, and that amino acid substitutions commonly lead to interactions not found in the native structure.

In a study in chicken TnC (54), it was observed that the native and the recombinant proteins differed in affinity for calcium at high-affinity sites. The high-affinity calcium binding constant of the native protein is four times larger than that of the recombinant TnC, as determined by far-UV circular dichroism (far-UV CD) calcium titrations. The sole difference between the high-affinity sites of the recombinant and native TnC is at position 130. In native TnC, position 130 is occupied by a threonine residue, whereas in the recombinant protein this position is occupied by an isoleucine. X-ray crystallographic studies of chicken TnC revealed that the threonine residue at position 130 is the N-cap residue that initiates helix G (residues 131-141) (Figure 1.5). The side chain oxygen of Thr-130 is at a distance of 21.7 and 21.1 Å from the bound calcium at sites III and IV, respectively. Therefore, Thr-130 is not directly involved in the ligation of metal ions. However, the side chain (Oγ1) of threonine forms a hydrogen bond to the amide group of aspartic acid-133, contributing to the stability of the helical structure of helix G. An isoleucine residue at position 130 would be expected to be destabilizing since it is unable to form hydrogen bonds. Therefore, differences in the

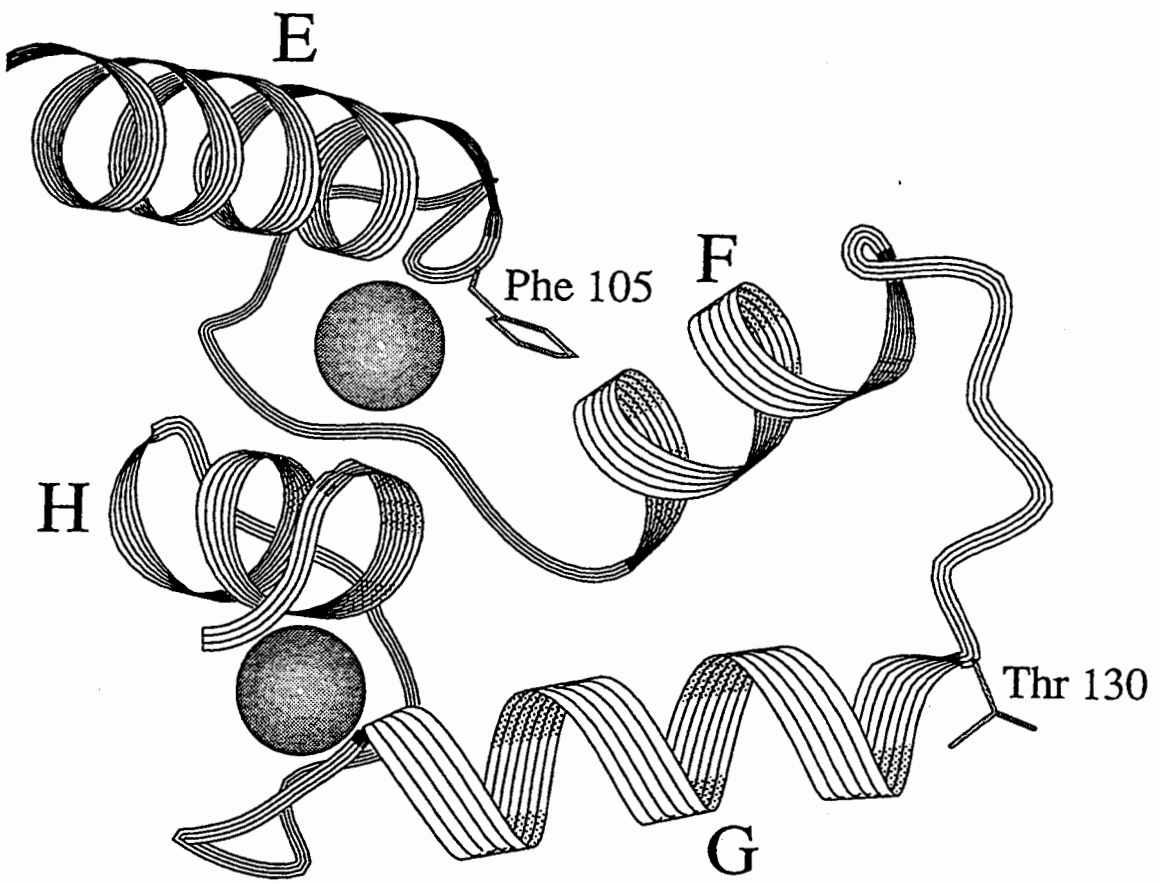

FIGURE 1.5. C-Domain of Troponin-C

The C-domain of troponin-C is represented with calcium ions (spheres) bound to sites III and IV. The positions of Thr-130 and Phe-105 are indicated.

binding constants of the high affinity sites of native and recombinant TnC, seem to reflect the relative abilities of threonine and isoleucine to stabilize helix G.

The study of the effect of different amino acids at the N-cap of helix G can give an insight into the role of the α-helix in metal ion binding. For this project, several site-specific mutations at position 130 were created, in order to probe relationships between the stability of helix G and high-affinity metal ion binding to TnC. The substitutions were made in the recombinant protein FW105, to create the double mutants FW105/IX130. X denotes the amino acid replacing isoleucine at position 130. High-affinity metal ion binding events could be monitored unambiguously by changes in the intrinsic fluorescence of the proteins. The amino acid substitutions at position 130 (Gly, Asp, Thr, Ser, Asn, Ile) were expected to influence the stability of the α-helix in a number of ways. Stabilizing effects were anticipated with amino acid residues whose side chains can hydrogen bond to main chain residues and / or that can interact with the α-helix dipole. The Asp-130 substitution was of interest since this residue has the potential to stabilize helix G by both means. Stabilizing effects were expected to be reflected in a higher affinity constant for these mutant proteins. Gly and Ile, unable to hydrogen bond would confer less stability to helix G and, therefore, these proteins would show lower affinity constants. Thus, the relative importance of the hydrogen bonding abilities and of interactions with the helix dipole in the high affinity sites of TnC could be studied.

1.4. Summary

The study of the function of TnC is important since the binding of calcium to this protein is believed to regulate muscle contraction. In order to better understand the contraction process, it is necessary to know how the different components of the muscle fiber function. It is therefore important to identify what aspects of the structure of TnC are important for metal ion binding, what are the features of the protein that give it

specificity for calcium or magnesium, how is the structure important in the equilibrium between the metal-free and metal-bound states.

It is also interesting that TnC has a structure common to other calcium binding proteins, the helix-loop-helix motif. Understanding aspects of the function and structure of TnC is therefore of relevance in the study of related proteins.

In this study, site-directed mutagenesis was used to introduce a tryptophan residue in chicken TnC. The usefulness of this chromophore as intrinsic reporter to monitor metal binding to TnC was evaluated. Since the studies in isolated TnC are, in some aspects, contradictory, it is important to find a sensitive technique to be able to confidently address structure/function questions in TnC. Site-directed mutagenesis was also used to prove relationships between the stability of helix G and metal ion binding. This study can give an insight on how the protein structure affects ion affinity. The results will be discussed in terms of an equilibrium between folded and unfolded TnC.

2. MATERIALS AND METHODS

2.1. Buffers And Other Solutions

Buffer A: 50 mM Tris-HCl pH 8.0, 1 mM EGTA, 25% sucrose, 0.5 mM PMSF.

Buffer B: Tris pH 8.0, 8 M Urea, 2 mM $MgCl_2$, 1 mM DTT, 85 mM KCl.

Buffer C: 50 mM Tris-HCl pH 8.0, 2 mM DTT, 1 mM $CaCl_2$, 0.1 mM PMSF.

Buffer D: Buffer C + 1 M NaCl.

Buffer E: 50 mM Tris-HCl pH 8.0, 0.1 M NaCl, 2 mM $CaCl_2$.

Buffer F: 50 mM MOPS pH 6.95, 150 mM KCl, 1 mM EGTA and 1 mM DTT.

10xPE 1 Buffer: 200 mM Tris-HCl pH 7.5, 100 mM $MgCl_2$, 500 mM NaCl, 10 mM DTT

10xPE 2 Buffer: 200 mM Tris-HCl pH 7.5, 100 mM $MgCl_2$, 100 mM DTT.

5 x Ligation Buffer: 0.25 M Tris-HCl pH 7.6, 50 mM $MgCl_2$, 5 mM ATP, 5 mM DTT, 25%(w/v) polyethyleneglycol-8000.

10 x Polynucleotide Kinase Buffer: 0.5 M Tris HCl pH 7.6, 0.1 M $MgCl_2$, 50 mM DTT, 1 mM spermidine HCl, 1 mM EDTA pH 8.0.

10 x CIP Dephosphorylation Buffer: 10 mM $ZnCl_2$, 10 mM $MgCl_2$, 100 mM Tris Cl pH 8.3

10 x T4 DNA Ligase Buffer: 200 mM Tris Cl pH 7.6, 50 mM $MgCl_2$, 50 mM DTT, 500 μg/mL bovine serum albumin.

TE pH 8.0: 10 mM Tris-HCl pH 8.0, 1 mM EDTA pH 8.0.

1 x TAE: 0.04 M Tris-acetate, 1 mM EDTA.

React 1 Buffer: 50 mM Tris-HCl, 10 mM $MgCl_2$.

React 2 Buffer: 50 mM Tris-HCl, 10 mM $MgCl_2$, 50 mM NaCl.

React 3 Buffer: 50 mM Tris-HCl, 10mM $MgCl_2$,100 mM NaCl.

5 x Sequencing Buffer: 200 mM Tris-HCl pH 7.5, 100 mM $MgCl_2$, 250 mM NaCl.

TfBI Buffer: 30 mM CH_3COOK, 50 mM $MnCl_2$, 100 mM KCl, 10 mM $CaCl_2$, 15 % glycerol. pH should be close to 7.0. Filter sterilize.

TfBII Buffer: 10 mM Na-MOPS pH 7.0, 75 mM $CaCl_2$, 10 mM KCl, 15% glycerol. Filter sterilize.

2.2 Bacteriological

2.2.1. Media

TY/Mg broth: 2% tryptone, 0.5% yeast extract, 0.5% NaCl, 10 mM $MgSO_4$. The $MgSO_4$ is added from a 1 M filter sterilized stock.

2 x TY broth: 1.6% tryptone, 1.0% yeast extract, 0.5% NaCl.

TY plate: 1.0% tryptone, 0.5% yeast extract, 1% NaCl, 2% agar.

2 x TY-Amp: 2 x TY broth with 100 µg/mL of ampicillin (Sigma).

TY-Amp plate: TY plate with 200 µg/mL of ampicillin.

2 x TY-Tet: 2 x TY broth with 50 µg/mL of tetracycline (Sigma)

TY-Tet plate: TY plate with 50 µg/mL of tetracycline.

H-top agar: 1.0% tryptone, 0.8% NaCl, 0.8% agar.

2.2.2 Bacterial Strains

***Escherichia coli* strain QY13** :Genotype (F- lac_{am} trp_{am} *B B'bio-256* N^+ *cI857* ΔH Sm^r*recA*).(55)

Growth conditions: On TY-Amp plates, incubation at 30°C. On 2xTY-Amp, incubation at 30°C or 37°C. This *E. coli* cell strain was used in the expression of Troponin C from the plasmid pLcIIFX-TnC. QY13 cells were transformed with expression vector and grown at 30°C. At this temperature, the cI857 temperature-sensitive repressor is active. The transcription from the P_L promoter is then repressed. The repressor is inactivated at

42°C and the cIIFX-TnC gene is then efficiently transcribed. Cells continue to grow at 37°C after induction.

***Escherichia coli* strain TG2** Genotype F'(*traD*36 *proAB*$^+$ *lacI*^{q} *lacZ* ΔM15) Δ(*lac-proAB*) *supE hsd*Δ*5 thi* Δ(*srl-recA*)306::Tn*10*(*tet*^{r}) (56).

Growth conditions: On TY-Tet plates. On 2xTY, or 2xTY-Tet. Incubation at 37°C.

***Escherichia coli* strain DH5α** Genotype *supE*44 Δ*lac*U169(Ø80 *lacZ*ΔM15) *hsd*R17 *recA*1 *endA*1 *gyrA*96 *thi*-1 *relA*1 (56).

Growth conditions: On TY plates. On 2xTY broth. Incubation at 37°C.

***Escherichia coli* strain K12cI:** This cell strain constitutively expresses cI repressor.

Growth conditions: On TY plate. On 2xTY broth. Incubation at 37°C.

***Escherichia coli* strain RZ 1032:** Dut-, Ung- cell line. A dut- strain does not synthesize the enzyme dUTPase (dUTP nucleotidohydrolase) that hydrolyzes dUTP into dUMP and PPi. An ung- strain lacks the enzyme uracil N-glycosylase that hydrolyzes uracil from single stranded and double stranded DNA.

Growth conditions: On TY-Tet plates. On 2xTY or 2xTY-Tet broth. Incubation at 37°C.

2.2.3. Preparation of Competent *E.coli* Cells

One mL of TY/Mg broth was inoculated with a fresh *E. coli* colony and incubated to a cell density = 0.5 (OD_{600} = 0.5) at the appropriate temperature (30°C or 37°C). This culture was then used to inoculate 20 mL of TY/Mg (pre warmed at 30°C or 37°C) in a 250 mL flask and incubated to OD_{600} = 0.5. Two hundred mL of TY/Mg (pre warmed at 30°C or 37°C) in a 1 L flask were inoculated with the 20 mL culture and incubated to an OD_{600} = 0.6. The cell culture was chilled on ice and then centrifuged at 3500 rpm for 15 min at 2°C. The cell pellet was resuspended in 40 mL of cold TfBI buffer and centrifuged as before. The cell pellet was then resuspended in 8 mL of cold TfBII buffer, aliquoted and frozen in tubes in a bath which was a mixture of dry ice and ethanol, then stored at

-70°C.

2.2.4. Transformation of *E.coli* Strains

2.2.4.1. Transformation of *E.coli* strain TG2 by Phage M13:

Recombinant M13 (section 2.3.1) DNA was added to 200 µL of competent TG-2 cells. The mixture was incubated on ice for 30 min then heat shocked for 2.5 min at 37°C. Heat shocked cells (150 µL) were mixed with 200 µL of an overnight TG-2 culture and 3 mL of H-top agar and poured onto a TY plate. Plaques containing M13 were visible on the lawn of TG2 growth after 6 hrs of incubation at 37°C.

2.2.4.2. Transformation of *E.coli* strain K12

Typically, 1 µL of pLcIIFX-TnC was added to 150 µL of competent *E.coli* strain K12cI. The culture was incubated on ice for 30 min and then heat shocked for 2.5 min at 37°C. After adding nine volumes of 2 x TY, the mixture was incubated for 2 hrs at 37°C. Then 0.2 mL was spread-plated onto a TY-Amp plate and incubated overnight at 37°C.

The same procedure was used to transform K12cI with 20 µL of diluted ligation mixture (section 2.5.4.). In this case, 1 and 0.2 mL of transformed cells were spread-plated onto TY-Amp plates.

2.2.4.3. Transformation of *E.coli* strain QY13 with Expression Vectors

The pLcIIFX-TnC expression vector that carried a mutated gene was added to 50 µL of competent *E.coli* QY13. The culture was incubated on ice for 30 min and then heat shocked for 2.5 min at 30°C. Nine volumes of 2xTY were added and the suspension incubated at 30°C for 2 hrs. Usually 0.2 mL of cells were spread-plated on TY-Amp and

incubated at 30°C for 36 hrs, until colonies were visible. Protein expression tests (section 2.6.1.) were done in fresh QY13 colonies only. QY13 should not be stored on plates in the refrigerator.

2.3. Plasmids and Bacteriophages

2.3.1. M13mp19 (M13) Bacteriophage:

F-specific rod-shaped filamentous phage of the mp series (57). A restriction map is shown in Figure 2.1 that contains the TnC gene:

2.3.2. pLcIIFX-TnC:

Expression vector which directs the synthesis of a fusion protein consisting of the 31 amino terminal residues of the lambda cII protein, the tetrapeptide Ile-Glu-Gly-Arg, and the complete Troponin C sequence (58). See Figure 2.2.

2.3.3. Determination of the Multiplicity of Viral Infection

The multiplicity of viral infection is expressed in plaque forming units (pfu) per bacterial cell (pfu/cell). To determine this, the number of pfu/mL of M13 bacteriophage suspension (section 2.3.1.1.), and the number of bacteria/mL in the inoculum of *E.coli* strain RZ1032 was determined as follows:

Dilutions of the bacteriophage suspension were prepared (10^{-4}, 10^{-6}, 10^{-7}). Ten µL of each dilution was mixed with 100 µL of a log phase *E.coli* TG2 culture and 3 mL of H-top agar and plated on TY plates. Plaques containing bacteriophage were counted after the plates were incubated overnight at 37°C, and the number of plaque forming units per volume (pfu/mL) of phage suspension was calculated.

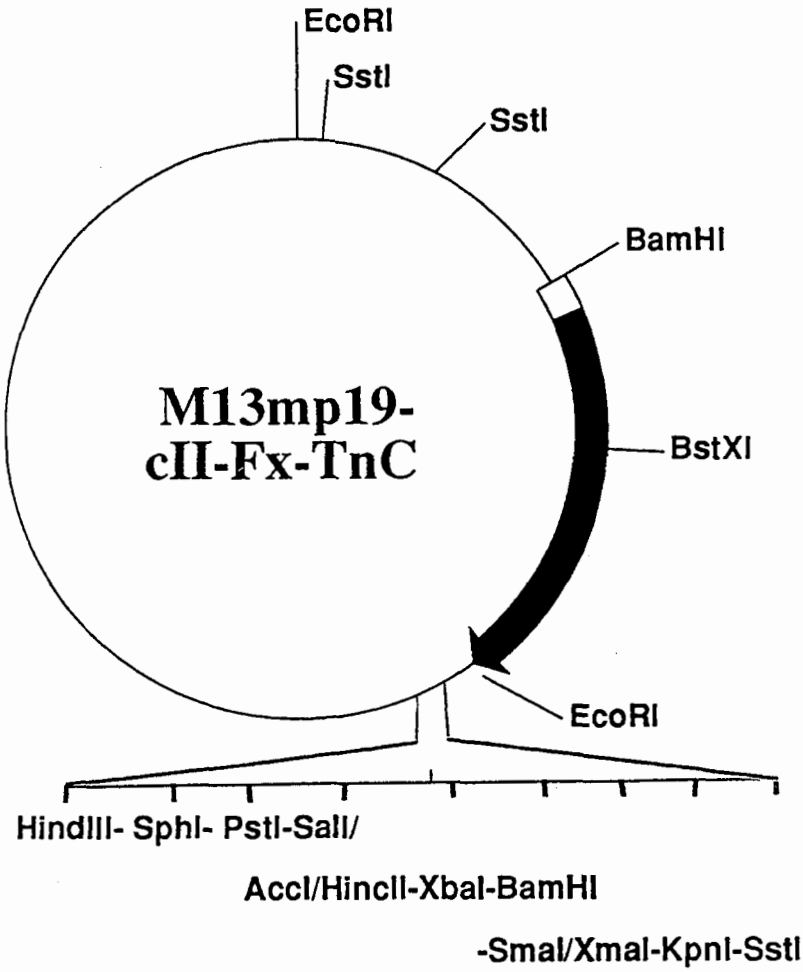

FIGURE 2.1. Bacteriophage M13mp19-cIIFX-TnC

Schematic representation of bacteriophage M13mp19 containing the coding region of the cIIFX-TnC fusion protein. The coding region for troponin C is indicated by a black arrow. Restriction sites are indicated, as well as the polylinker region.

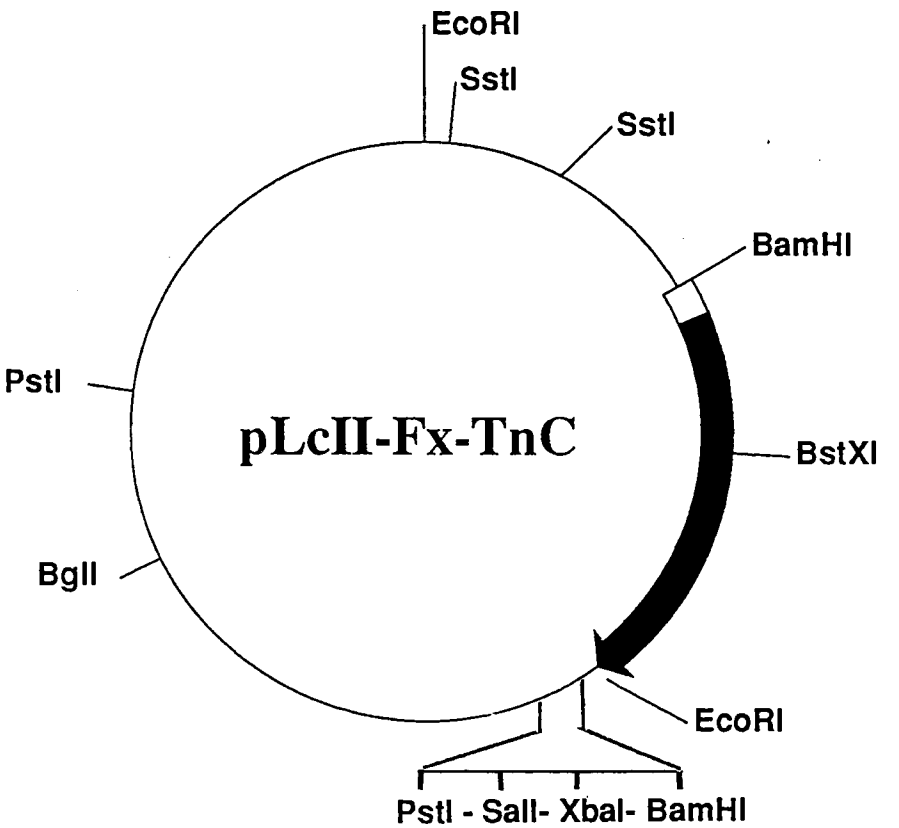

FIGURE 2.2. Plasmid pLcIIFX-TnC

Schematic representation of the expression vector pLcIIFX-TnC. The coding region for troponin C is indicated by a black arrow. Restriction sites are indicated, as well as the polylinker region.

Dilutions of the bacterial suspension were prepared (10^{-2}, 10^{-4}, 10^{-5}, 10^{-6}). One hundred µL of each dilution was spread plated onto TY-Tet plates. The number of colonies in each plate was counted after incubation overnight at 37°C, and the number of bacteria / mL of inoculum calculated.

2.3.4. Preparation of Single Stranded M13 (ssM13) DNA For Sequencing

Two mL aliquots of 2xTY were inoculated with single plaques produced by M13 (section 2.2.4.1.) and 20 µL of an overnight TG-2 culture (typically 24 to 48 clones were screened for mutations by DNA sequencing). After incubation for 5 hrs at 37°C, the cultures were centrifuged to pellet the cells. About 1.2 mL of the culture supernatant was added to 200 µL of a solution of 20% polyethyleneglycol and 3.5 M ammonium acetate. After 15 min, the precipitated bacteriophage particles were recovered by centrifugation at 12,000 rpm for 5 min. The pellets were resuspended in 100 µL of TE buffer pH 8.0. Fifty µL of phenol was added, mixed, and the aqueous phase was withdrawn after the phases were separated by centrifugation. Then 100 µL of chloroform was combined with the aqueous phase, mixed and the aqueous phase separated as before. DNA was precipitated by combining the aqueous layer with 10 µL of 3 M sodium acetate (pH 5.5) and 250 µL of 95% ethanol, and incubating for 15 min. The suspension was centrifuged at 12,000 rpm for 10 min. The pellet was washed with 200 µL of 70% ethanol, dried under vacuum and finally resuspended in 40 µL of ddH_2O.

2.3.5. Large Scale Preparation of Replicative Form M13 (RF M13) and Plasmid pLcIIFX-TnC

Five mL of 2xTY were inoculated with 25 µL of an overnight culture of TG-2 and a single plaque of M13 picked from a lawn of transformed TG-2 (section 2.2.4.1.).

The cultures were incubated for 4 hrs at 37°C and centrifuged for 10 min at 12,000 rpm. to pellet cells. Supernatants were kept at 4°C as M13 bacteriophage stocks.

Two hundred mL of 2 x TY medium was inoculated with 2 mL of a mid-log phase TG-2 culture and incubated for 2 hrs at 37°C. A 1 mL aliquot of M13 stock solution (section 2.3.1.) was added and the culture grown overnight at 37°C with shaking. The culture was then centrifuged at 8,000 rpm for 10 min at 4°C. The cell pellet was resuspended in 10 mL of Solution I (50 mM glucose, 10 mM EDTA, 25 mM Tris-HCl pH 8.0, and 4 mg/mL of lysozyme), and incubated for 10 min. Then, 20 mL of freshly prepared solution II (0.2 N NaOH, 1% SDS) was added and the mixture was allowed to stand at room temperature until it became clear. A 15 mL aliquot of Solution III (5 M potassium acetate,60 mL; 11.5 mL acetic acid; 20 mL H_2O) was added and it was incubated for 5 min. The solution was centrifuged for 10 min at 8,000 rpm. The supernatant was removed and extracted with 25 mL of phenol and 15 mL of chloroform, then with 25 mL of chloroform. Two volumes of ethanol were added and the solution incubated for 10 min to precipitate DNA. The precipitated DNA was recovered by centrifuging at 9,000 rpm for 15 min. The pellet was dried under vacuum and then resuspended in 500 µL of H_2O. To the DNA solution, RNase A (0.5mg/mL) and RNase T1 (0.5 mg/mL) were added and it was incubated for 2 hrs at 37°C. An extraction with one equal volume of phenol/chloroform (60:40) and then with one volume of chloroform was performed. DNA was precipitated by combining the DNA solution with 125 µL of 10.0 M ammonium acetate and 1 mL of 95% ethanol and incubating for 30 min. The suspension was centrifuged for 15 min at 12,000 rpm. The resulting pellet was resuspended in 200 µL of TE pH 8.0, and precipitated again by incubation for 30 min with 20 µL of 3.0 M sodium acetate (pH 7.5) and 450 µL of 95% ethanol. The suspension was again centrifuged. The DNA pellet was dried under vacuum and finally resuspended in 200 µL of sterile ddH_2O.

The large scale preparation of pLcIIFX-TnC was essentially the same as that described for M13 except that 1 mL of 2 x TY-Amp was inoculated with a single pLcIIFX-TnC infected K12 colony (section 2.2.4.2.), and incubated for 6 hrs at 37°C. The resulting culture was inoculated into 200 mL of 2 x TY-Amp and grown overnight with shaking at 37°C. Cells were harvested by centrifugation at 8,000 rpm for 10 min at 4°C. DNA was extracted and purified from cell pellets as described above for RF M13 DNA.

2.4. Site-directed Mutagenesis of Troponin C DNA

The coding region of chicken TnC had been cloned into the Eco RI site of bacteriophage M13mp19 (Figure 2.1). A modified recombinant M13 DNA bearing the substitutions phenylalanine-29 to tryptophan-29 and phenylalanine-105 to tryptophan-105 (FW29/FW105) was obtained from K. Racher and T. Borgford (SFU). Recombinant M13 DNA FW29/FW105 and FW29/FW105/IN130 (the third substitution of isoleucine-130 by asparagine-130 was available after the first set of mutations using FW29/FW105 as template) were used as templates for the mutagenesis reactions in order to create the FW105/IX130 mutant proteins.

Mutagenesis of the Troponin C DNA was performed by the Kunkel method (56). In the Kunkel method, a phage DNA template is used that contains uracils instead of thymine (U-DNA). U-DNA is obtained from M13 bacteriophage that has been grown on a *E. coli* dut^-, ung^- strain like RZ1032. In the mutagenesis reaction, the mutagenic oligonucleotide is annealed to the U-DNA template. During the *in vitro* synthesis of the complementary strand, only thymine is incorporated. When this double stranded DNA is used to transform a *E. coli* ung^+ strain like DH5α, the wild type template strand (that contains uracil) is degraded. Therefore, the majority of the progeny phage produced should contain DNA with the desired mutation.

2.4.1. Preparation of U-DNA

Uracil containing ssDNA (U-DNA) was prepared from *E.coli* strain RZ1032 infected with the recombinant M13 bacteriophage stocks FW29/FW105 or FW29/ FW105/IN130 (section 2.3.1). To prepare a stock of M13 bacteriophage, 2 mL of 2xTY were inoculated with a single plaque of bacteriophage M13 (section 2.2.4.1) and 0.2 mL of an overnight culture of *E. coli* TG2. The culture was incubated at 37°C for 2 hrs, and then at 60°C for 5 min. The supernatant, which contained the bacteriophage, was recovered by centrifugation at 12,000 rpm for 10 min at 4°C, and stored at 4°C.

Three 50 mL aliquots of 2xTY containing 0.25 μg/mL of uridine, in 500 mL flasks, were inoculated with 1 mL from a 5 mL overnight RZ1032 culture and 50 μL of the bacteriophage M13 stock solution. The mixture was incubated at 37°C with shaking (300 rpm) for 6 hrs. The multiplicity of infection was 0.02-0.2 pfu/cell (section 2.3.3.). The cultures were then centrifuged at 8,000 rpm for 30 min in a GSA centrifuge rotor at 4°C. The supernatant was collected and U-DNA was purified essentially as described previously (56). The concentration of U-DNA was determined spectrophotometrically (56).

2.4.2. Mutagenic Oligonucleotides

Oligonucleotides were purchased from the Regional DNA Synthesis Laboratory at the University of Calgary (Dr. R. Pons), from (Oligonucleotide Synthesis Laboratory at the University of British Columbia) (Dr. T. Atkinson), and at the I.M.B.B synthesis facilities (SFU). Table 2.1. shows the sequence of the oligonucleotides used and Table 2.2. indicates their mutagenic capabilities.

TABLE 2.1. Oligonucleotide Sequences

Mutagenic Oligonucleotides

Oligonucleotide IT130:
5'- G C A C G T C A C C G A G G A G G A C -3'

Oligonucleotide IX130-1:
5'- G C A C G T C A A C G A G G A G G A C -3'
G G
C

Oligonucleotide IX130-2:
5'- G C A C G T C G G C G A G G A G G A C -3'
T C
T

Oligonucleotide IX130-3:
5'- G C A C G T C G A T G A G G A G G A C -3'
C C A

Underlined in each oligonucleotide is the sequence heterogeneity at the position complementary to codon 130. The mutagenic capabilities are presented in Table 2.2.

Sequencing Primers

FW105 primer:
5'- C C G C A T C T G G G A C A A G A -3'

FW29 primer:
5'- T T G A C A T G T G G G A T G C G G A C G -3'

SEQ 1 primer:
5'- T C G A G A G T G C G T T G C T T -3'

2.4.3. Kinasing of Primers

The 5'-end of the oligonucleotide sequencing primer Seq 1 and the 5'-end of mutagenic oligonucleotides (Table 2.1) were phosphorylated enzymatically (56). The reaction mixtures (20 μL) contained oligonucleotide (0.2 nmoles), 10 mM rATP and 10 x polynucleotide kinase buffer (2 μL). T4 DNA Kinase (10 Units) was added and the solution was incubated at 37°C for 1 hr. The kinase was then inactivated by heating at 68°C for 10 min.

TABLE 2.2. Mutagenic Capabilities of Oligonucleotides

IX130-1		IX130-2		IX130-3	
codon	amino acid	codon	amino acid	codon	amino acid
G G C	Gly	G G C	Gly	G A T	Asp
G A C	Asp	G C C	Ala	G A A	Glu
A G C	Ser	G T C	Val	G C T	Ala
A A C	Asn	T G C	Cys	G C A	Ala
C G C	Arg	T C C	Ser	C A T	His
C G C	Arg	T C C	Ser	C A T	His
				C C T	Pro
				C C A	Pro

2.4.4. Site-specific Mutagenesis

Site-specific mutagenesis was performed by the oligonucleotide-directed method (59) using double primers (60). The primers were the mutagenic oligonucleotide and Seq 1 (Table 2.1). Seq 1 is complementary to the cII gene in the recombinant M13 DNA (see the DNA sequence of cIIFX-TnC in Figure 2.3).

FIGURE 2.3. DNA and Amino Acid Sequences of cIIFX-TnC

Nucleotides are indicated by the name of the corresponding base. Amino acids are indicated underneath the DNA sequence by the one letter code. The beginning and end of the cII, FX_a and TnC DNA sequences are indicated above the sequence.

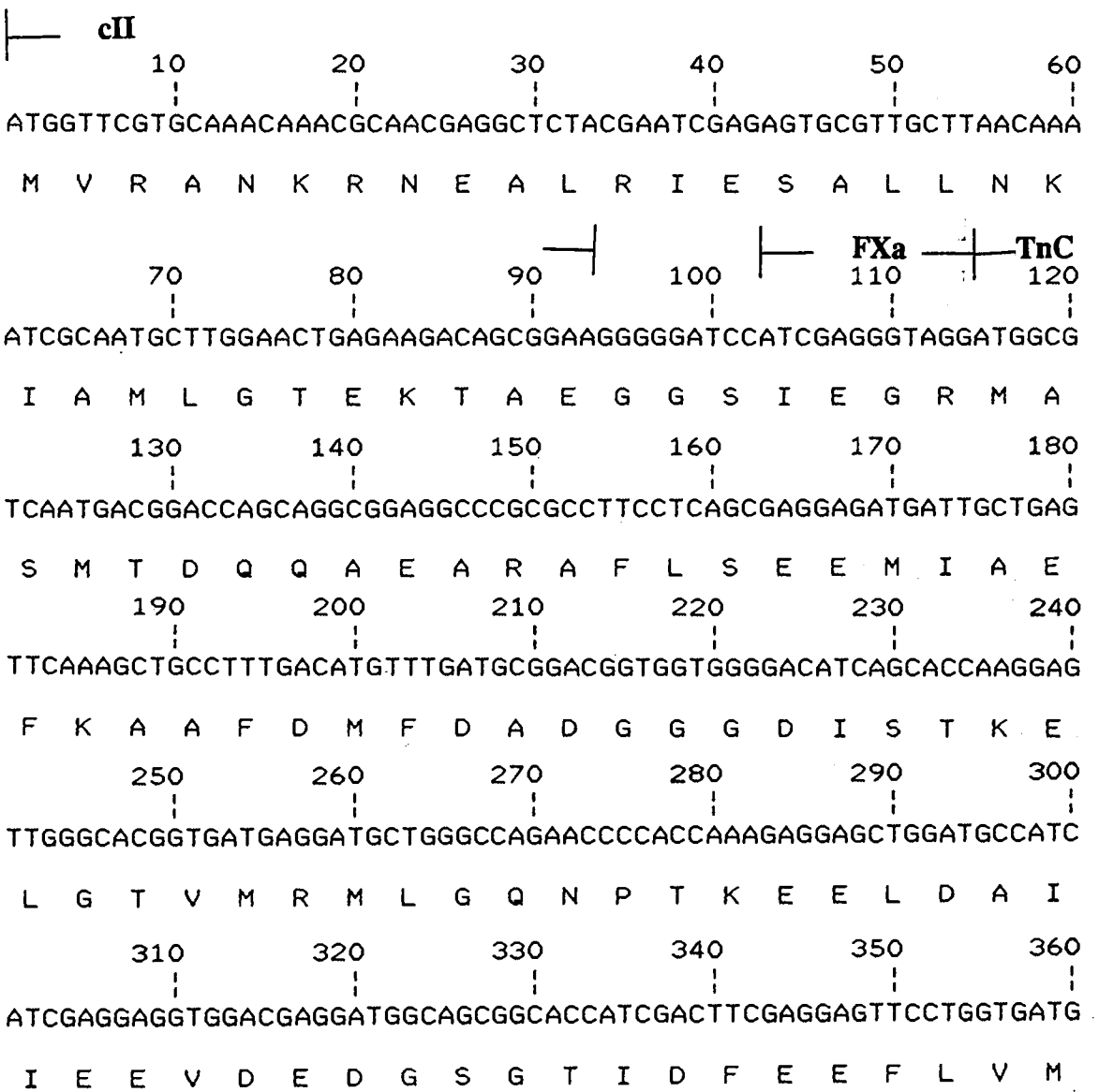

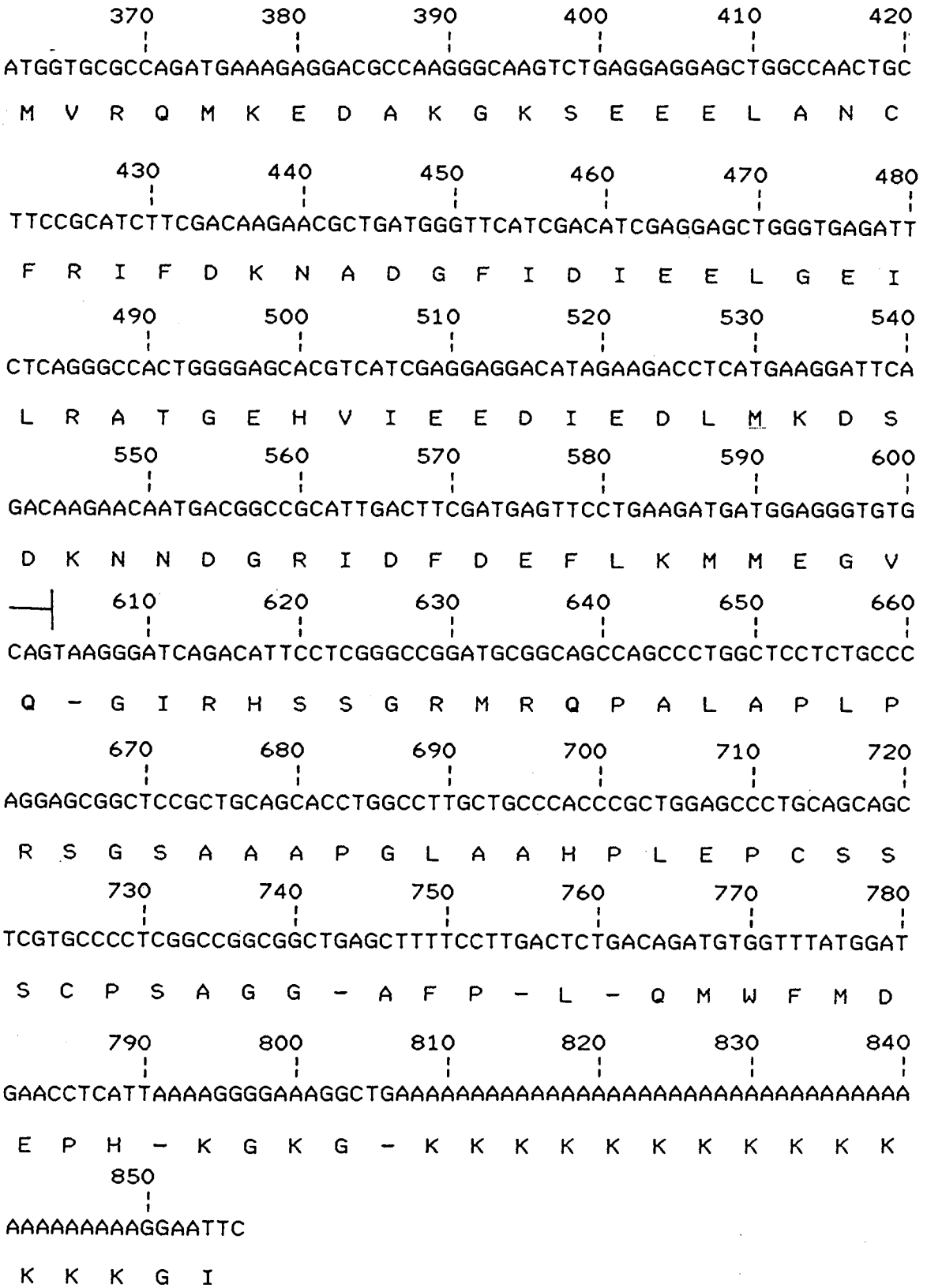
370 380 390 400 410 420
ATGGTGCGCCAGATGAAAGAGGACGCCAAGGGCAAGTCTGAGGAGGAGCTGGCCAACTGC
M V R Q M K E D A K G K S E E E L A N C
430 440 450 460 470 480
TTCCGCATCTTCGACAAGAACGCTGATGGGTTCATCGACATCGAGGAGCTGGGTGAGATT
F R I F D K N A D G F I D I E E L G E I
490 500 510 520 530 540
CTCAGGGCCACTGGGGAGCACGTCATCGAGGAGGACATAGAAGACCTCATGAAGGATTCA
L R A T G E H V I E E D I E D L M K D S
550 560 570 580 590 600
GACAAGAACAATGACGGCCGCATTGACTTCGATGAGTTCCTGAAGATGATGGAGGGTGTG
D K N N D G R I D F D E F L K M M E G V
610 620 630 640 650 660
CAGTAAGGGATCAGACATTCCTCGGGCCGGATGCGGCAGCCAGCCCTGGCTCCTCTGCCC
Q - G I R H S S G R M R Q P A L A P L P
670 680 690 700 710 720
AGGAGCGGCTCCGCTGCAGCACCTGGCCTTGCTGCCCACCCGCTGGAGCCCTGCAGCAGC
R S G S A A A P G L A A H P L E P C S S
730 740 750 760 770 780
TCGTGCCCCTCGGCCGGCGGCTGAGCTTTTCCTTGACTCTGACAGATGTGGTTTATGGAT
S C P S A G G - A F P - L - Q M W F M D
790 800 810 820 830 840
GAACCTCATTAAAAGGGGAAAGGCTGAAAAAAAAAAAAAAAAAAAAAAAAAAAAAAAAA
E P H - K G K G - K K K K K K K K K K K
850
AAAAAAAAAGGAATTC
K K K G I

The annealing reaction (10 μL) contained U-DNA (0.5 pmoles), phosphorylated mutagenic oligonucleotide (10 pmoles), phosphorylated Seq 1 (10 pmoles) and 10 x PE 1 buffer (1 μL). Annealing reaction mixtures were incubated for 10 min at 80°C or at 67°C. The mixtures were allowed to cool slowly to room temperature.

Ten μL of a solution that contained dNTP (1 mM), rATP (1 mM) and 10 x PE 2 Buffer (1 μL) was added to the 10 μL of annealing mixture described above. T4 DNA ligase (1 Unit) was added, then T4 DNA polymerase (3 Units). This extension ligation mixture was incubated for 5 min on ice, then for 5 min at room temperature and finally for 2 hrs at 37°C. *E. coli* strain DH5α was transformed with the extension/ligation mixture.

2.4.5. Transformation of *E.Coli* strain DH5α

The entire extension / ligation mixture from a mutagenesis reaction was added to 50 μL of competent DH5α and incubated on ice for 30 min. The cells were heat shocked at 37°C for 2.5 min and then combined with 0.2 mL aliquots of an overnight TG-2 culture and 3 mL of H-top agar. The entire mixture was poured onto a TY plate. Plaques of M13 carrying putative gene mutants were visible after overnight incubation at 37°C. Single stranded M13 DNA (ssM13) was obtained from M13 plaques (section 2.3.4) and screened for mutations by DNA sequencing (section 2.4.6).

2.4.6. Sequencing of ssM13

Single stranded M13 DNA (section 2.3.4) was sequenced by the Chain Termination Method (61), using the enzyme Sequenase (Version 2.0) and protocols provided by the United States Biochemical Corporation). Once a mutation at position

130 was identified (FW29/FW105/IX130 mutants), replicative form M13 was prepared (section 2.3.5).

2.5. Cloning into pLcIIFX-TnC Expression Vector

Wild type troponin C DNA had been cloned into the expression vector pLcIIFX (24) yielding the expression vector pLcIIFX-TnC. In the cloning procedure, fragments of DNA bearing the mutations FW105/IX130 were isolated from enzyme digests of replicative form M13. The fragments were then ligated to the pLcIIFX-TnC, which had been previously treated with the same restriction enzymes, creating pLcIIFX-TnC_{mut}.

2.5.1. Restriction Digestion of M13 and pLcIIFX-TnC

The DNA fragments bearing the substitution FW105/IX130 were obtained from replicative form M13 by digestion with the restriction endonucleases Sal I (Pharmacia) and BstX I (BRL) or with Cla 1, Sal I and BstX I (see restriction sites in Figure 2.1). pLcIIFX-TnC was similarly digested with Sal I and BstX I (see restriction sites in Figure 2.2). Typically, 10 µL of RF M13 DNA or of plasmid DNA (section 2.3.5) was digested in a total volume of 100 µL, with 30 units of Sal I in React 3 Buffer (10 µL) and 1 mM DTT. The reaction was incubated at 37°C for 2 hrs. Then, 30 units of BstXI was added and the mixture incubated at 55°C for further 2 hrs.

An alternative procedure was used in the restriction digestion of M13 bearing Thr-130 and Asp-130. M13 DNA was incubated with 30 units of Cla 1 in React 1 Buffer (10 µL) for 3 hrs. An extraction was performed with one volume of phenol and chloroform (60:40) and then with one volume of chloroform. The DNA was precipitated by incubation for 30 min with 3 M sodium acetate pH 5.6 (1/10 volumes) and 2 volumes of 95% ethanol. The pellet was resuspended in ddH_2O (90 µL) and incubated with 30

units of Sal I in React 3 Buffer (10 µL) for 1.5 hrs at 37°C. Another 30 units of enzyme was added and the reaction was incubated for further 1.5 hrs. Then, 1 mM DTT and 30 units of BstXI were added and incubated for 1.5 hrs at 55°C. A second addition of BstXI was done, and the reaction was incubated for another 1.5 hrs. The DNA was purified by extractions with one volume of phenol and chloroform (60:40), then with one volume of chloroform. The DNA was ethanol precipitated as described above, dried under vacuum and finally resuspended in 10 - 20 µL of sterile ddH_2O.

The digested pLcIIFX-TnC and M13 fragments were purified as described in section 2.5.3. Plasmid DNA (pLcIIFX-TnC) was dephosphorylated (Section 2.5.2) prior to purification.

2.5.2. Dephosphorylation of pLcIIFX-TnC Fragment

The dephosphorylation reaction (60 µL) contained pLcIIFX-TnC_{mut} digestion fragments (section 2.5.1), 2 units of Calf Intestine Phosphatase (Boehringer Mannheim) and 6 µL of 10 x CIP dephosphorylation buffer. The reaction was incubated at 50°C for 1 hr and then at 65°C for 15 min. The DNA was purified by extracting with one volume of phenol and chloroform (60:40), then with one volume of chloroform. Then 1/10 volume of sodium acetate (pH 5.6), and 2 volumes of 95% ethanol was added, and the solution incubated for 30 min. The precipitated DNA was recovered by centrifugation, air dried and resuspended in 20 µL of sterile ddH_2O.

2.5.3. Purification of pLcIIFX-TnC and M13 Fragments

The DNA was loaded onto a 0.8% agarose gel containing 0.001 mg/mL ethidium bromide. Electrophoresis was performed at 70 V for 1.5 hrs, using lambda DNA digested with Cla I as a size marker. A band corresponding to a DNA fragment of the correct size

was cut from the gel with a scalpel and placed in dialysis tubing with 200-300 µL of TE buffer pH 8.0. The tubing was immersed in 1/2 TAE buffer in a gel electrophoresis apparatus and the DNA was electroeluted at 200 V for 15 min. The polarity was reversed for 15 sec to release DNA from the walls of the dialysis bag. The solution was then transferred to a microfuge tube and the DNA was precipitated by combining it with 1/10 volume 0.3 M sodium acetate, 2 volumes of 95% ethanol and 1 µL of PAP. The pelleted DNA fragment was recovered after centrifuging for 20 min at 12,000 rpm, and was then resuspended in 5-10 µL of sterile dd H_2O.

2.5.4. Ligation of pLcIIFX-TnC and M13 Fragments

The pLcIIFX-TnC and M13 fragments were ligated to create the mutant pLcIIFX-TnC_{mut}. The concentration of vector and insert was estimated by visualization on a 1% agarose gel containing 0.001 mg/mL ethidium bromide. The ligation reaction (in 7 µL) contained an approximately 1:1 molar ratio of vector to insert and 1 unit of T4 DNA ligase in 5 x ligation buffer. After incubating for 3 hrs, the solution was diluted with 20 µL of ddH_2O.

E.coli strain K12cI was transformed with 20 µL of diluted ligation mixture (section 2.2.4.2.). Plasmid pLcIIFX-TnC_{mut} was obtained from infected K12cI and screened for mutant genes by sequencing.

2.5.5. Sequencing of pLcIIFX-TnC_{mut}

Three mL aliquots of 2xTY-Amp were inoculated with single colonies of *E.coli* strain K12cI infected with ligation mixture and incubated at 37°C for 8 hrs. Cells were recovered by centrifugation at 13,000 rpm for 5 min. Plasmid DNA was prepared and purified as in section 2.3.5.

One μg of DNA was added to 200 mM NaOH/0.2 mM EDTA (17 μL total volume) and left at room temperature for 3 min. Then 3 μL of 3 M sodium acetate pH 4.8 and 50 μL of 95% ethanol were added and the mixture was incubated at room temperature for 5 min. The DNA was recovered by centrifugation at 12,000 rpm for 5 min and then dissolved in 7 μL of sterile ddH_2O.

For the annealing reaction (in 10 μL), the DNA solution was mixed with 5 x sequencing buffer and 0.5 pmole of the appropriate primer (Seq 1, FW29 or FW105). The solution was then incubated at 37°C for 15 min, left for 10 min at room temperature and then kept on ice until needed. The sequencing reaction was performed as described for ssM13 (section 2.4.6).

Once the presence of a mutation gene was confirmed by DNA sequencing, plasmid DNA was used to transform *E.coli strain* QY13 (section 2.2.4.3), and the recombinant host was tested for protein expression (section 2.6.1).

Expression plasmids containing the substitutions phenylalanine-29 to tryptophan-29 (FW29), phenylalanine-105 to tryptophan-105 (FW105) and the double mutant (FW29/FW105) were obtained from K. Racher and T. Borgford (SFU).

2.6. Expression of cIIFX-TnC Mutant Genes in *E. coli* Strain QY13

2.6.1. Test for Expression

Two mL aliquots of 2xTY-Amp were inoculated with single QY13 colonies infected with pLcIIFX-TnC_{mut} (section 2.2.4.3) and grown at 30°C to an $OD_{600} = 0.5$. The cultures were heat shocked at 42°C for 10 min to induce expression, and then incubated at 37°C for 2 hrs. Cells were harvested by centrifugation at 13,000 rpm for 10 min and then resuspended in 50 μL of TE pH 8.0 buffer with 0.5 mM PMSF. Cells were lysed by three cycles of freezing and thawing and then sonicated for 10 min in a bath sonicator (Branson Model B-32, SmithKline company). The suspension was centrifuged

at 12,000 rpm for 12 min. Expression of fusion troponin C, cIIFX-TnC (Figure 2.3) was determined by SDS polyacrylamide gel electrophoresis of cell supernatant fractions and comigration with known standards (62).

2.6.2. Large Scale Expression

2.6.2.1. Growth of Cultures

Four 1 L aliquots of 2xTY-Amp were inoculated with pLcIIFX-TnC_{mut} infected *E.coli* strain QY13 and the culture was incubated at 30°C with shaking until a cell density OD_{600} = 0.8 was reached. Cultures were then heat shocked at 42°C and subsequently incubated at 37°C in an environmental shaker for 4 hrs. After incubation, the flasks were rapidly cooled on ice and cells were harvested by centrifugation at 8,000 rpm in a Sorvall GS3 centrifuge rotor at 4°C.

2.6.2.2. Release of Troponin C by Cell Lysis

Cell pellets were resuspended in 110 mL of Buffer A. Ten mL of a 24 mg/mL lysozyme solution were added to the suspension, and the mixture was incubated on ice for 30 min. After lysozyme treatment, 1.2 mL of a 1 mg/mL solution of DNase I, 2.4 mL of a 1.0 M solution of $MgCl_2$ and 120 µL of a 1.0 M solution of $MnCl_2$ were added to the suspension and it was further incubated on ice for 30 min. After the addition of 0.6 mL of a 100 mM stock of PMSF in isopropanol, the suspension was sonicated with three 20 seconds bursts at a maximum power from a probe sonicator (Fisher Sonic-Dismembrator model 300) fitted with a medium sized probe. Cell debris was removed from the homogenate by centrifugation at 18,000 rpm in a Sorvall SS34 rotor.

2.6.3. Purification of Troponin C

2.6.3.1. Purification of Fusion Troponin C

Ninety-six grams of urea, 31 mg of DTT and 200 µL of 1.0 M solution of Tris-HCl pH 7.5 were dissolved in the QY13 homogenate. The entire mixture was loaded onto a 2.6 x 40 cm chromatography column packed with 160 mL of Q-Sepharose Fast Flow (Pharmacia) and pre-equilibrated in Buffer B. The column was washed with 500 mL of Buffer B and proteins were then eluted with a linear gradient of KCl from 85 mM to 1 M at a flow rate of 200 mL/hr. The column fractions containing fusion troponin-C were identified by SDS-PAGE, then pooled and desalted on a 2.6 cm x 90 cm chromatography column packed with 500 mL of G-25 Sephadex (Pharmacia). The column was pre-equilibrated in 0.1% TFA (in H_2O) and eluted with the same solvent at a flow rate of 85 mL/hr. Fractions containing fusion proteins were pooled, lyophylized and stored desiccated at -20°C. Typically, 200 mg of fusion protein (cIIFX-TnC sequence, 200 amino acids long) was recovered from 4 L of cell culture.

Fusion protein (10mg) was resuspended in 2 mL of Buffer C and further purified by ion exchange chromatography on a Pharmacia FPLC system equipped with a HR 5/5 or HR 10/10: Mono Q (Pharmacia) column. cIIFX-TnC was eluted from the column in a 40 min linear gradient extending from 80% Buffer C/20% Buffer D to 100% Buffer D. Purified recombinant cIIFX-TnC was flash frozen and stored at -20°C until needed. Fusion FW105 and fusion FW105/IX130 mutants were purified by this method.

2.6.3.2. Digestion of Fusion Protein with Factor X_a

X_a was obtained from Dr T.J.Borgford (SFU). Conditions for the digestion of each preparation of fusion TnC by Factor X_a were determined empirically. Typically,

complete digestion was achieved after incubating the fusion protein with Factor X_a (800:1 weight ratio) for 12 hrs at room temperature in Buffer E.

Full length TnC (authentic TnC 162 amino acids long) was purified from Factor X_a digests by reversed phase chromatography on a Spectra-Physics model 8810 HPLC equipped with a 10 mm x 25 cm C4 (Vydac) column. The full length protein was eluted from the column in a 20 min linear gradient extending from 65% Solvent A (0.2% TFA/H_2O) / 35% Solvent B (0.2% TFA/acetonitrile) to 50% Solvent A / 50% Solvent B. Purified recombinant TnC was lyophylized and stored at -20°C until needed. FW29, FW105 and FW29/FW105 were purified by this method.

2.6.4. Preparation of Purified Proteins for Spectroscopic Analysis

Studies of FW105/IX130 mutants were performed on fusion proteins purified by FPLC as described in section 2.6.3.1. Column fractions were precipitated by the addition of ammonium sulphate to 50% (w/v). Proteins were recovered by centrifugation for 30 min at 5,000 rpm in a SS34 rotor and pellets were resuspended in 2 mL of 50% Buffer B / 50% Buffer F and 3 mM DTT. TnC samples were resuspended in Buffer F with 3 mM DTT. Protein solutions (cIIFX-TnC and TnC samples) were dialysed for 30 hrs at 4°C against two 500 mL changes of Buffer F.

Buffer F was prepared with ddH_2O and filtered through a chelating resin. To ensure free Ca^{2+} conditions, only acid washed (6N HCl) and thoroughly rinsed (ddH_2O) plastic containers were used. Stock protein solutions were flash frozen and stored at -70°C until analysis.

Protein concentrations were estimated by a modified version (63) of the method of Lowry (64).

2.6.4.1. Calcium Concentration in Stock Solutions

Total calcium concentration in calcium chloride stock solutions was determined by atomic absorbance on a Perkin-Elmer model 1100B atomic absorption spectrophotometer. A 1.0 mg/mL calcium chloride standard (BDH) was used to calibrate measurements. All samples were prepared according to protocols supplied by Perkin-Elmer (standard conditions for calcium).

2.7. Metal Binding Properties of Purified Proteins

2.7.1. Fluorescence Spectroscopy

Fluorescence spectra and calcium and magnesium titration of protein solutions were recorded on a Photon Technology model LS-100 fluorimeter equipped with a thermostated cell assembly and interfaced with a microcomputer. Spectra and titrations were performed at 25 ± 1°C in 1 cm square quartz cuvettes (OD_{280}<0.05). For spectroscopic studies, protein stock solutions were diluted to 5 μM with Buffer F. The buffer was previously equilibrated to room temperature and sparged with helium to displace dissolved oxygen. Protein solutions were pre-warmed to 25°C before the assay. The excitation wavelength was 278 nm (the excitation maxima) for all titrations. Emissions were monitored at 335 nm (FW29 mutant) or 366 nm (FW105, FW29/FW105 and FW105/IX130 mutants) in calcium titrations, and at 345 nm in the magnesium titrations. The intrinsic fluorescence of the recombinant proteins was titrated by the incremental addition of calcium chloride or of magnesium chloride with a 25 μL Hamilton syringe. The fluorescence emission spectra of the proteins was recorded before and after the titration with the metal ion.

The relative fluorescence quantum yield was determined using a tryptophan solution in buffer F as standard. The quantum yield of Trp is 0.12 (65). The excitation

wavelength was 286 nm and fluorescence emission was integrated between 295 nm and 420 nm. Relative fluorescence quantum yields were determined before and after the addition of calcium chloride or of magnesium chloride to a final free calcium concentration of 0.18.mM or a final free-magnesium concentration of 89 mM. The protein concentration was 5 μM.

2.7.2. Circular Dichroism

Circular dichroism spectra and calcium titration of full length TnC proteins (FW29, FW105 and FW29/FW105) were recorded on a Jasco J=20 spectropolarimeter that was equipped with a thermostated cell assembly and interfaced to a microcomputer. Spectra and titrations were performed on samples in a quartz cuvette of 2.0 mm path length. The instrument was calibrated with D-pantolactone (Θ=-16200 at 219 nm, concentration=0.015 %w/v (66)). The far-UV CD spectra of the fusion FW105/IX130 mutants were performed on a Jasco J710 spectropolarimeter fitted with a thermostated cell compartment. The instrument was calibrated with ammonium d-10-camphorsulfonate (ACS) (Θ= +7910 at 290.5 nm, concentration=0.06 %w/v). All spectra were obtained at 25°C in either 1.0 mm or 0.5 mm path length cells. Ellipticities were measured at 10 nm/min scan speed, 1.0 nm band width, 4 second response time, and 0.05 nm step resolution. Two to five measurements were made for each mutant. Absolute ellipticities were converted to mean residue ellipticities, based on the protein concentrations and 200 residues in the cIIFX-TnC fusion protein. The curves were smoothed with filter settings of 4 (top) and 10 (bottom).

Prior to spectral analysis protein solutions were diluted to a concentration about 10 μM in a total volume of 1 mL or 1.15 mL, with buffer F. In the case of the FW105/IX130 mutant proteins Buffer F was previously warmed to 25°C and sparged with helium,. All protein solutions were pre-warmed to 25°C before the assay.

Protein ellipticity at 221 nm was titrated by the incremental addition of calcium chloride. The far UV CD spectra of the recombinant proteins was obtained before and after titration.

2.7.3. UV Absorbance and UV Absorbance Difference Spectra

UV absorbance spectra were recorded on a Hewlett Packard model 8452A Diode Array Spectrophotometer with a 1 cm path length cell and 2.0 nm resolution. A split cell of 0.487 cm path length was used to generate absorbance difference spectra. Protein samples prepared in Buffer F were placed in one chamber of the split cell and calcium chloride or magnesium chloride solutions in Buffer F were placed in the other chamber. An unmixed reference spectrum was recorded. Difference spectra were generated by subtracting the spectrum of the sample after mixing of protein and metal solutions, from the spectrum of the unmixed blank.

Two calcium chloride additions were done. The first addition to a final calcium concentration of 0.9 μM, ensured the saturation of the high-affinity calcium binding sites. The second addition, to a final 0.18 mM ensured the saturation of the low-affinity sites. The absorbance difference spectra was recorded before and after each calcium addition.

The absorbance difference spectra was also recorded before and after the addition of magnesium chloride to a concentration of 12.1 mM.

2.8. Calculations

Free calcium or magnesium concentrations were calculated from total metal ion in chelating buffers by a computer algorithm (67) adapted to the MacIntosh microcomputer by Dr. B. Sykes and Mr. J. Boyko. The logarithmic binding constants for

metals and H^+ to EGTA used were: H^+ to $EGTA^{4-}$, 9.46; H^+ to $HEGTA^{3-}$, 8.85; H^+ to H_2EGTA^{2-}, 2.68; H^+ to H_3EGTA^{1-}, 2.0; Ca^{2+} to $EGTA^{4-}$, 10.72; Ca^{2+} to $HEGTA^{3-}$, 4.07; Mg^{2+} to $EGTA^{4-}$, 5.21; Mg^{2+} to $HEGTA^{3-}$, 3.38. Titration data was fitted by an iterative, derivative free curve fitting routine (BMDP Statistical Software,Inc.) on the IBM model 3081 computer.

Titration data was fitted to an equation that assumes there is a single class of sites:

$$y = (K_1[Ca^{2+}])^h \times 100 / 1+(K1[Ca^{2+}])^h$$

or to an equation that assumes there are two classes of sites:

$$y = (K_1[Ca^{2+}])^{h1} \times N_1 / 1+(K_1[Ca^{2+}])^{h1} + (K_2[Ca^{2+}])^{h2} \times N_2 / 1+(K_2[Ca^{2+}])^{h2}$$

The percent saturation is given by y, K is an association constant, *h* the Hill coefficient, and N the percentage contribution to fluorescence of sites of class 1 or 2.

The free energy change associated with metal binding to TnC can be expressed as

$$\Delta G = -RT \ln K$$

G is the Gibbs free energy, R is the universal gas constant, T is the temperature and K is the dissociation constant. A $\Delta\Delta G$ term was calculated that corresponds to the difference in free energy change associated with metal binding,

between two mutant proteins 1 and 2:

$$\Delta\Delta G = - RT \ln K_2 / K_1$$

3. RESULTS

3.1. Mutagenesis

The Kunkel method was used in site-specific mutagenesis of TnC DNA (section 2.4). In a first mutagenesis reaction, FW29/FW105 U-DNA was used as a primer, and IX130-1 or IX130-2 as oligonucleotides. The transformation of *E. coli* strain DH5α with the extension/ligation mixture from the reactions resulted in different number of plaques of M13, as indicated in Table 3.1:

TABLE 3.1. Annealing Reaction Conditions and Results.

Annealing Temperature	Seq 1 Primer Concentration	Number of Plaques of M13 Obtained With Oligonucleotides	
		IX130-1	IX130-2
80°C	10 pmoles	800	300
85°C	5 pmoles	20	5

The best results were obtained with 10 pmoles of Seq 1 and an annealing temperature of 80°C.

Single stranded DNA was prepared from 24 M13 clones (plaques) from each IX130-1 and IX130-2 transformation (section 2.3.4) and then sequenced (section 2.4.6). The autoradiography in Figure 3.1. shows the DNA sequence in the region of amino acid 130. Out of 40 samples sequenced, 31 were mutants. Four different mutations were

FIGURE 3.1. Autoradiography of Mutant M13 DNA Sequences

The picture shows the autoradiography of the M13 DNA sequence of 3 clones in the region that codes for amino acid 130. A, G, C, T, correspond to the initials of the deoxynucleotides dATP, dGTP, dCTP and dTTP. The site of the mutation, the codon and the corresponding amino acid are indicated.

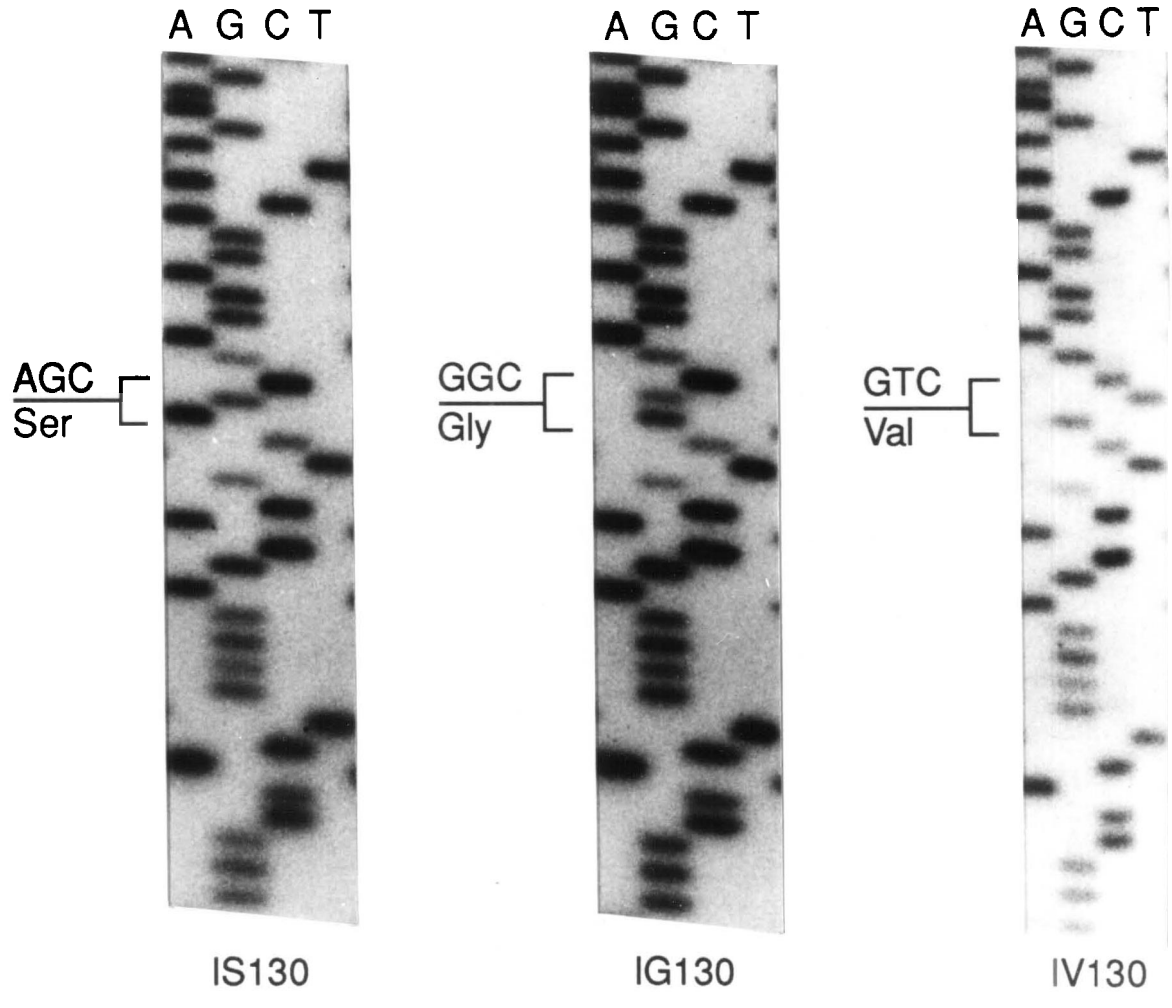
A G C T
AGC
Ser
IS130
A G C T
GGC
Gly
IG130
A G C T
GTC
Val
IV130

obtained in that first mutagenesis experiments: Gly-130, Ser-130, Val-130 and Phe-130. Table 3.2 shows the sequencing results of the first mutagenesis experiments.

TABLE 3.2. Sequencing Results.

Mutant Amino acid 130	Number of Mutants Obtained IX130-1	IX130-2	Total
Serine	12		12
Glycine	5	4	9
Valine		9	9
Phenylalanine		1	1

Table 3.3 summarises the results of the mutagenesis experiments. It indicates the mutagenic oligonucleotide and U-DNA template used in the reactions to obtain the different amino acid substitutions at position 130. Also, the codon that corresponds to the amino acid substitution identified by sequencing of the DNA, and the name of the mutant protein created.

The mutations Asn-130 and Asp-130 could not be obtained by annealing at 80°C. In order to favour the annealing of oligonucleotides of low melting temperature (Tm), subsequent annealing reactions were performed at a temperature only 5°C above the Tm. Asn-130 was obtained by annealing at 67°C. In an attempt to create the Asp-130, FW29/FW105/IV130 U-DNA was prepared and annealed to oligonucleotide IX130-1. The codon for Val-130 was G T C. The codon for Asp in IX130-1 was G A C. Since there is a difference of only one base between the template and the oligonucleotide, their annealing should be favoured. However, the yield of this U-DNA was very low, and mutagenesis experiments were not successful. Asp-130 was finally obtained as indicated

TABLE 3.3. Summary of Site-Directed Mutagenesis Experiments

Mutant Amino Acid 130	Oligonucleotide	U-DNA Template	Codon	Mutant Protein*
Asparagine	IX130-1	FW29/FW105	A A C	FW105/IN130
Aspartic acid	IX130-3	FW29/FW105/IN130	G A T	FW105/ID130
Serine	IX130-1	FW29/FW105	A G C	FW105/IS130
Valine	IX130-2	FW29/FW105	G T C	FW29/FW105/IV130
Glycine	IX130-2	FW29/FW105	G G C	FW105/IG130
Phenylalanine	IX130-2	FW29/FW105	T T C	FW29/FW105/IF130
Glutamic acid	IX130-3	FW29/FW105/IN130	G A A	
Histidine	IX130-3	FW29/FW105/IN130	C A T	
Threonine	IT130	FW29/FW105	A C C	FW105/IT130

*Note: Some subcloning protocols (i.e. subcloning protocols of mutant DNA from M13 to expression vector) resulted in mutant proteins with one tryptophan. In other cases, subcloning resulted in double tryptophan mutants.

in Table 3.3. From that same mutagenesis reaction His-130 and Glu-130 were obtained.

Restriction digestion reactions and subsequent cloning into the expression vector was done for the M13 mutant DNA carrying the mutations FW29/FW105/IX130 with the substitutions at position 130 being Gly-130, Asn-130, Asp-130, Ser-130, Thr-130, Val-130 and Phe-130 only. M13 DNA bearing the mutations His-130 and Glu-130 were identified by DNA sequencing only, and left at that stage.

3.2. Cloning into pLcIIFX-TnC

The success of the cloning of the M13 inserts into pLcIIFX-TnC was confirmed by plasmid sequencing (section 2.5.5). The sequencing of Val-130 and Phe-130 mutants in the expression plasmid showed that they had Trp-29 and were FW29/FW105/IX130 mutants. The corresponding mutant proteins were expressed in *E.coli* QY13 (section 2.6.2) but their activity was not tested. For the purpose of this project, these mutations were not of great importance and the restriction digestion of M13 and the subsequent ligations were not attempted again.

3.3. Protein Expression and Purification

The fusion TnC mutant proteins successfully expressed in *E.coli* strain QY13 were: FW29, FW105, FW29/FW105, FW29/FW105/IV130, FW29/FW105/IF130, FW105/IT130, FW105/IN130, FW105/IS130, FW105/IG130 and FW105/ID130. The cells were lysed (section 2.6.2.2), and the cell lysate was loaded onto a Q-Sepharose column (section 2.6.3.1). TnC is an acidic protein, and fusion proteins could therefore be purified in this anion exchange column by eluting it with KCl. Native TnC has been purified in the past using a DEAE-Sephadex anion exchange column (6). Figure 3.2 shows the chromatogram of the fractions eluted from the column. The fractions that

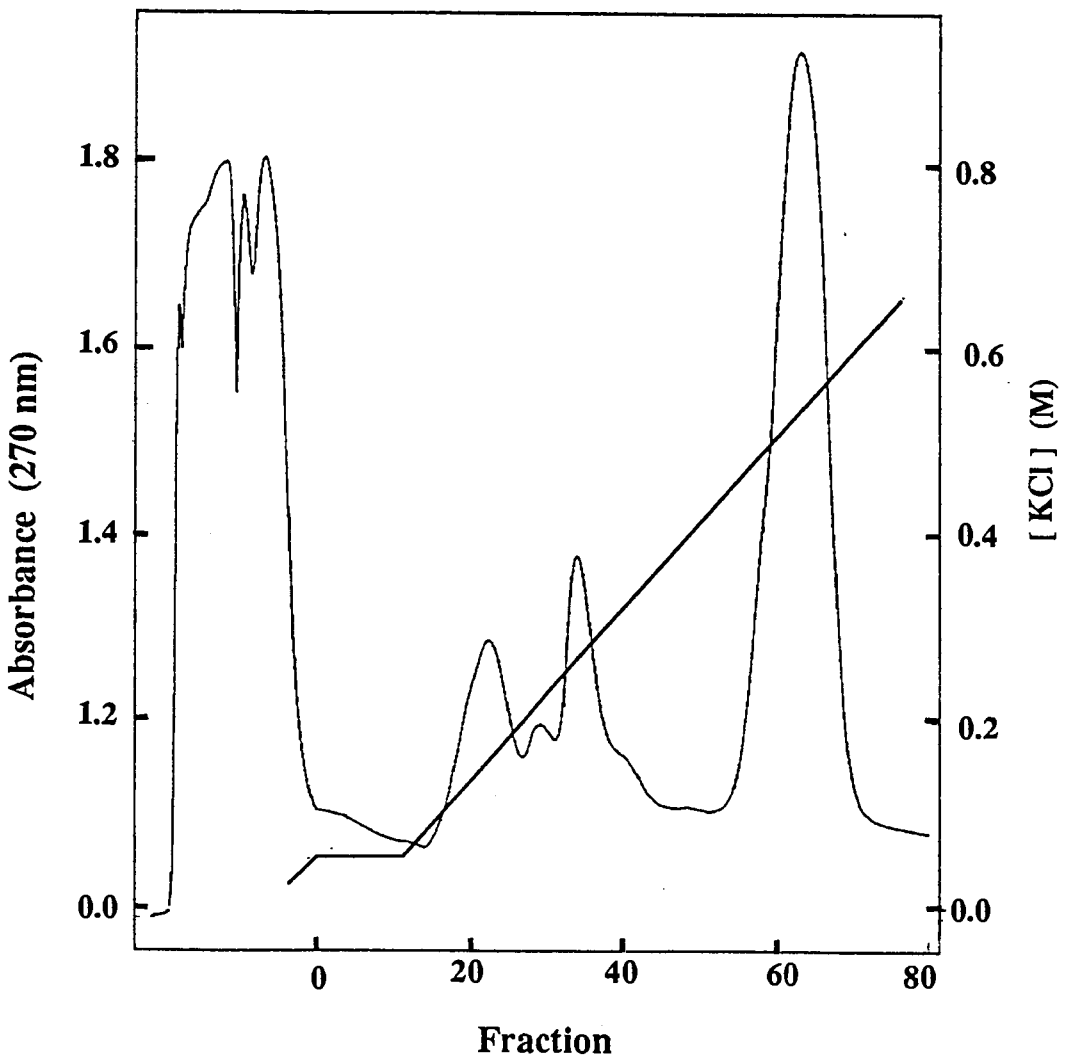

FIGURE 3.2. Anion Exchange Chromatography of *E.coli* Extract

The figure corresponds to a chromatogram of a cell lysate sample eluted from a Q-Sepharose column (section 2.6.3.1.). TnC was identified in fractions 33 to 38, as determined by SDS Polyacrylamide Gel Electrophoresis (Figure 3.3).

contained TnC were identified by SDS PAGE (Figure 3.3). Lane B, which corresponds to cell lysate, shows that recombinant TnC was the major protein expressed by *E.coli* QY13. The conductivity of the samples that eluted from the Q-sepharose column was measured. It was established that wild type recombinant TnC eluted at a KCl concentration between 0.16 M and 0.19 M (conductivity of 18.7 mS/cm to 21.1 mS/cm).

The Q-sepharose eluent that contained TnC was desalted in a G-25 gel filtration column. After this purification step fusion TnC was recovered from the column free of urea. Figure 3.4 represents the chromatogram from the gel filtration column (section 2.6.3.1), and shows that TnC eluted as a single peak.

Proteins were further purified by either HPLC or FPLC. In theory, HPLC gives superior purity but lower yields. However, FPLC gave a product as highly pure as HPLC and higher yield.

The fusion FW105/IX130 mutant proteins were further purified by FPLC (section 2.6.3.1). Figure 3.5 shows the FPLC chromatogram. The protein eluted as one single peak at a NaCl concentration between 0.36 M and 0.4 M.

Fusion FW29, FW105 and FW29/FW105 were digested with FX_a (section 2.6.3.2) in order to obtain full length TnC. That the digestion reaction had gone to completion was confirmed by SDS PAGE. The SDS PAGE in Figure 3.6. shows in Lanes 3 and 4, two bands. One comigrates with a full length TnC standard. The band of lower molecular weight appears to be the first 31 amino acids of the cII protein. Reversed phase HPLC was used to purify full length TnC from the digestion reaction mixture (2.6.3.2). The chromatogram presented in Figure 3.7 shows that TnC elutes from the column as a single peak.

FIGURE 3.3. SDS Polyacrylamide Gel of Troponin C

SDS PAGE of Lane A: Pure FW29 standard. Lane B: Cell lysate before loaded onto the Q-sepharose anion exchange column. Lanes 28 to 38 correspond to the number of the fractions eluted from the Q-sepharose column (Figure 3.2).

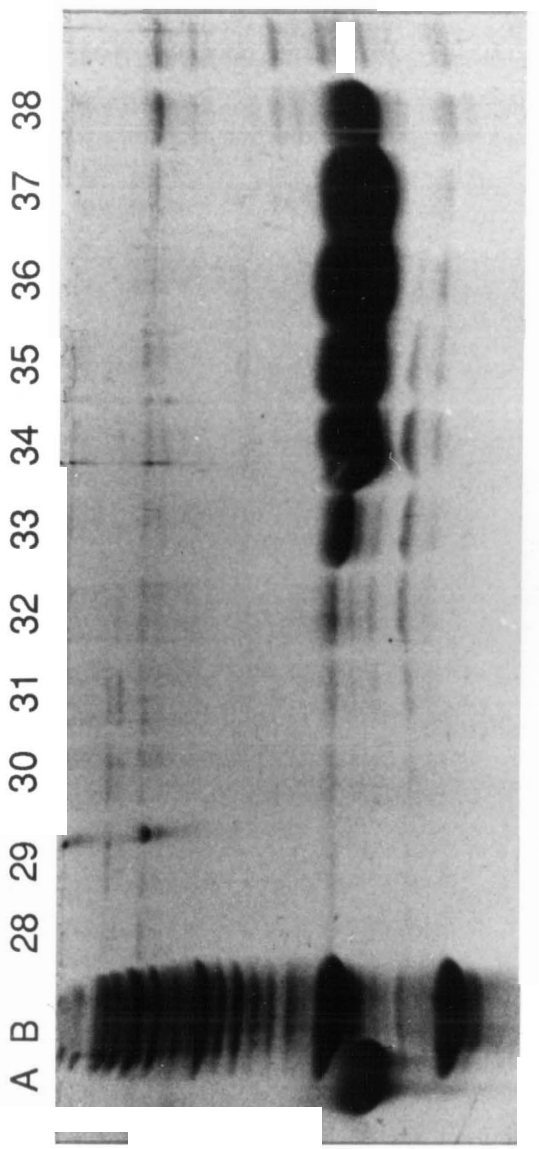
A B
28
29
30
31
32
33
34
35
36
37
38

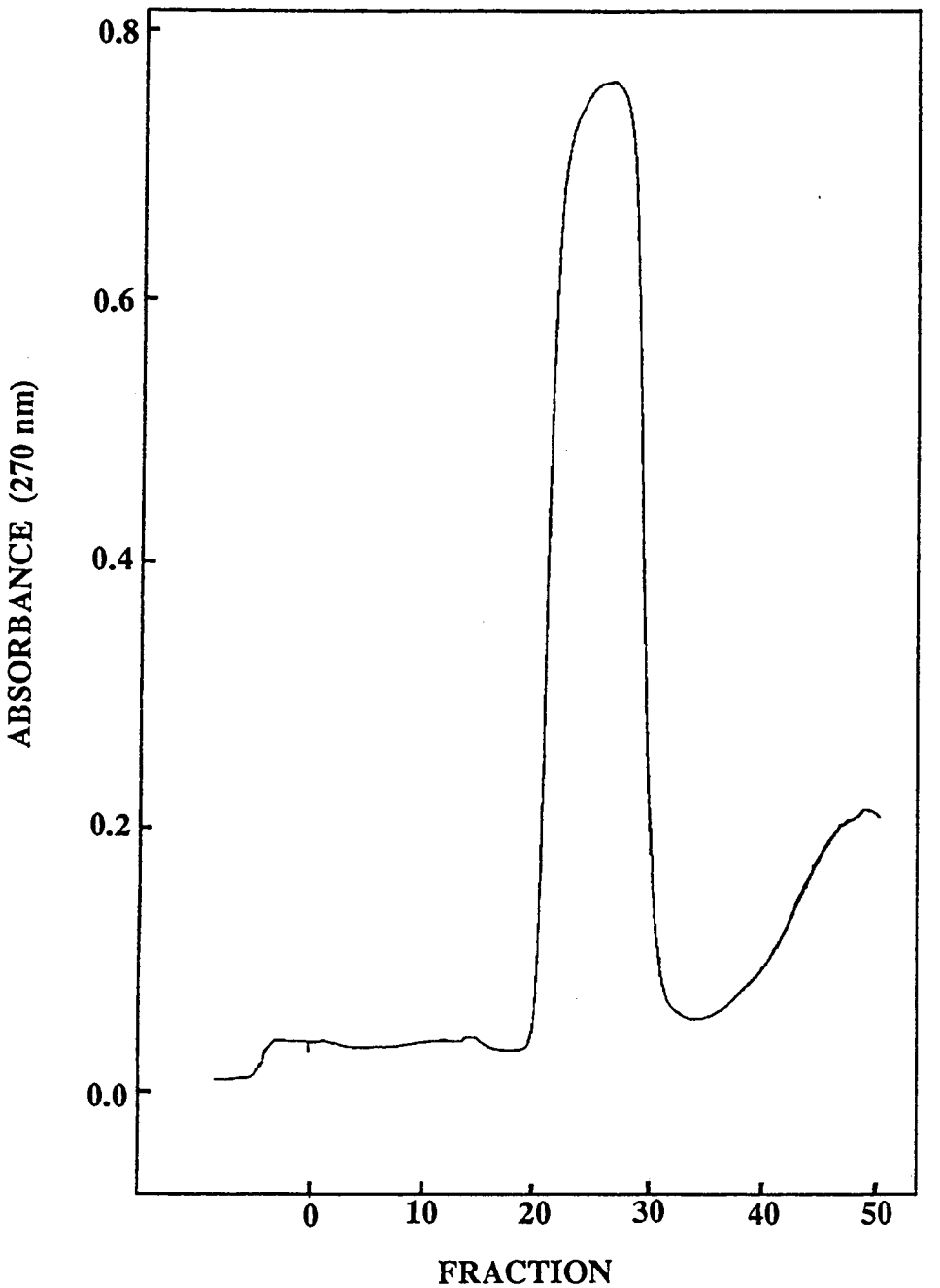

FIGURE 3.4. Gel Filtration Chromatography of Fusion Troponin C

The figure corresponds to the chromatogram of TnC samples eluted from a G-25 gel filtration column (section 2.6.3.1). Troponin C was collected from fractions 22 to 30.

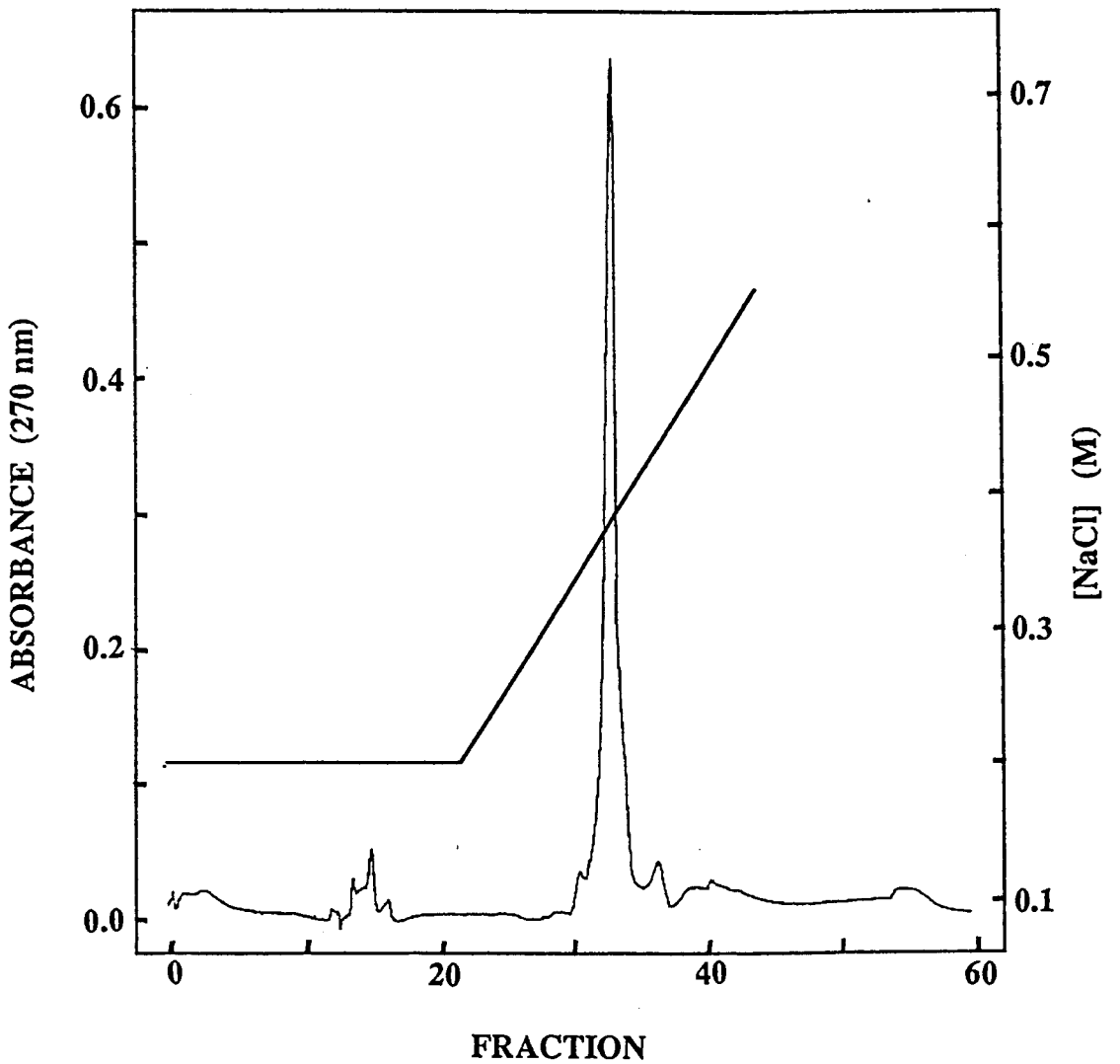

FIGURE 3.5. FPLC Chromatography of Fusion Troponin C

The figure corresponds to the chromatogram of fusion TnC eluted from an FPLC mono-Q column (section 2.6.3.1). The protein eluted as a single peak at a NaCl concentration between 0.35 and 0.4 M.

FIGURE 3.6. SDS Polyacrylamide gel of Troponin C Digested with FX_a

SDS PAGE shows on Lane 1: Fusion TnC standard. Lane 2: Pure TnC standard. Lanes 3 and 4: Digestion reaction of TnC with FX_a (section 2.6.3.2).

3
2
1

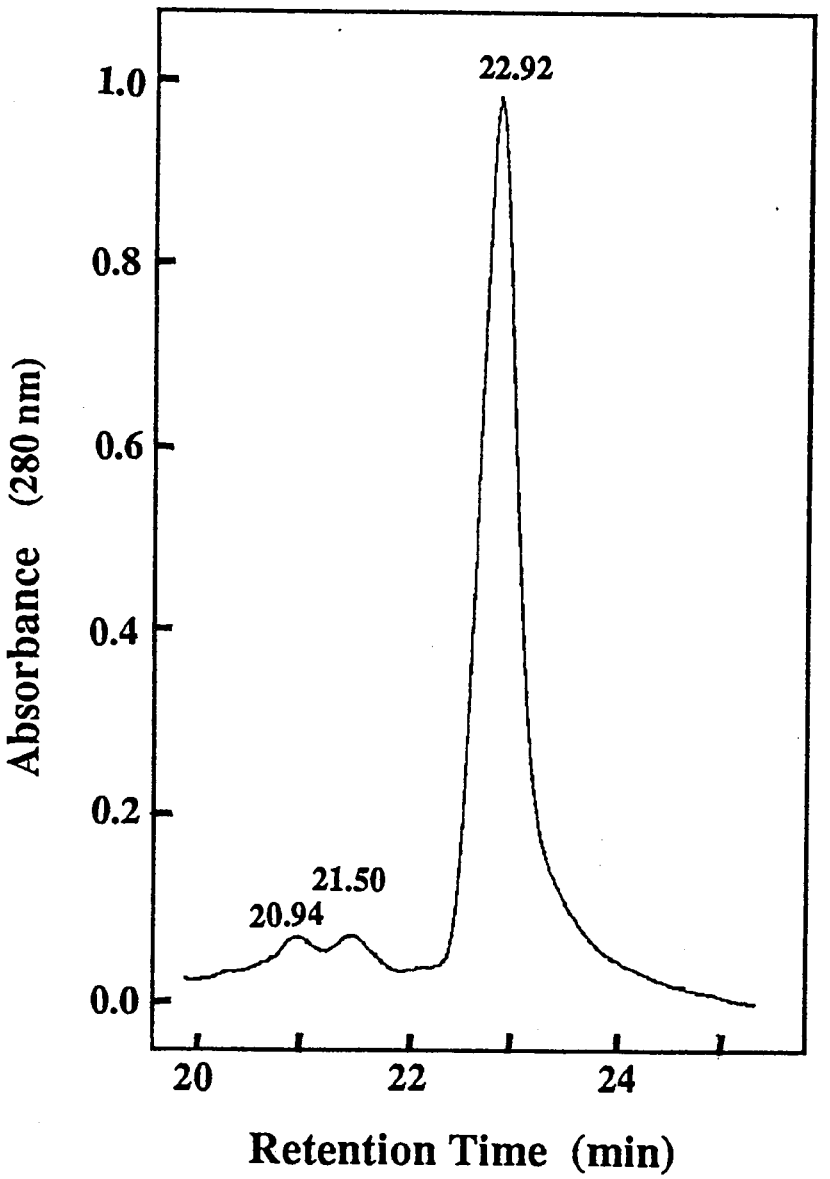

FIGURE 3.7. HPLC Chromatography of Authentic Troponin C

The figure corresponds to the chromatogram of a sample of TnC digested with FX_a. The peak with a retention time = 22.92 corresponds to purified TnC. Chromatography conditions are described in section 2.6.3.2.

3.4. Metal Binding Properties of FW29, FW105 and FW29/FW105

3.4.1. Far-UV Circular Dichroism

The Far UV CD spectra of the recombinant mutants FW29, FW105 and FW29/FW105, with and without calcium chloride at saturation (pCa<4.0) appear in Figure 3.8. The corresponding ellipticity values and changes in ellipticity at 221 nm are presented in Table 3.4. In the presence of calcium, all three mutant proteins showed an increase in the negative ellipticities. This is associated with an increase in the helical content of both high- and low-affinity sites of TnC. Although the absolute ellipticities of recombinant proteins varied, the relative changes in going from the calcium-free states of the proteins to calcium saturated states were approximately equivalent and averaged -6.51×10^3 deg cm^2 $dmole^{-1}$.

The results of far-UV CD calcium titrations are shown in Figure 3.9 and binding parameters are in Table 3.5. The titration data indicate that approximately 60% to 70% of the total calcium-induced change in ellipticity is contributed by calcium ion binding to the high-affinity sites. Only 30% to 40% of the change is contributed by metal ion binding to the low-affinity sites. The data were best fit to a monophasic curve, of the form $y = (K_1[Ca^{2+}])^h \times 100 / 1+(K1[Ca^{2+}])^h$ (section 2.8.), although in each case there is a deviation from an ideal curve. The average half saturation point for the three mutants was at a pCa = 6.73 ± 0.03 with a Hill Coefficient for binding of 1.59 ± 0.78.

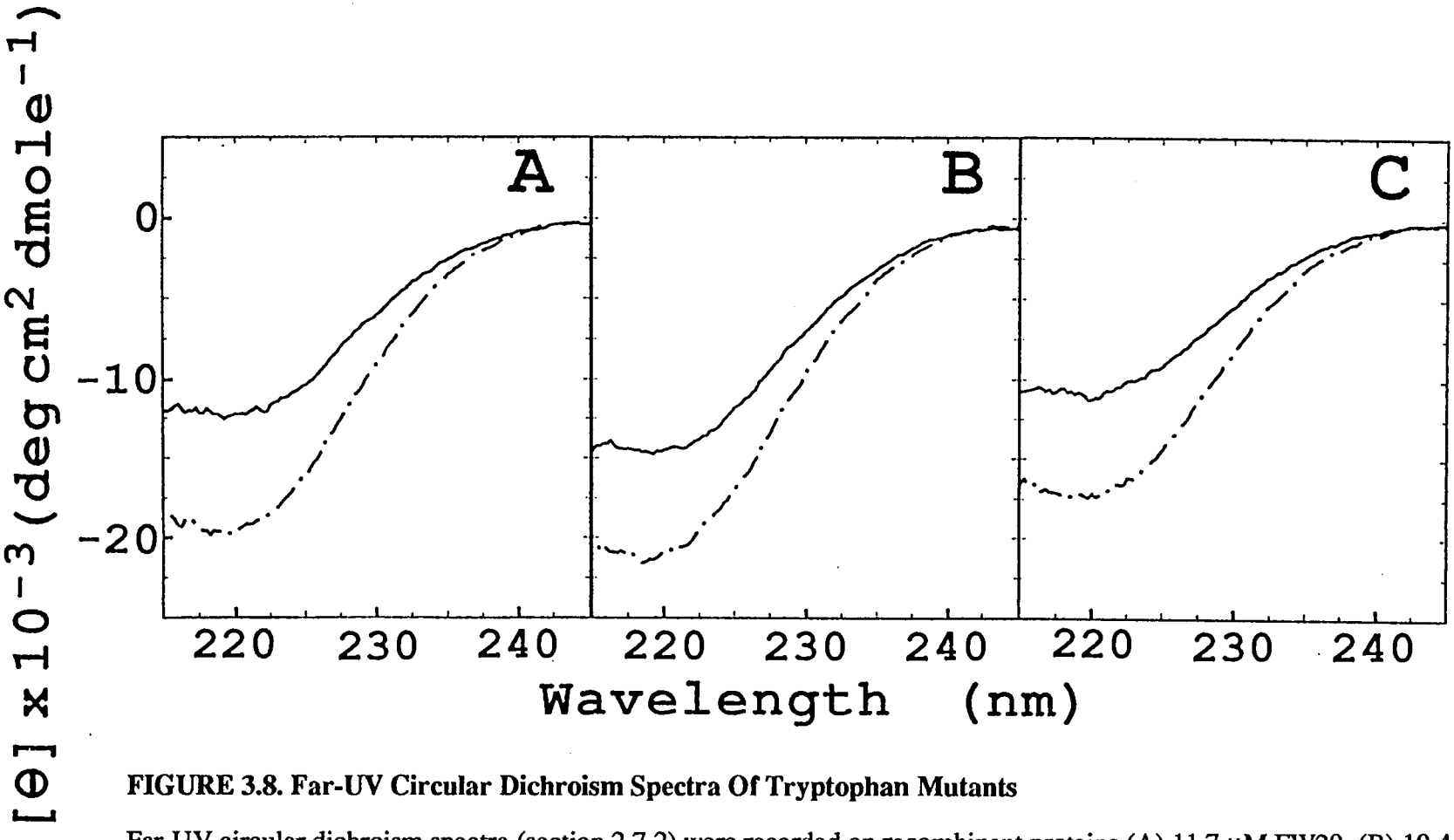

FIGURE 3.8. Far-UV Circular Dichroism Spectra Of Tryptophan Mutants

Far-UV circular dichroism spectra (section 2.7.2) were recorded on recombinant proteins (A) 11.7 μM FW29, (B) 10.4 μM FW105, (C) 10.1 μM FW29/FW105 in Buffer F, before (solid lines) and after (broken lines) the addition of calcium chloride to saturation.

TABLE 3.4. Relative Fluorescence Quantum Yields[a] and Far UV Ellipticities[b] of Tryptophan Mutants

Mutant	Q_{rel}			$[\Theta]_{221} \times 10^{-3}$ (deg · cm^2 · dmole^{-1})		$\Delta\Theta$
	metal free	+Ca^{2+}	+Mg^2	metal free	+Ca^{2+}	
FW29	0.052	0.159		-11.76	-18.96	-7.20
FW105	0.066	0.054	0.104	-14.39	-20.52	-6.13
FW29/FW105	0.083	0.155		-10.63	-16.83	-6.20

[a] Fluorescence quantum yields are relative to free tryptophan Q = 0.12 (REF) dissolved in Buffer F. Relative quantum yields were determined before, and after, the addition of metal ions (as $CaCl_2$ or $MgCl_2$) to a final free-calcium concentration of 0.18 mM or a final free-magnesium concentration of 89 mM. Assay conditions were as described in section 2.7.1.

[b] Protein ellipticities were determined at 221 nm in the absence of calcium and after the addition of calcium to saturation (ie. pCa<4.0).

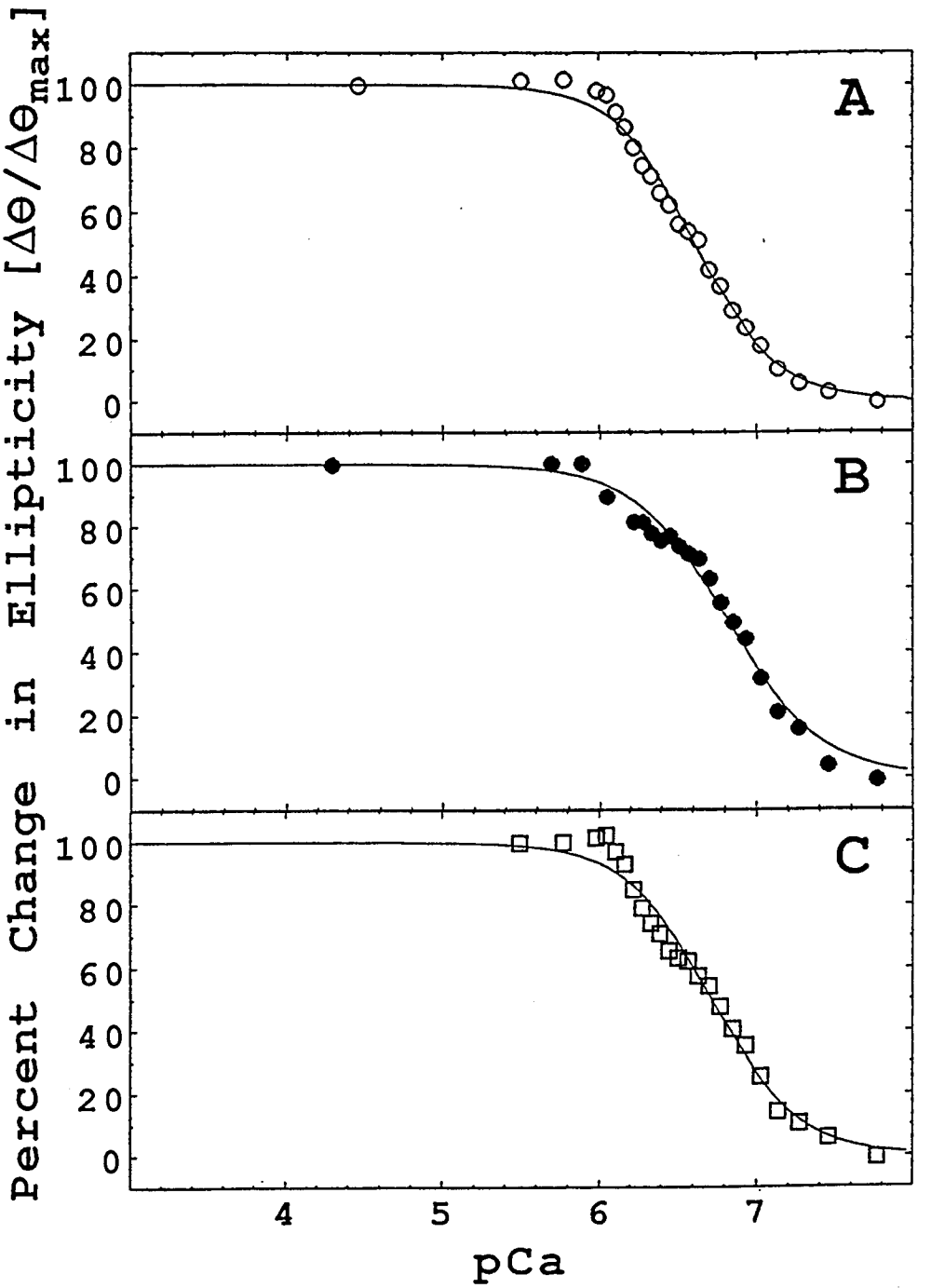

FIGURE 3.9. Titration of Far-UV Circular Dichroism

Titration of the far-UV protein ellipticity of (A) FW29, (B) FW105, (C) FW29/FW105. Experimental conditions are described in section 2.7.2.

TABLE 3.5. Binding Parameters from Far-UV Circular Dichroism

Mutant Protein	Kassoc (M^{-1})	Hill Coefficient
FW29	$4.15 \pm 0.1 \times 10^6$	1.71 ± 0.07
FW105	$6.55 \pm 0.23 \times 10^6$	1.46 ± 0.77
FW29/FW105	$5.23 \pm 0.2 \times 10^6$	1.59 ± 0.10

3.4.2. Absorbance Difference Spectra

The absorbance difference spectra of recombinant mutants perturbed with calcium appear in Figure 3.10. Difference spectra were generated for the mutant proteins at two free calcium concentrations 0.9 μM and 0.18 mM. Based on the results of titration experiments (Figure 3.13), only high affinity sites were expected to be occupied at a free calcium concentration of 0.9 μM and all sites are expected to be occupied at a free calcium concentration of 0.18 mM. After the first addition of calcium chloride (0.9 μM), no change in the environment of the tryptophan residue in the FW29 mutant (Figure 3.10-A) was apparent. Alternatively, significant changes were observed in the absorbance of the FW105 (Figure 3.10-B) and FW29/FW105 (Figure 3.10-C) at that same concentration. The second addition of calcium to a final free calcium concentration of 0.18 mM caused further transitions in the spectra and tryptophan environments of FW29 and FW29/FW105 only, but no further change in FW105. The absorbance spectra of FW105 perturbed with magnesium is shown in Figure 3.12-A.

In every case, absorbance difference spectra of mutant proteins were positive in response to calcium and magnesium ions. Therefore, the absorbance spectra of the substituted tryptophans are red shifted by metal ions.

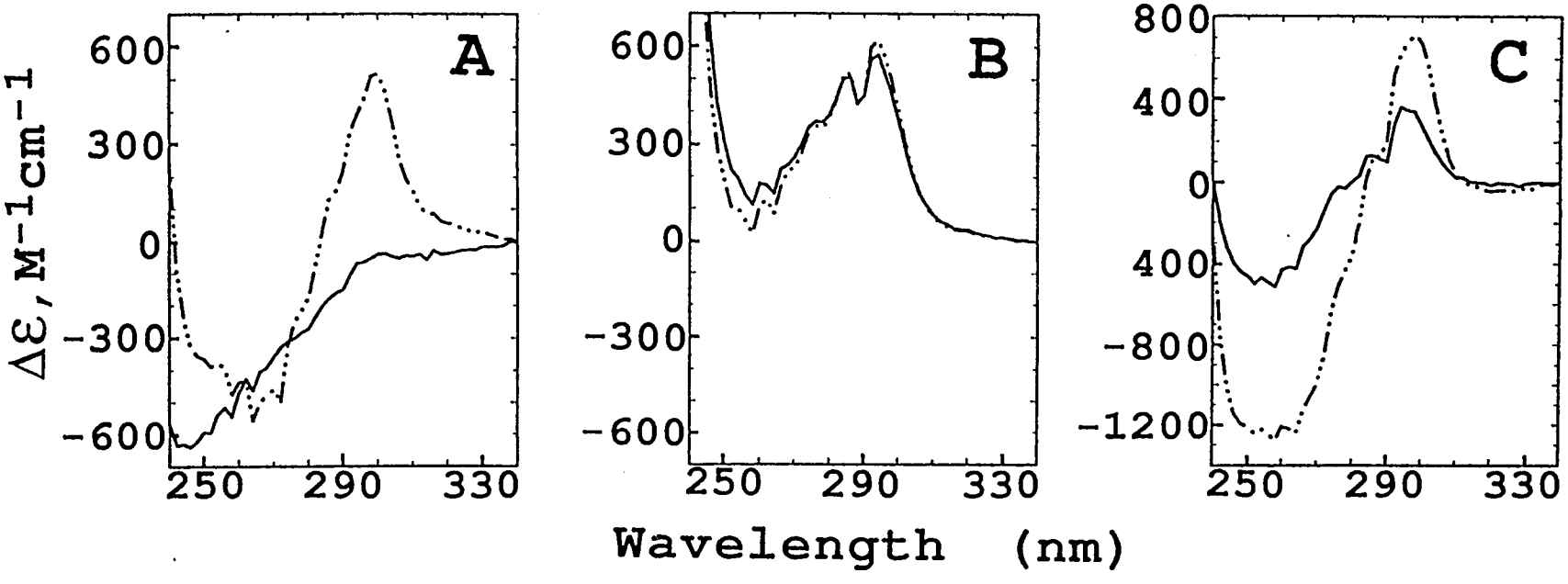

FIGURE 3.10. Absorbance Difference Spectra of Tryptophan Mutants

Absorbance difference spectra of (A) FW29, (B) FW105, (C) FW29/FW105 (section 2.7.3). Solid lines represent the difference spectra of samples at a final protein concentration of 5 μM and a free calcium concentration of 0.9 μM. Broken lines represent the difference spectra of samples at a final protein concentration of 5 μM and calcium at 0.18 mM.

3.4.3. Fluorescence

The fluorescence excitation spectra of all three mutant proteins, recorded at an emission wavelength of 335 nm, were characteristic of tryptophan and closely resembled the near UV absorbance spectra of the proteins.Fluorescence emission spectra of the recombinant proteins recorded before and after the addition of calcium appear in Figure 3.11. The corresponding relative fluorescence quantum yields are presented in Table 3.4. Calcium induced a 3.1 fold increase in the relative fluorescence quantum yield of FW29. The addition of calcium to FW105 caused a 1.22 fold reduction in fluorescence quantum yield and a blue shift in the absorbance maximum from 344 nm (without calcium) to 334 nm (with calcium). Calcium induced a 1.9 fold increase in the fluorescence quantum yield of FW29/FW105 and a small blue shift in the emission spectrum from 336 nm to 333 nm. The largest difference in the fluorescence intensity of the FW105 apoprotein and Ca^{2+}-saturated FW105 occurred at 366 nm and calcium titrations were monitored at this wavelength for both FW105 and FW29/FW105 proteins.

The fluorescence emission spectra of FW105 before and after the addition of magnesium is presented in Figure 3.12-B. The fluorescence quantum yield appears in Table 3.4. Magnesium induced a 1.6 fold increase in the fluorescence quantum yield of FW105. Alternatively, magnesium had no influence on the fluorescence spectrum of FW29.

Metal-ion induced changes in the fluorescence spectra of the mutant proteins allowed calcium binding to be titrated at low-affinity (Ca^{2+} specific) sites, and calcium and magnesium binding to be titrated at high-affinity (Ca^{2+}/Mg^{2+}) sites. The calcium titration curves of FW29, FW105 and FW29/FW105 mutants appear in Figure 3.13 and binding data are presented in Table 3.6. The fluorescence titration data of FW29 and FW105 were best fit by monophasic titration curves of the form:

$$y = (K_1[Ca^{2+}])^h \times 100 / 1+(K1[Ca^{2+}])^h \text{ (section 2.8)}$$

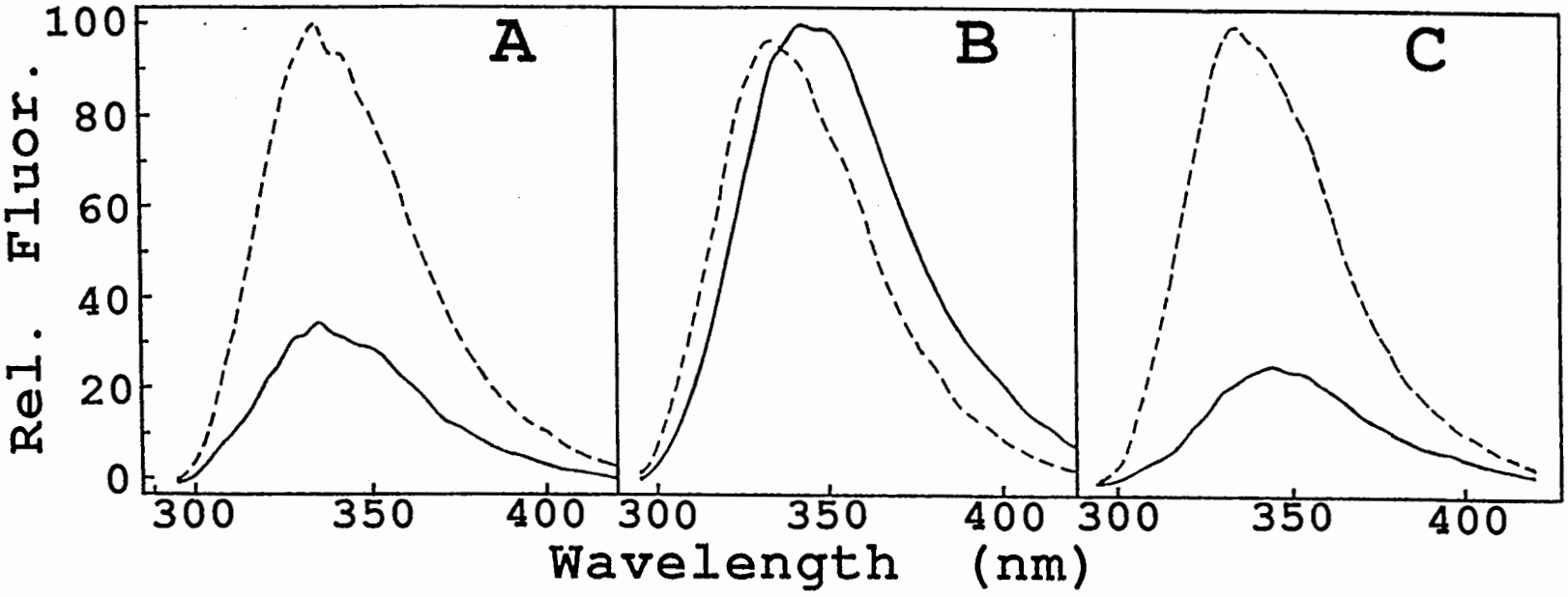

FIGURE 3.11. Fluorescence Emission Spectra of Tryptophan mutants

Fluorescence intensities (relative to maximal fluorescence) are graphed as a function of wavelength. The fluorescence emission spectra (section 2.7.1) of recombinant proteins (A) 5.0 μM FW29, (B) 5.0 μM FW105, (C) 5.0 μM FW29/FW105 in Buffer F were recorded before (solid lines) and after (broken lines) the addition of calcium chloride to a final free calcium concentration of 0.5 mM or 1.5 mM.

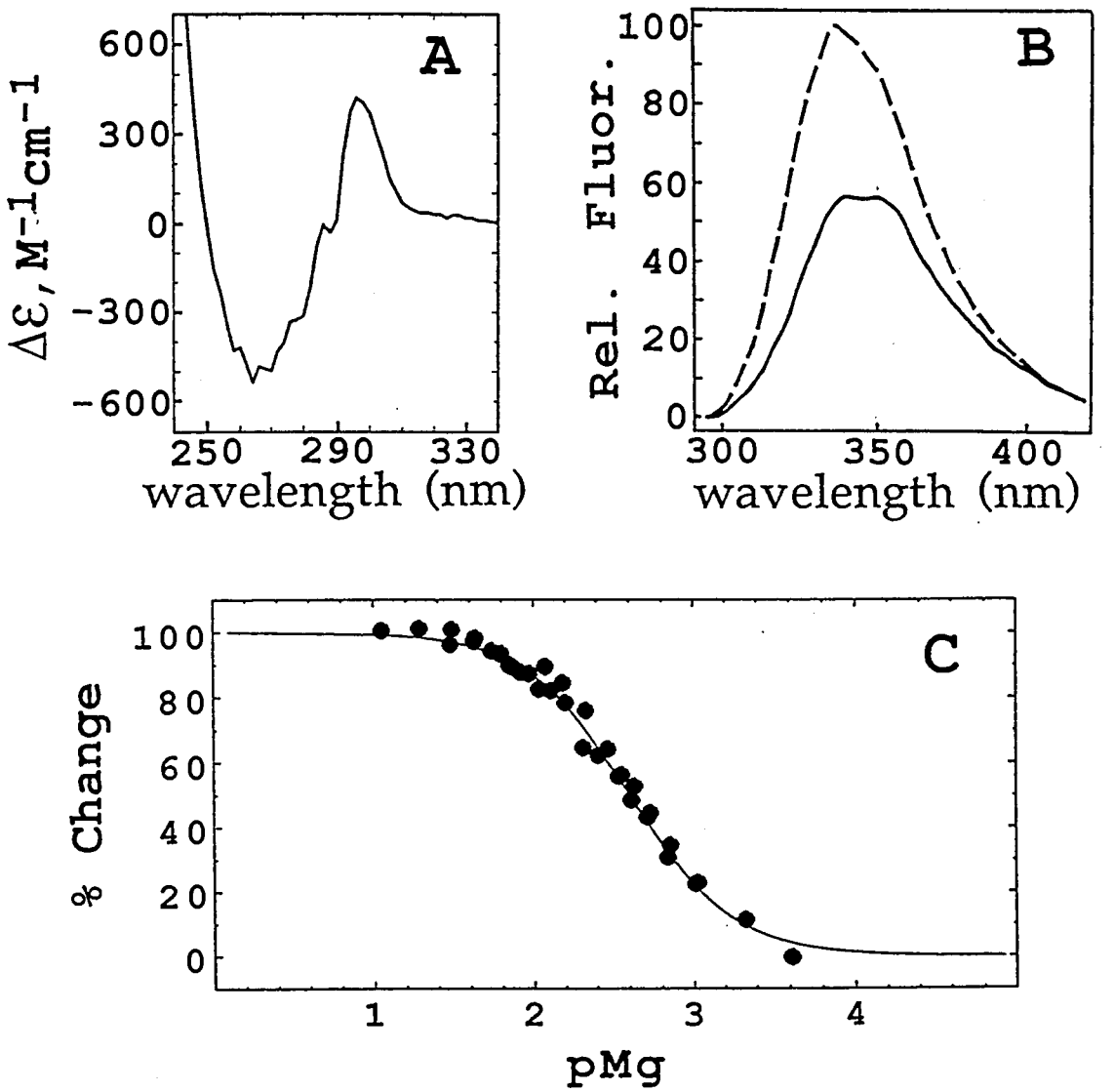

FIGURE 3.12. Spectroscopic Properties of FW105 in Response to Magnesium

(A) Absorbance difference spectrum of 5 μM of FW105 at a free magnesium concentration of 12.1 mM (section 2.7.2). (B) Fluorescence emission spectra of 5 μM FW105 before (solid line), and after (broken line) titration to a final free magnesium concentration of 89 mM (section 2.7.1). (C) Titration of the magnesium-induced change in tryptophan fluorescence of FW105 (section 2.7.1).

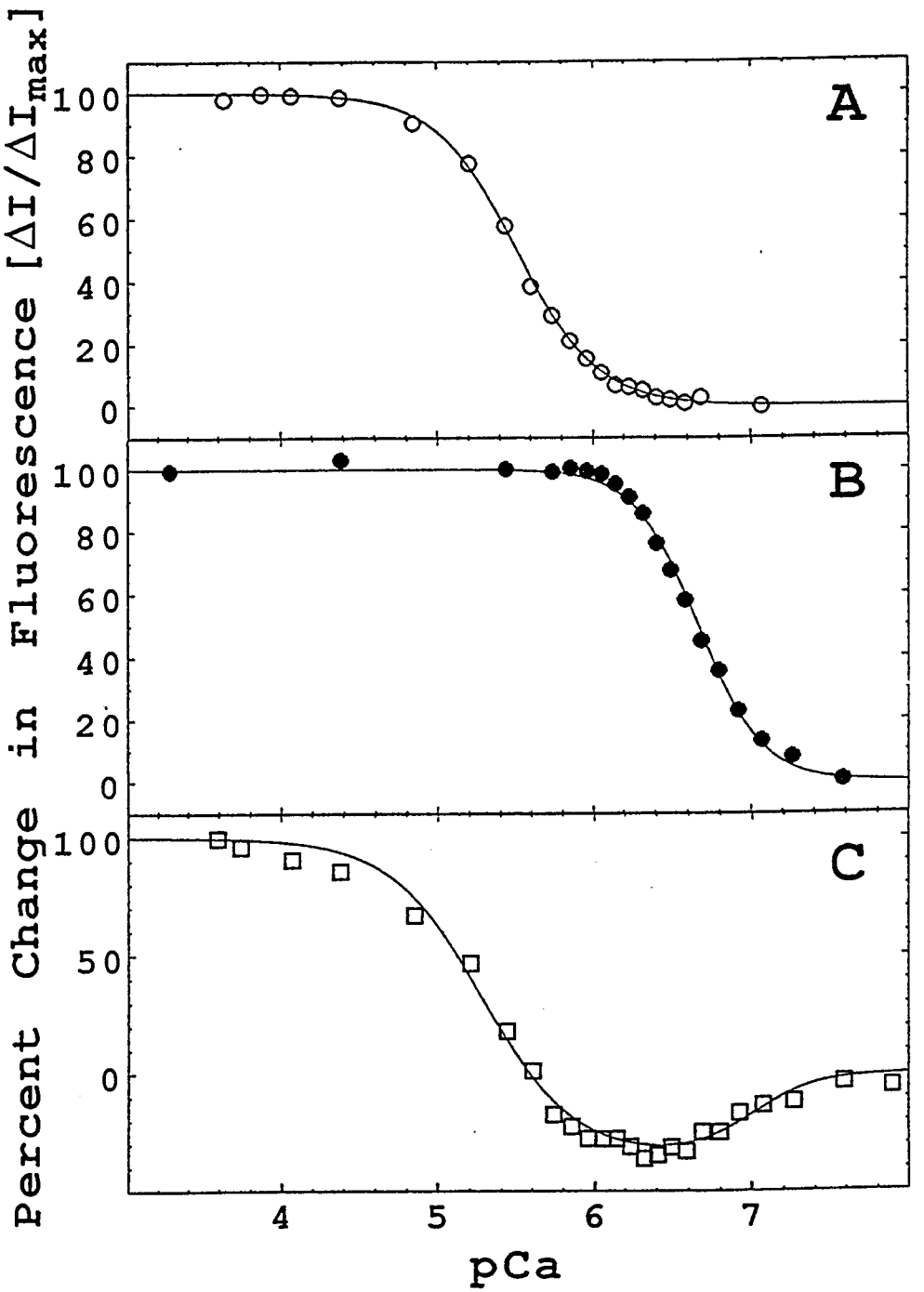

FIGURE 3.13. Titration of the Fluorescence of the Tryptophan Mutants

Titration of the intrinsic tryptophan fluorescence of (A) FW29, (B) FW105, (C) FW29/FW105. Experimental conditions are described in section 2.7.1. Titration data are plotted as a percentage of the absolute change in the fluorescence intensity.

TABLE 3.6. Binding Parameters Determined by Titration of Fluorescence of Tryptophan Mutants

		Calcium		Magnesium	
Mutant	**Class**	$K_{assoc.}$ (M^{-1})	*h*	$K_{assoc.}$ (M^{-1})	*h*
FW29	1 (Low)	$3.29 \pm 0.01 \times 10^5$	1.66 ± 0.03		
FW105	1 (High)	$4.66 \pm 0.08 \times 10^6$	2.15 ± 0.07	$4.64 \pm 0.01 \times 10^2$	1.44 ± 0.05
FW29/FW105	1 (High)	$9.91 \pm 1.26 \times 10^6$	2.15 ± 0.53		
	2 (Low)	$1.90 \pm 0.10 \times 10^5$	1.47 ± 0.09		

Titration data were fitted, as described in section 2.8, to an equation that assumes there is a single class of sites: $y=\frac{(K_1[Ca^{2+}])^h \cdot 100}{1+(K_1[Ca^{2+}])^h}$, as in the case of FW29 and FW105, or to an equation that assumes there are two classes of sites: $y = \frac{(K_1[Ca^{2+}])^{h1} \cdot N_1}{1+(K_1[Ca^{2+}])^{h1}} + \frac{(K_2[Ca^{2+}])^{h2} \cdot N_2}{1+(K_2[Ca^{2+}])^{h2}}$, as in the case of FW29/FW105. The percent saturation is given by y , K is an association constant, h the Hill Coefficient, and N the percentage contribution to fluorescence. The subscripts 1 and 2 refer to the first and second class of sites, respectively.

The titration data of FW29/FW105 was best fit by a binding equation that assumes there are two classes of binding sites:

$y = (K_1[Ca^{2+}])^{h1} \times N_1 / 1+(K_1[Ca^{2+}])^{h1} + (K_2[Ca^{2+}])^{h2} \times N_2 / 1+(K_2[Ca^{2+}])^{h2}$ (section 2.8).

The best fitting of these binding data assumed that the parameters N1 and N2 were equal to -35 and 135, respectively.

The magnesium titration curve of FW105 appears in Figure 3.12-C, and binding parameters appear in Table 3.6.

3.5. Metal Binding Properties of Fusion FW105/IX130 Proteins

The metal binding studies were performed on fusion FW105/IX130 mutant proteins (200 amino acids). Since the study of helix stability would be a comparative study, working with the fusion protein was convenient, as long as the fusion proteins could be titrated with calcium and magnesium. Working with the fusion protein reduced the number of purification steps and therefore the risks of protein deterioration.

3.5.1. Far-UV Circular Dichroism

The far-UV CD spectra of the recombinant mutants FW105/IX130. with and without calcium chloride at saturation (pCa < 4.0) appear in Figure 3.14. Calcium induced an increase in the negative ellipticity in all the mutant proteins. The relative change in ellipticity in going from the calcium-free to the calcium-saturated states of the protein is presented in Table 3.7. The changes in ellipticity values are approximately equivalent.

FIGURE 3.14. Far-UV Circular Dichroism of FW105/IX130 Mutants

The far-UV circular dichroism (section 2.7.2) of (A) FW105/I130, (B) FW105/IG130, (C) FW105/ID130, (D) FW105/IN130, (E) FW105/IS130 and (F) FW105/IT130 was recorded before (solid lines) and after (broken lines) the addition of calcium to saturation

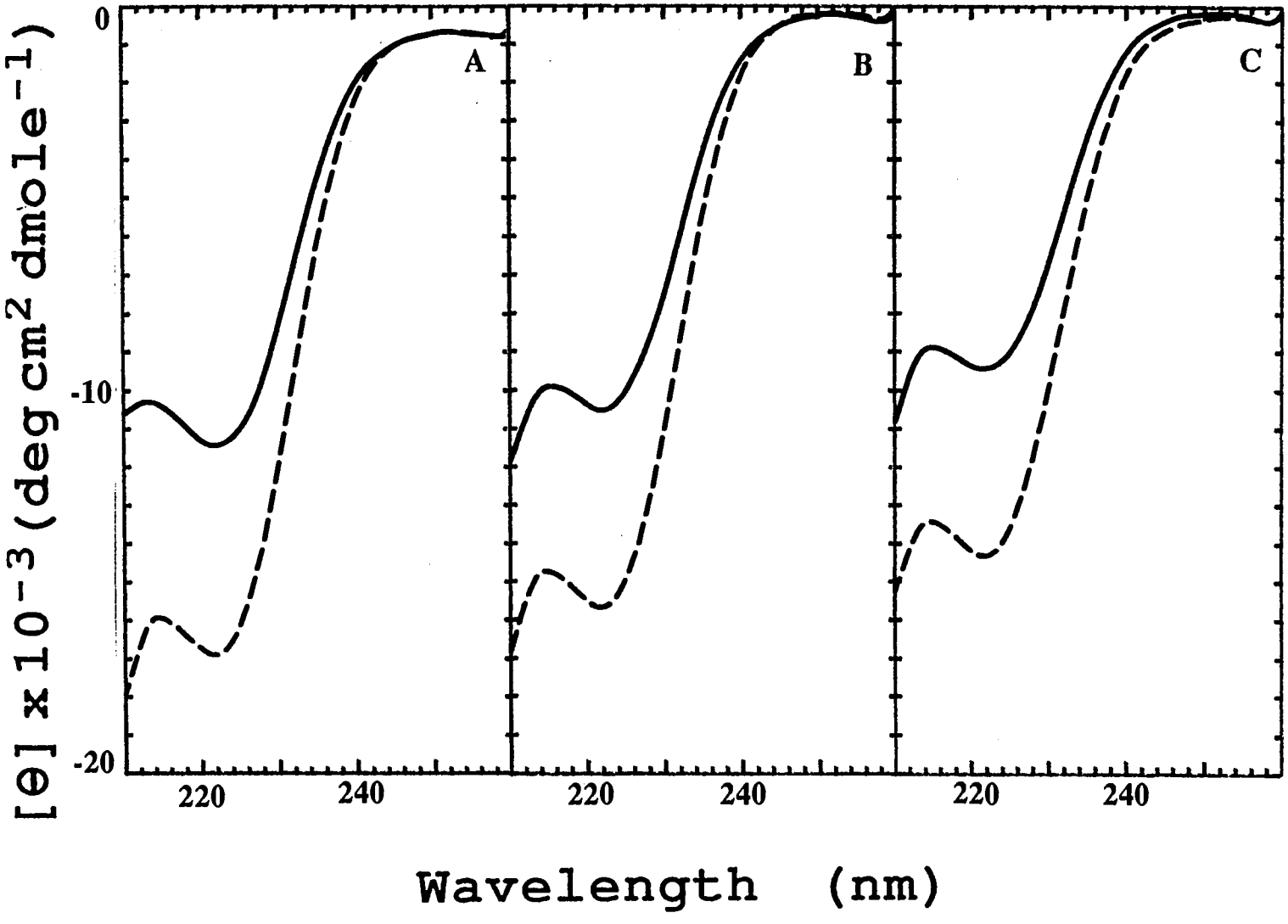
0
-10
-20
[θ] x 10⁻³ (deg cm² dmole⁻¹)
A
B
C
220
240
220
240
220
240
Wavelength (nm)

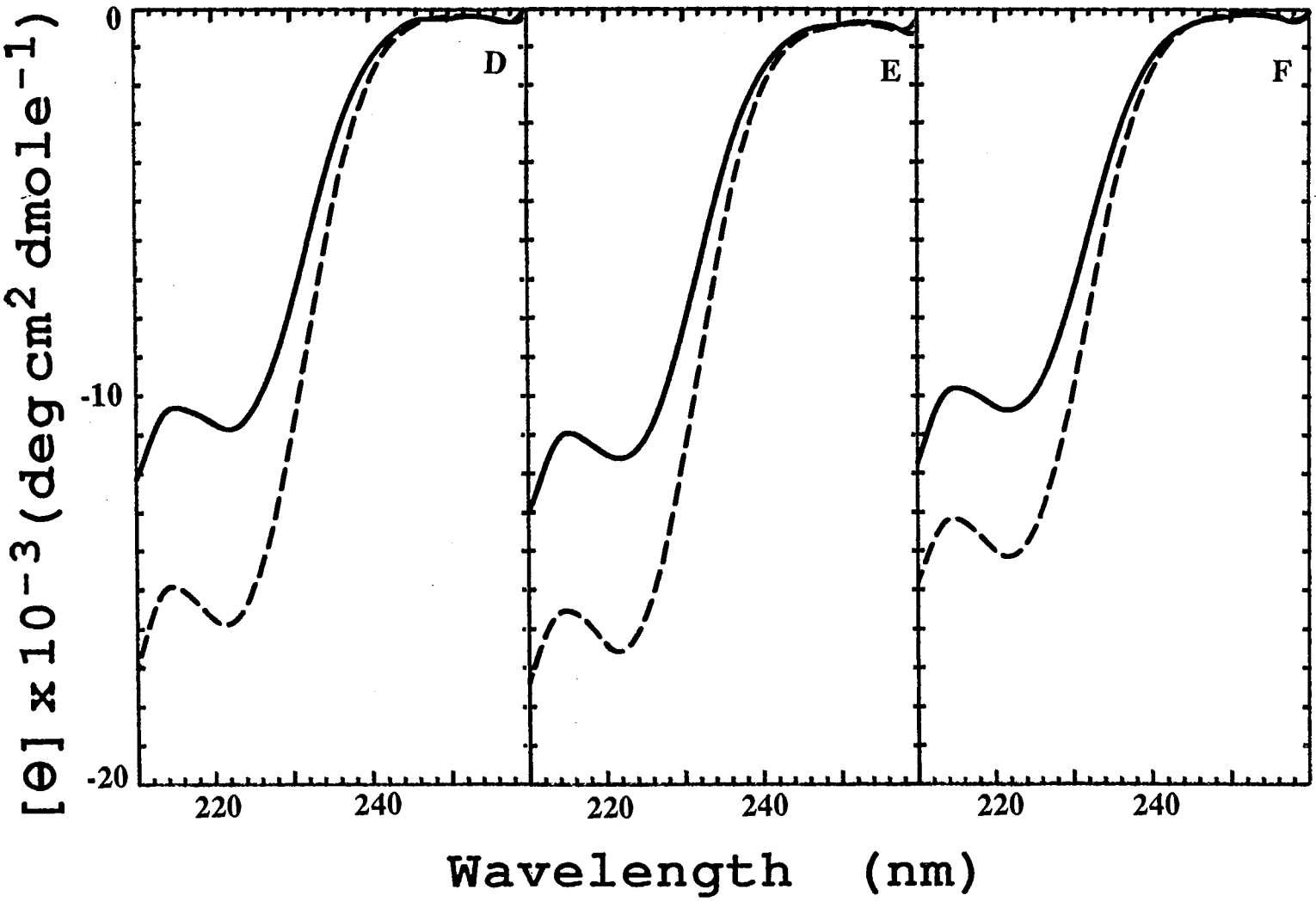
0
-10
-20
[θ] x 10⁻³ (deg cm² dmole⁻¹)
D
E
F
220
240
220
240
220
240
Wavelength (nm)

TABLE 3.7. Summary of FW105/IX130 Spectroscopic Data

Mutant	All Sites	High Affinity Sites		
	$\Delta[\theta]_{221}$ ($\times 10^{-3}$) (deg·cm^2·dmol^{-1})	-log Kd	$\Delta\Delta G_{Ile->Mut}$ (kcal·mol^{-1})	Hill Coefficient
FW105/I130	-5.4±0.1	7.462±0.013	0.00	2.1±0.1
FW105/IG130	-5.8±0.8	7.608±0.009	0.20±0.02	2.1±0.1
FW105/ID130	-5.3±0.6	7.691±0.011	0.31±0.02	1.9±0.1
FW105/IN130	-5.3±0.3	7.752±0.011	0.40±0.02	1.8±0.1
FW105/IS130	-5.1±0.2	7.945±0.012	0.66±0.02	2.0±0.1
FW105/IT130	-4.4±0.9	7.943±0.012	0.66±0.02	1.7±0.1

$\Delta[\theta]_{221}$ values represent the mean change in protein ellipticity at 221 nm upon the addition of calcium chloride to saturation (pCa<4.0), for 2 - 5 experiments. Protein samples had a concentration between 7.86 μM and 10.63 μM.

Titration data were fitted, as described in section 2.8, to an equation that assumes there is one single class of binding sites. $\Delta\Delta G$ was estimated as indicated in section 2.8.

3.5.2. Fluorescence

The fusion FW105 protein undergoes a magnesium induced increase in fluorescence emission intensity similar to that of the full length FW105. Calcium induced a similar decrease in the intensity of the fluorescence of both full length and fusion FW105. The fluorescence emission spectrum of all FW105/IX130 mutant proteins was recorded before and after the addition of calcium chloride (Figure 3.15) or of magnesium chloride (Figure 3.16). Saturating concentrations of metal ions were obtained from titration experiments (section 2.7.1). Fusion FW105/IX130 proteins responded differently to the addition of Ca^{2+} and of Mg^{2+}. Calcium induced a decrease in the intrinsic fluorescence of all the fusion proteins, whereas magnesium induced an increase in the intrinsic fluorescence.

Figure 3.15 shows that the fluorescence spectra of the mutant apoproteins are the same, as are the spectra of the calcium-saturated mutants. The reporter group then, undergoes the same calcium-induced change in environment, regardless of the secondary amino acid substitution at position130. The addition of magnesium to saturation induced the same increase in the fluorescence emission spectra of all the fusion FW105/IX130 proteins (Figure 3.16). That is, the reporter group undergoes the same magnesium-induced change in environment, regardless of the secondary amino acid substitution at position 130.

The calcium titration curves of the fusion FW105/IX130 mutant proteins appear in Figure 3.17 and binding data are presented in Table 3.7. The fluorescence titration data were best fit by monophasic titration curves (section 2.8). Calcium titrations of the fluorescence change show that there is an increase in the affinity for calcium in the order Ile < Gly < Asp < Asn < Thr < Ser. The binding curves for FW105/IT130 and FW105/IS130 superimpose and these two mutant proteins show essentially identical affinities for calcium. The largest difference in half-saturation point is of 0.48 pCa units

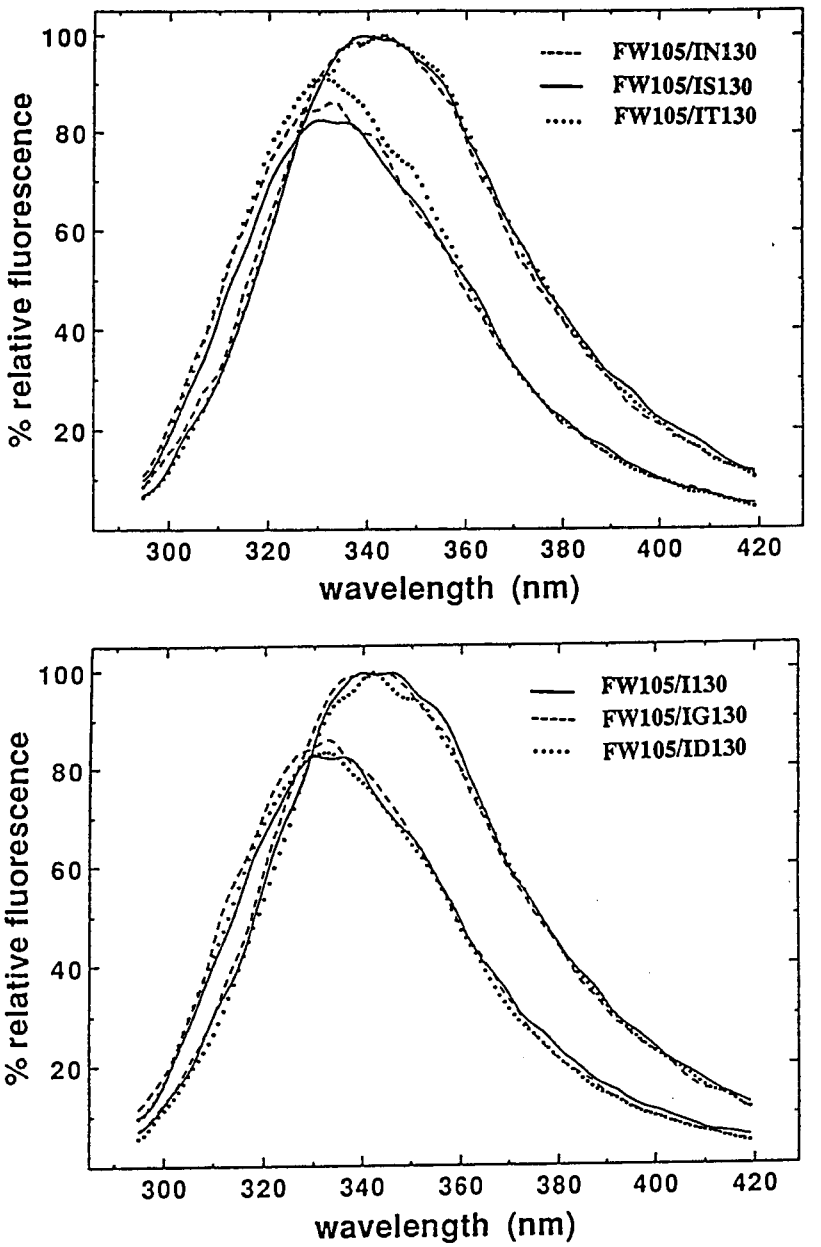

FIGURE 3.15. Effect of Calcium on the Fluorescence Emission Spectra of FW105/IX130 Mutants

Fluorescence emission spectra of FW105/IX130 mutant proteins were recorded before and after the addition of calcium chloride to a final free calcium concentration of 0.5 mM (section 2.7.1). The apoproteins presented the maximum fluorescence intensities, while the metal bound forms showed only a fraction of the intensity.

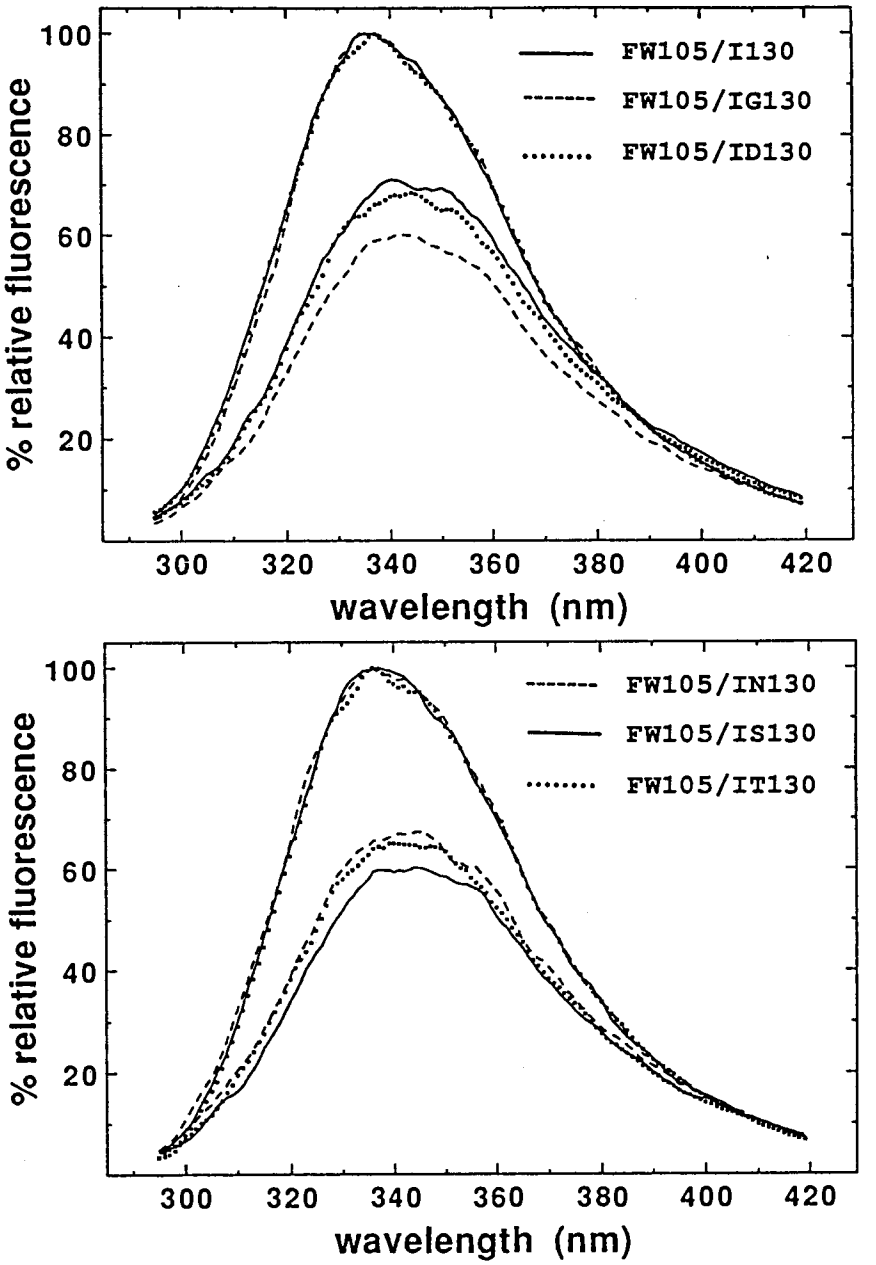

FIGURE 3.16. Effect of Magnesium on the Fluorescence Emission Spectra of FW105/IX130 Mutants

Fluorescence emission spectra of FW105/IX130 mutant proteins were recorded before and after the addition of magnesium chloride to a final free magnesium concentration of 12 mM (section 2.7.1). The metal bound form presented the maximum fluorescence intensities, while the apoproteins showed only a fraction of the intensity.

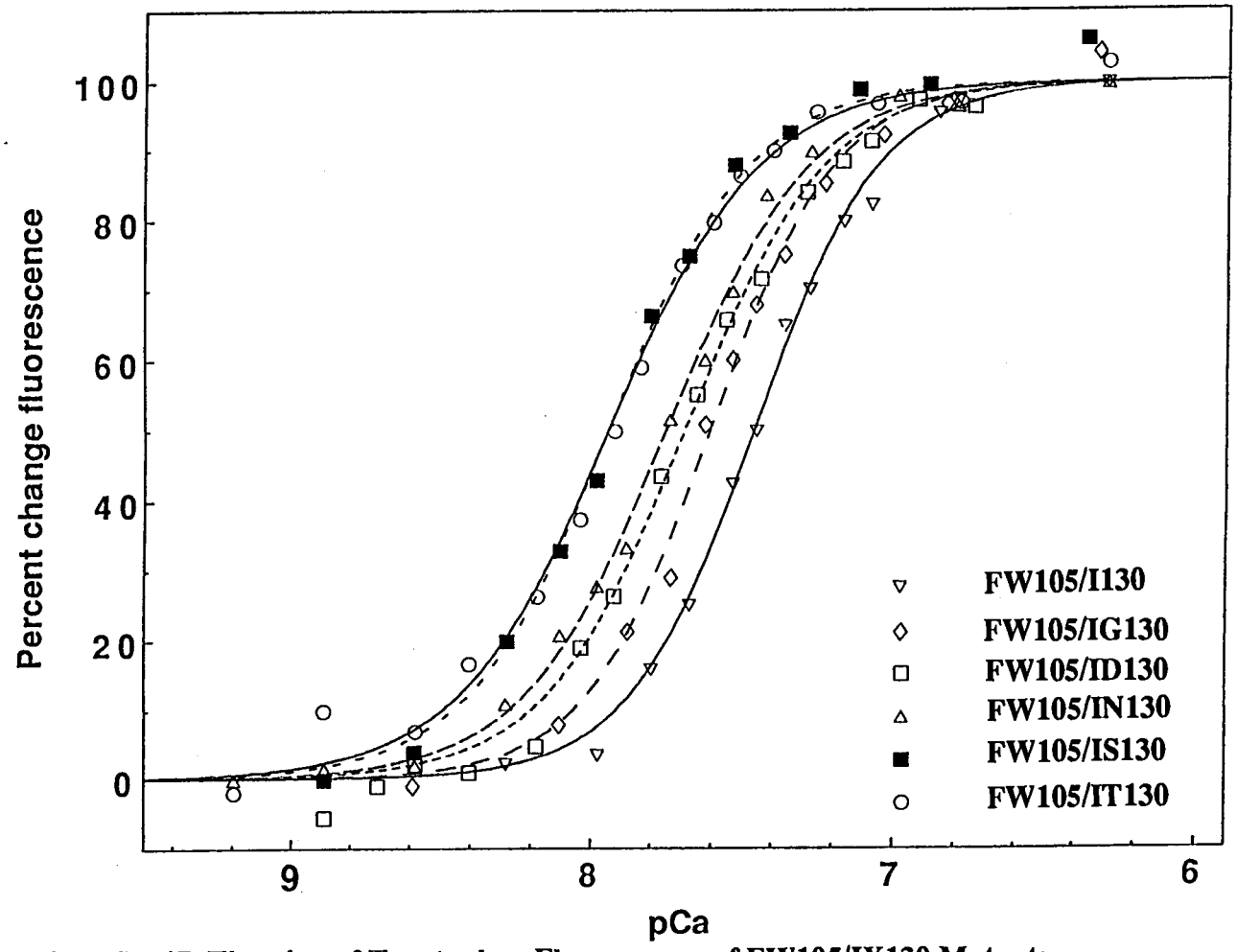

FIGURE 3.17. Titration of Tryptophan Fluorescence of FW105/IX130 Mutants

Titration of the tryptophan fluorescence in FW105/IX 130 mutant proteins was done as described in section 2.7.1.

between FW105/I130 and FW105/IT130 or FW105/IS130 mutants. The amino acid substitutions did not seem to affect the degree of cooperativity between the high-affinity sites, as indicated by the similarity of the Hill coefficient in the six fitted curves.

The difference in free energy change between every FW105/IX130 mutant and FW105/I130, $\Delta\Delta G$ was calculated (section 2.8) and the values appear in Table 3.7.

4. DISCUSSION

4.1. Troponin C - Tryptophan Mutants

The release of calcium ions from the sarcoplasmic reticulum produces an increase in the concentration of intracellular calcium (1, 2). Calcium binds to TnC in the thin filaments and this initiates the process of muscle contraction. Calcium binding produces a conformational change in TnC, which affects the interactions between the troponin subunits, and between troponin and tropomyosin and actin (thin-filament proteins). This causes an increase in myosin (thick-filament protein) crossbridge attachment to actin, and increase in actomyosin ATPase activity which results in tension development in the muscle fiber. It was the objective of this study to characterize the interaction between calcium and TnC, and to identify the structural features of TnC that are important for its function. TnC is the key protein in the regulation of muscle contraction and its study is important for a better understanding of the contraction process.

The X-ray crystal structure of chicken troponin C (14) shows a protein that has two domains connected by a long central α-helix. Each calcium binding domain consists of a pair of binding sites with helix-loop-helix (H-L-H) structural motifs. This structural arrangement is a common feature of a family of highly homologous intracellular calcium binding proteins. Like TnC, their activities are regulated by the binding of calcium ions. A better knowledge of the relationship between the function and structure of TnC can help in understanding the way these structurally related proteins work. The results obtained in the study of TnC can be extrapolated to other proteins and thus be of a more general value.

The gene that codes for chicken TnC has been successfully cloned and expressed in *Escherichia coli* (24), and this makes it possible to study relationships between the

structure and function of the protein by site-directed mutagenesis. The X-ray crystal structure of native chicken TnC (14) is now available at high resolution. Structure information is essential in the design of useful mutant proteins. An interesting feature of the native chicken TnC, is that there are no tyrosine or tryptophans in the amino acid sequence. These amino acids are unique in that they have absorbance maxima close to 280 nm, high extinction coefficients and high fluorescence quantum yields (68). Their absorption and fluorescence properties are sensitive to changes in environment and therefore tyrosine and tryptophan can be useful as reporters of ligand binding and of conformational changes in proteins. Site-directed mutagenesis can be used to introduce one of these amino acid residues in the TnC sequence, where it can be useful as site-specific probe or reporter, of ligand binding and conformational change in TnC. Phenylalanines at position 29 or 105 were substituted by a tryptophan residue to create the mutant proteins FW29 and FW105, respectively. Also the double mutant FW29/FW105 was created. The tryptophan residue in the TnC sequence allowed us to unambiguously assign the fluorescence and absorbance properties of the mutant TnCs to the position of the substitution in the high-affinity or low-affinity domains.

Phe-29 and Phe-105 occupy equivalent positions in the TnC sequence. Phe-29 precedes the first coordinating residue of binding loop I in the low-affinity domain (Figure 1.4). Phe-105 precedes the first coordinating residue of binding loop III in the high-affinity domain. These positions were chosen since the spectral properties of tryptophans, so close to the binding loops, were predicted to be strongly influenced by metal ion binding and conformational change (26). The first step in the project was to characterize the spectral properties of the tryptophan mutant proteins. Trp-29 was predicted to be able to report binding events occurring in the N-domain. Similarly, FW105 was designed so that Trp-105 would report binding events and conformational changes occurring in the C-domain of TnC. In other words, FW29 and FW105 were

expected to be useful in measuring calcium binding to the N- and C-domains, independently.

The increase in the helical content of TnC, observed in the far-UV CD spectra, indicates that the protein is undergoing a conformational change as calcium ions bind. The changes in ellipticity observed on going from the calcium-free to the calcium bound forms were similar for all three tryptophan mutants and in good agreement with other reports (22, 23). For rabbit skeletal TnC, an average change in protein ellipticity of 8.86 x 10^3 deg cm^2 $dmole^{-1}$ was reported (22), comparable to 6.51 x 10^3 deg cm^2 $dmole^{-1}$ at pH 6.95 in this study.

The data for the titration of the ellipticity of the mutant proteins (Figure 3.9) could not be accurately fit to a model that involves two classes of binding sites. In agreement with reports from studies of rabbit skeletal TnC, changes in far-UV circular dichroism of all the Trp mutant proteins predominantly reflect structural changes in the high-affinity binding domains. In fact, it was found that approximately 60% to 70% of the total calcium induced change in ellipticity is contributed by calcium binding to the high-affinity sites. However, the data was not fit to a biphasic curve that assumes there are two classes of binding sites. This would have required a good estimate of the contribution of each set of sites to the ellipticity change. Since the titration curves of high- and of low-affinity sites overlap, the estimate would have been very imprecise and of little statistical relevance.

The far UV CD studies were important in evaluating the integrity of the mutant proteins. Regardless of the location of the tryptophan in the mutant proteins in the high-affinity (FW105), low-affinity (FW29) or both (FW29/FW105) domains, calcium induced similar changes in their CD spectra. These results suggest that the tryptophan substitutions did not have an effect on the overall conformation of the protein or on its function.

The UV absorbance difference spectra of the mutant proteins (Figure 3.10) indicate that there is a change in the environments of Trp-29 and of Trp-105, due to the calcium-induced structural transitions in the domains. A positive difference in the extinction coefficient is observed in the difference spectra in the UV region that corresponds to Trp absorbance bands (from approximately 275 nm to 320 nm). This red shift in the tryptophan absorbance is attributed to the tryptophan moving from a relatively polar to a relatively non polar environment as calcium binds to the protein (69).

The spectra of FW105 (Figure 3.10-B) showed a calcium-induced transition after the first addition only. At that concentration, only high-affinity sites were expected to be saturated. No further changes were observed with the second addition of calcium. This indicates that Trp-105 is, in fact, reflecting structural changes occurring at the C-domain only.

In contrast, the spectra of FW29 (Figure 3.10-A) were virtually unaffected by the first addition of calcium, in the region of the tryptophan absorbance bands. A change in the environment of the Trp-29 was only evident after the second addition of calcium, at an ion concentration enough to saturate the low-affinity sites.This observation is good evidence that Trp-29 is a useful probe for monitoring calcium binding in the N-domain.

Magnesium ions also induced a red shift in the absorbance spectrum of FW105 at wavelengths above 275 nm (Figure 3.12-A). It is interesting that the spectra in Figures 3.12-A and 3.10-A are very similar. The calcium-induced change in the environment of Trp-29 in the N-domain, is virtually identical to the magnesium-induced change in the environment of Trp-105 in the C-domain.

The red shifts observed in the absorbance spectra of FW29 and FW105 imply that Trp residues become more buried in the protein when calcium is bound. There is a difference between these experimental results and the conformational change model proposed by Herzberg *et. al* (13), according to which Phe-29 would become more

exposed. The model is based on the high homology in the sequence and helical arrangement of the C- and N-domains of TnC. The three dimensional crystal structure shows that only the C-domain is occupied by calcium, whereas the N-domain is calcium free. The tertiary structure of the N-domain is in these circumstances quite different from the structure of the C-domain. According to the model, the N-domain would undergo a structural rearrangement on binding calcium. The tertiary structure of the low-affinity domain would then more closely resemble that of the calcium-bound high-affinity sites. In the model, the change in conformation would result in Phe-29 becoming more exposed. The change in surface exposure for that residue would be from 46.2 $Å^2$ to 55.7 $Å^2$, an increase of 9.5 $Å^2$. A possible explanation for the difference between the experimental results and the model is that tryptophan at position 29 may adopt a conformation somewhat different to phenylalanine. Or the conformational change model may not be entirely accurate.

Fluorescence was the most sensitive and reproducible method of monitoring metal ion binding to TnC.

Calcium induced very different responses in the spectra of FW29 and FW105, as indicated by the relative fluorescence quantum yield values (Table 3.4 and Figure 3.11-A and B). The results from FW29 show that a 3.1 fold increase in the relative fluorescence quantum yield is associated with calcium induced transitions of the low-affinity sites. The data from FW105 indicates a reduction in the relative quantum yield and a blue shift in the absorbance maxima related to calcium induced structural transitions of the high affinity sites.

The calcium induced increase in the fluorescence intensity of FW29 allowed the titration of the low-affinity sites at 335 nm and the calcium-induced decrease in the fluorescence intensity of FW105 allowed the titration of the high-affinity sites at 366 nm. In the double mutant FW29/FW105, the tryptophans were titrated at 366 nm, in order to be able to detect the transition of Trp-105. Since the titration curves overlap and, since

the contributions of the two tryptophans in FW29/FW105 to total fluorescence are not equivalent, it was not possible to estimate binding constants with the same precision as in the single mutants.

Magnesium had no effect on the fluorescence emission of FW29 nor did it effect the absorbance properties of the mutant. These observations are in agreement with previous reports that magnesium does not bind at the N-domain and that the low-affinity binding sites are calcium-specific (16). On the other hand, the fluorescence emission spectrum of FW105 was significantly affected by magnesium. It is interesting to note that the increase in fluorescence quantum yield (1.6 fold) of FW105 to magnesium is similar to the response of FW29 to the addition of calcium. As was pointed out above, magnesium induces a change in the absorbance spectrum of FW105 similar to that induced by calcium in FW29.

The magnesium-induced increase in the fluorescence intensity of FW105 allowed the titration of the high affinity sites at 345 nm (Figure 3.12-C). The association constant was estimated $Ka = 4.64 \pm 0.01 \times 10^2$. At the high magnesium concentrations used in the titration experiments, it is possible for calcium to be an important contaminant. This could mean that there is a chance that calcium rather than magnesium is titrating the sites. The absorbance difference spectra for FW105 in Figures 3.10-B and 3.12-A, clearly show that calcium and magnesium have quite different effects on the environment of the tryptophan. Therefore, the magnesium titration of FW105 is a true estimate of the magnesium binding constant.

The absorbance difference spectra and fluorescence experiments show that calcium and magnesium have different effects on the absorbance and fluorescence properties of Trp-105. This is not so surprising considering that the coordination number for magnesium is predominantly six, and has ionic radius of 0.64 Å. Calcium has an ionic radius of 0.99 Å and a seven coordinate geometry. Therefore, the conformation that best accommodates calcium is not optimal for the coordination of magnesium. In other

words, for a calcium-binding site to bind magnesium, a slightly different organization in the binding loop would be required (15), which would be reflected in the absorbance and fluorescence experiments.

Both fluorescence and far-UV CD calcium titrations show clear evidence of cooperativity between Ca^{2+} specific and Ca^{2+}/Mg^{2+} sites. The evidence of cooperativity in troponin-C in the literature is contradictory. The techniques that have been used so far in metal binding studies on TnC - extrinsic fluorescence probes and equilibrium dialysis - may be disruptive to TnC, as analyzed by Golosinka *et.al.* (12). The use of tryptophan chromophores introduced by site-directed mutagenesis, as intrinsic reporters seems a less disruptive alternative for the study of TnC.

The binding constants estimated for the high-affinity sites in the recombinant protein FW105 are lower than those found in the literature for the native TnC. Ka = $2x10^7$ (23), Ka = $1.8x10^7$ (22) for calcium binding, Ka = $4x10^3$ (70), Ka = $3x10^3$ (16) for the binding of magnesium. This difference was attributed to the difference in the amino acids located in position 130. In both rabbit skeletal TnC and in the chicken TnC (non-recombinant proteins), this position in the high-affinity domain is occupied by a threonine residue. Instead, the recombinant protein has an isoleucine at position 130. The effects of having a threonine or an isoleucine residue at position 130 in chicken TnC will be discussed later in this thesis.

Site-directed mutagenesis seems an efficient alternative to chemical methods for the introduction of reporter groups into recombinant TnC. Trp29 and Trp-105 proved to be useful as intrinsic reporter groups to monitor metal binding in one domain of the protein, independently of binding events in the other domain. This was particularly important in the current study since titration curves overlapped. Titration data for FW29 and FW105 mutants could be fit to an equation that assumes there is a single class of sites. Only two parameters are involved in the calculation: 1 binding constant and 1 Hill coefficient. Calculations from the data of the double mutant FW29/FW105 and from far-

UV CD experiments was complicated by the fact that two classes of sites were been titrated. Fitting the data involves six parameters: 2 binding constants, 2 Hill coefficients and the relative contributions of each class of site to the spectral features. The statistical significance of the estimated constants is then lower.

Future mutagenesis studies in this recombinant protein should be greatly simplified by the use of the tryptophan chromophore in the single mutants. Problems regarding the N-domain should be easier to study using FW29, whereas FW105 would be useful for studies at the C-domain. In the second part of this project, Trp-105 was used as an intrinsic reporter in calcium binding experiments in the double mutants FW105/ IX130.

4.2. Stability of Helix G

In the second part of the project, an interesting structural aspect of chicken TnC was studied in relation to the function of the protein. The mutant proteins FW105/IX130 were created to probe the relationship between N-cap residue, stability of helix G and affinity for metal ions in TnC. Trp-105 was used to monitor metal binding at the high-affinity site of the proteins.

The N-cap is the residue that initiates an α-helix (47). It has non helical dihedral angles, but it participates in the hydrogen bonding network. The N-cap residue is believed to play an important role in the stability of helices. In fact, a preference at the N-cap position for amino acids whose side chain can hydrogen bond to main chain atoms >NH groups of an amino acid 2 to 3 positions towards the C-terminal (n+2 or n + 3) (47) has been attributed to the stabilizing effect this hydrogen bond would have on the helix. The helix could also be stabilized by the favorable interaction of charged amino acids with the helix dipole (45, 50). The N-cap residue that inititates helix G in the high-affinity domain is Thr-130 in native TnC and Ile-130 in the recombinant protein (Figure

1.4 and 1.5). Position 130 was chosen for this study since it was previously reported that native and recombinant TnC, which differ in the amino acid at position 130, differed also in their affinity for calcium. That is, amino acid residues that are likely to have different effects on the stability of the helix, confer different affinities for calcium ions. In fact, the 3 dimensional crystal structure shows that the side chain of Thr-130 hydrogen bonds to aspartic acid at position 133 (14). This stabilizing effect on helix G would be absent in the recombinant TnC where Ile-130 cannot provide a hydrogen bond acceptor. It is then interesting to explore the effect of different amino acids at position 130 on the affinity for calcium, as a model to prove relationships between N-cap residue and helix stability in proteins. Determining the effect of each amino acid substitution on the stability of helix G contributes to the understanding of the relationship between amino acid sequence and secondary structure (helix folding) in proteins.

It is widely accepted that metal binding induces conformational changes in TnC. Far-UV circular dichroism experiments show that the helical content of the apo protein increases from 36 % to 55 % in the metal-bound state (71). This equilibrium between the metal-free and metal-bound forms of TnC can be said to be homologous to the equilibrium between an unfolded and folded protein. The metal-free conformation of TnC can be viewed as an unfolded stable or semistable TnC. The transition to a structure of greater helical content in the metal-bound state would correspond to the transition to a fully folded TnC. The studies on Barnase (53) and T4 lysozyme (51) show that amino acid substitutions at the N-cap of α-helices shift the equilibrium between folded and unfolded forms of these enzymes. Similarly, it was predicted that amino acid substitutions at the N-cap of helix G in TnC would shift the equilibrium between a partially folded (metal-free) and fully folded (metal-bound) protein. If Thr-130 as N-cap provides greater stability to the helix compared to Ile-130, it would be equivalent to say that Thr-130 favours a fully folded conformation of TnC and Ile-130 favours a partially folded conformation. The effect of the amino acid substitutions at the N-cap can be

interpreted in terms of the relative contribution of the amino acid to the equilibrium between folded and partially folded proteins.

Far-UV CD experiments done on peptide fragments of TnC (71), show that the increase in helical content in the native troponin C corresponds to an increase in the number of helical residues from 57 in the calcium-free form, to 87 in the calcium-bound form. Substitutions at the N-cap are expected to contribute to the stability of helix G (51, 53) and favor the calcium-bound form of the protein in the equilibrium between bound and free states. Therefore, an increase in the helical content of TnC solutions relative to FW105/I130 mutant might be observed before the addition of calcium. However, CD measures the global helical content of the protein in solution, and the increase in the number of helical residues due to the contribution of the N-cap would be negligible compared to the overall helical content. Consequently, CD is not sensitive enough to detect this small change and no significant differences in the helical content of the mutant proteins were observed (Figure 3.14).

The far-UV CD spectra of the FW105/IX130 proteins (Figure 3.14) show the expected increase in negative ellipticity with calcium bound, and changes in ellipticity for all the mutant proteins are approximately equivalent (Table 3.7). The changes in fluorescence intensity when calcium or magnesium bind are also the same for all the mutant proteins, as indicated by the overlap of the spectra (Figure 3.15 and 3.16). Therefore, though the spectra are not sensitive enough to detect small changes in the equilibrium between bound and free states of TnC, they do indicate that the amino acid substitutions did not affect the global structure of TnC or the conformation and function of the high-affinity sites.

Titration data in Table 3.7 show that the Hill coefficient of all FW105/IX130 mutants do not vary significantly, that is, the amino acid substitutions at position 130 do not affect the cooperativity of the high-affinity sites. This is evidence that the high-affinity binding sites function in unison.

The data from the titration of the fluorescence of the FW105/IX130 mutants show differences in their binding constants. FW105/IG130 and FW105/I130 have the lower affinities for calcium. FW105/IS130 and FW105/IT130 show the highest and FW105/ ID130 and FW105/IN130 have intermediate values of Ka.

Ile and Gly had the expected effect on the calcium affinity at the high affinity sites in the mutants FW105/I130 and FW105/IG130. Both amino acid residues at the N-cap are unable to hydrogen bond to unpaired backbone >NH groups and cannot contribute to the formation of the N-terminus of helix G. There is a difference of 0.14 pCa units between Ile and Gly, which corresponds to a difference in free energy change of 0.2 kcal/mole between FW105/I130 and FW105/IG130. Between FW105/IT130 and FW105/I130 there is a difference of 0.48 pCa units and a $\Delta\Delta G = 0.66$ kcal/mole. Thr-130 in the wild type TnC participates in several H-bond interactions that involve water molecules and residues in helix G . Oγ1 of Thr-130 H-bonds to the main chain N of Asp-133 and to a structured water (# 36). At the same time this water molecule is H-bonded to Oε2 of Glu-132 and to another structured water molecule (#52). Ile would not participate in these interactions and would destabilize the helix. This could explain the large difference in affinity for calcium between FW105/IT130 and FW105/I130. Gly would allow more space for a more adequate hydrogen bonding with water, which would account for the higher affinity for calcium observed for FW105/IG130 with respect to the Ile mutant protein.

The titration curves of FW105/IS130 and FW105/IT130 overlap and have estimated Ka that are very similar. These amino acid residues differ only by a γ-methyl group. In the crystal structure this γ-methyl group does not appear to have hydrophobic interactions with neighboring residues. It can be expected then that Ser and Thr at the N-cap position will not differ very much in their contributions to the stability of helix G. This can explain the similar calcium affinities of FW105/IS130 and FW105/IT130 mutants.

Aspartic acid and asparagine at position 130 were expected to show higher affinities than what was observed experimentally. The side chain of aspartic acid can serve as H-bond acceptor and will thus stabilize the helix. On the other side, the negative charge of aspartic acid could favorably interact with the helix dipole at the N-terminal end. However, FW105/ID130 is not the best N-cap. To explain this, the structure that surrounds the N-cap position must be considered. The sequence immediately following position 130 is Glu - Glu - Asp. The high concentration of negatively charged residues close to the N-cap position may lead to charge repulsion interactions. Aspartic acid at position 130 would then have a more destabilizing than stabilizing effect.

These results may indicate that the preference for one amino acid over another will depend on the sequence context in which the amino acid is found. Aspartic acid might be a preferred N-cap when there are no adjacent negative charges in the sequence.

According to the study by Richardson *et. al.* (47), asparagine is highly preferred as N-cap residue. Experimentally it was observed that FW105/IN130 has an affinity lower than FW105/IT130 by 0.19 pCa units, which corresponds to a $\Delta\Delta G = 0.26$ kcal/mole. It is difficult to explain this difference, since the carbonyl oxygen (Oγ) in asparagine can accept a hydrogen bond from the backbone >NH group. The side chain - NH_2 group is available for other hydrogen bond interactions with water, for instance. It is also possible for the-NH_2 group to discourage helix propagation in the N-terminal direction, since it can compete with the backbone to provide the interaction. In the absence of a crystal structure for this mutant protein, it is difficult to interpret these results. Contrary to what was expected, Asn was not the best N-cap for helix G. These results agree with those from a study on Barnase (53) where the substitution of Thr by Asn at the N-cap was also destabilizing.

The overall results indicate that threonine is the preferred residue, together with serine at the N-terminus of helix G. It is worth noting that Thr is always the N-cap in helix G and in helix C of TnC and of calmodulin. Either Ser or Thr are the N-cap

residues in helices A, B and E (15). In the case of TnC, the results show that the native protein has a N-cap residue that guaranties the highest affinity for calcium at the N-domain.

Substitutions at the N-cap had a measurable effect on the affinity for calcium in the C-domain of TnC. The evidence from the literature (40, 45, 47, 50, 51, 53), shows that the N-cap residues affect the stability of helices. Therefore, it is possible that the observed difference in ion affinity is due to the different contribution of the N-cap residues to the stability of helix G. If a thermodynamic relationship truly exists between helix stability and ion affinity in the C-domain, the same relationship may exist in the N-domain and in structurally related proteins. Factors that affect the stability of the helix will regulate the affinity for calcium, and in this way calcium-affinity is fine-tuned in calcium binding proteins with helix-loop-helix motifs.

More detail and a better understanding of the relationship between N-cap residue, stability of helix G and calcium affinity would be possible if the structure of mutants proteins were determined, for example, by ^{1}H-NMR or X-ray crystallography.

If the N-cap residue is important in determining the equilibrium between metal-free and metal-bound states of TnC, it would also be important in the equilibrium between unfolded and folded TnC. It would be interesting to characterize the mechanism by which the N-cap contributes to this equilibrium. The N-cap residue could destabilize the unfolded free-state of TnC, it could stabilize the folded, metal-bound state, or both. These situations are represented in Figure 3.18 for the FW105/IT130 mutant, relative to FW105/I130. ΔG_a^T represents the destabilization of the unfolded free-state of TnC by Thr-130, ΔG_b^T represents the stabilization of the folded, metal-bound state, and (ΔG_c^T) represents both situations occurring simultaneously. These possibilitites could be analyzed in a future study by urea denaturation experiments on both the metal-free and metal-bound FW105/IX130 mutants.

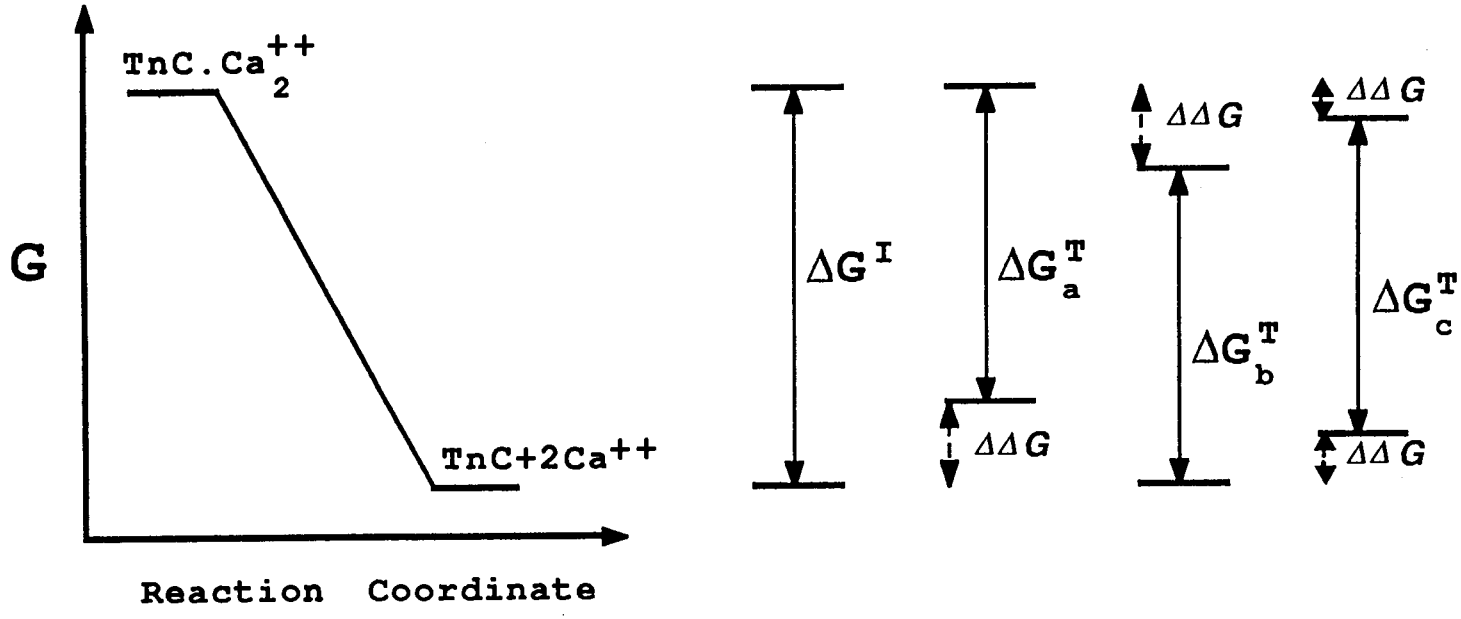

Figure 3.18. Comparative Gibbs Free Energy Diagram of FW105/IT130 versus FW105/I130

The figure represents the Gibbs free energy (G) diagram for the equilibrium between calcium-bound (TnC . Ca_2^{2+}) and calcium-free forms (TnC + $2Ca^{2+}$) of the high-affinity sites in the mutants FW105/I130 and FW105/IT130. The upper bars represent the calcium-bound forms of the protein, the lower bars the calcium-free forms. ΔG is the free energy change in the equilibrium between these two protein forms. ΔG_a^T , ΔG_b^T and , ΔG_c^T represent three possibilities for the threonine mutant to have a smaller ΔG than the isoleucine mutant (ΔG^I), accounting for the $\Delta\Delta G$ observed experimentally.

In other future studies, it will be interesting to determine the physiological consequences that mutations at the N-cap position can have. Muscle fibers depleted of TnC can be reconstituted with FW105/IX130 variants. TnC with different high-affinities for calcium incorporated into a fibre system can tell about the contribution of the C- and N-domains to the regulation of muscle contraction.

4.3. Conclusions

The characterization of the tryptophan mutants was an important first step in the study of TnC by the method of site-directed mutagenesis. FW29 and FW105 enable us to monitor metal binding to the N-domain without interferences due to metal binding at the C-domain. Trp-105 proved to be sensitive to subtle changes in the conformation of the high-affinity sites. This can be as important in future mutagenesis studies of structure and function relationships in TnC as it was in the study of the FW105/IX130 mutants.

The substitutions at position 130 by site-directed mutagenesis revealed important aspects of the function of the high-affinity sites in TnC. The calcium affinity at the C-domain appears to be related to the stability of an α-helix, and this relationship could also exist in the N-domain, and maybe in structurally related proteins. Future experiments with the FW105/IX130 mutants will help to obtain a more complete view of the function of the high-affinity domain in the regulation of muscle contraction by TnC.

Site-directed mutagenesis was a useful method to probe the structure and function of TnC. Other aspects of the structure and function of this important muscle protein can also be addressed in future experiments using this powerful technique.

5. REFERENCES

1. Zot, A., Potter, J. (1987) *Ann. Rev. Biophys. Chem.* **16**, 535-559

2. Potter, J.D., & Johnson, J.D. (1982) in *Calcium and Cell Function.* **2**, 145-173., ed. W. Cheung, New York: Academic

3. Ebashi, S. (1963) *Nature* **200**, 1010.

4. Ebashi, S., & Ebashi, F. (1964) *J. Biochem.* **55**, 604-613

5. Ebashi, S., Kodama, A., & Ebashi, F. (1968) *J. Biochem.* **64**, 465-477

6. Greaser, M.L., & Gergely, J. (1971) *J. Biol. Chem.* **246**, 4226-4233

7. Greaser, M.L., & Gergely, J. (1973) *J. Biol. Chem.* **248**, 2125-2133

8. Darnell, J., Lodish, H., & Baltimore, D. (1986) in *Molecular Cell Biology*, pp 821. Ed. W. H. Freeman and Company, N.Y.

9. Stryer, L. (1988) in *Biochemistry*, pp 933. Ed. W. H. Freeman and Company, N.Y.

10. Collins, J.H., Potter, J.D., Horn, M.J., Wilshire, G. & Jackson, N. (1973) *FEBS Lett*, **36**, 268-272

11. Wilkinson, J.M. (1976) *FEBS Lett.* **70**, 254-256

12. Golosinka, K., Pearlstone, J.R., Borgford, T., Oikawa, K., Kay, C.M. Carpenter, M.R. & Smillie, L.B. (1991) *J. Biol. Chem.* **266**, 15797-15809

13. Herzberg, O., & James, M.N.G. (1985) *Nature* **313**, 653-659

14. Satyshur, K.A., Rao, S.T., Pyzalska,D., Drendel,W., Greaser,M., & Sundaralingam, M. (1988) *J. Biol Chem.* **263**, 1628-1647

15. Strynadka, N.C.J., & James, M.N.G. (1989) *Ann. Rev. Biochem.* **58**, 951-998

16. Potter, J., & Gergely, J. (1975) *J. Biol. Chem.* **250**, 4628-4633

17. Sheng, Z., Strauss, W.L., Francois, J., & Potter, J.D. (1990) *J. Biol. Chem.* **265**, 21554- 21560

18. Zot, H.G., Guth, K., & Potter, J.D. (1986) *J. Biol. Chem.* **261**, 15883-15890

19. Grabarek, Z., Grabarek, J., Leavis, P.C., & Gergely, J. (1983) *J. Biol. Chem* **258**, 14098-14102

20. Grabarek, Z., Tan, R., Wang, J., Tao, T., & Gergely, J. (1990) *Nature* **345**, 132-135

21. Iida, S. (1988) *J. Biol.* **103**, 482-486

22. Hincke, M.T., Mc Cubbin, W.D., & Kay, C.M. (1978) *Can. J. Biochem.* **56**, 384-395

23. McCubbin, W.D., Oikawa, K., Sykes,B.D. & Kay, C.M. (1982) *Biochemistry* **21**,5948-5956

24. Reinach, F.C., & Karlsson, R. (1988) *J. Biol. Chem.* **263**, 2371-2376

25. Xu, G-Q., & Hitchcock-DeGregori, S.E. (1988) *J. Biol. Chem*, **263**, 13962-13970

26. Pearlstone, J.R., Borgford, T., Chandra, M., Oikawa, K., Kay, C.M. & Smillie, L.B. (1992) *Biochemistry* accepted for publication

27. Forsen, S., Vogel, H.J., & Drakenberg, T. (1986) *Calcium and Cell Function* (Cheung,W.Y.ed) **6**, 113-157, Academic Press,N.Y.

28. Haiech, J., Klee, C.B., Demaille, J.G. (1981) *Biochemistry* **20**, 3890-3897

29. Linse, S., Brodin, P., Drakenberg, T., Thulin, E., Sellers, P., Elmden, K., Grundstrom, T., & Forse, S. (1987) *Biochemistry* **26**, 6723-6735

30. Tsuda, S., Hasegawa, Y., Yoshida, M., Yagi, K. & Hickichi, K. (1988) *Biochemistry* **27**, 4120-4126

31. Yamakita, Y., & Iio, T. (1989) *J. Biochem.* **105**, 870-874

32. Brandt, P.W., Cox, R.N., & Kawai, M. (1980) *Proc. Natl. Acad. Sci.* **77**, 4717-4720

33. Grabarek, Z., Grabarek, J., Leavis, P.C. & Gergely,J. (1983) *J. Biol. Chem.* **258**, 14098-14102

34. Ogawa, Y. (1985) *J. Biochem.* **97**, 1011-1023

35. Zot, H.G., & Potter, J.D. (1987) *J. Musc. Res. Cell. Motil.* **8**, 428-436

36. Leavis, P.C., Rosenfeld, S.S., & Gergely. (1978) *J. Biol. Chem.* **253**, 5452-5459

37. Grabarek, Z., Leavis, P.C., & Gergely, J. (1986) *J. Biol. Chem.* **261**, 608-613

38. Iida, S. (1988) *J. Biochem.* **103**, 482-486

39. Richardson, J.S. *Adv. Protein. Chem.* (1981) **34**, 167

40. Presta, L.G., & Rose, G.D. (1988) *Science* **240**, 1632-1641

41. Chou, P.Y., & Fasman, G.D. (1974) *Biochemistry* **13**, 211-222

42. Hol, W.G.J. (1985) *Prog. Biophys, Molec. Biol.* **45**, 149-195

43. Hol, W.G.J., van Duijnen, P.T., & Berendsen, H.J.C. (1978) *Nature* **273**, 443-446

44. Marqusee, S., & Baldwin, R.L. (1987) *Proc. Natl. Acad. Sci.* **84**, 8898-8902

45. Shoemaker, K.R., Kim, P.S., York, E.J., Stewart, J.M., & Baldwin,R.L. (1987) *Nature* **326**, 563-567

46. Shoemaker, K.R., Kim ,P.S., Brems, D.N., Marqusee, S., York, E.J., Chaiken, I.M., Stewart, J.M., & Baldwin, R.L. (1985) *Proc. Natl. Acad. Sci.* **82**, 2349-2353

47. Richardson, J.S., & Richardson, D.C. (1988) *Science* **240**, 1648-1652

48. Fairman, R., Shoemaker, K.R., York, E.J., Stewart, J.M., & Baldwin, R.L. (1989) *Proteins: Structure, Function, and Genetics* **5**, 1-7

49. Shaw, G.S., Hodges, R.S., & Sykes, B.D. (1991) *Biochemistry* **30**, 8339-8347

50. Nicholson, H., Becktel, W.J., & Mathews, B.W. (1988) *Nature* **336**, 651-656

51. Nicholson, H., Anderson, D.E., Dao-pin, S., & Mathews, B.W. (1991) *Biochemistry* **30**, 9816-9828

52. Sali, D., Bycroft, M., & Fersht, A.R. (1988) *Nature* **335**, 740-743

53. Serrano, L., & Fersht, A.R. (1989) *Nature* **342**, 269-299

54. Golosinka, K., Pearlstone, J.R., Borgford, T., Oikawa, K., Kay, C.M. Carpenter, M.R., & Smillie, L.B. (1991) *J. Biol. Chem.* **266**, 15797-15809

55. Nagai, K., Perutz,M.F., & Poyart,C.(1985) *Proc.Natl.Acad.Sci.* USA **82**, 7252-7255

56. Sambrook, J., Fritsch,E.F., & Maniatis, T. 1989. Molecular Cloning, 2nd Ed. Cold Spring Harbor Laboratory Press.

57. Messing, J.(1983) *Methods Enzymol.***101**, 20-78

58. Nagai,K., & Thogersen,H.C. (1987) *Methods Enzymol.* **153**, 461-481

59. Zoller,M., & Smith,M.(1982) *Nucleic Acids Res.* **10**, 6487-6500

60. Carter,P., Bedouelle,H., & Winter,G.(1985) *Nucleic Acids Res.***13**, 4431-4443

61. Sanger, F., Nicklen, S., & Coulson, R.(1977) *Proc.Natl.Acad.Sci.* USA **74**, 5463-5467

62. Laemmli, U.K. (1970) *Nature* **227**, 680-685

63. Markwell, M.A.K., Haas, S.M., Tolbert, N.E., & Bieber,L.L. (1981) *Methods Enzymol.***72**, 296-303

64. Lowry, O.H., Rosebrough, N.J., Farr, A.L., & Randall, R.J.(1951) *J.Biol.Chem.***193**, 5-275

65. Borresen, H. C. (1967) *Acta. Chem. Scand.* 21, 920-936

66. Schippers, P.H., & Dekkers, H.P.J.M.(1981) *Anal.Chem.***53**, 778-782

67. Perrin, D.D., & Sayce, I.G.(1967) *Talanta***14**, 833-842

68. Cantor, C.R., & Schimmel, P.R. in *Biophysical Chemistry. Part II: Techniques for The Study of Biological Structure and Function.*

69. Donovan, J.W. (1969) in *Physical Principles and Techniques of Protein Chemistry*, Part A (Leach, S.J., Ed) pp 101-170, Academic Press, N.Y.

70. Johnson, J.D., Collins, J.H., & Potter, J. D. (1978) *J. Biol. Chem.* **253**, 6451-6458.

71. Reid, R.E., Gariepy, J., Saund, A.K., & Hodges, R.S. (1981) *J. Biol. Chem.***53**, 2742-2751.